LINKAGE ANALYSIS AND CANDIDATE GENE APPROACH IN THREE DISORDERS

by

Yeşerin Yıldırım

B.S., Molecular Biology and Genetics, Boğaziçi University, 2007

Submitted to the Institute for Graduate Studies in
Science and Engineering in partial fulfillment of
the requirements for the degree of
Master of Science

Graduate Program in Molecular Biology and Genetics
Boğaziçi University
2010

ACKNOWLEDGMENTS

I would like to sincerely thank my thesis supervisor Prof. Aslı Tolun, whose guidance, support and encouragement throughout the study helped me understand how the fundamental approach to scientific research should be. My appreciation is also extended to the members of my thesis committee, Prof. S. Hande Çağlayan and Prof. S. Nur Buyru for allocating their time to evaluate this work.

I sincerely thank all present and previous KOMMAGENE lab members, especially Sibel Uğur and Murat Çetinkaya for all their contribution to my learning lab techniques and dicipline and for their comments, Çiğdem Köroğlu, Renin Hazan and Ayşe Güven for their great friendship.

I thank all my friends in MBG, especially Emine Dindar, İzzet Akiva, Tuncay Şeker and Burçak Özeş for their support, their friendship and making my life pleasant. I would like to thank Sunay Usluer and İnanç Fidancı for their practical help and Arzu Öztürk for sharing her knowledge with me and for her friendship.

I am indebted to my family for encouraging and supporting me patiently.

This work has been supported by the Scientific and Technological Research Council of Turkey (106T596 and 108S011) and Boğaziçi University Research Funds (BAP 08M102).

dedicated to my beloved mother Çakır Ayşe

ABSTRACT

LINKAGE ANALYSIS AND CANDIDATE GENE APPROACH IN THREE DISORDERS

Genetically inherited diseases are powerful resources for defining new gene functions. Genetic linkage analysis is the tool used for identifying the locus/loci harboring the gene(s) responsible for a particular disease. The analysis of the genotypes generated with highly dense markers using computer programs for lod score calculations are the basis of genetic linkage analysis. In this study, genome scan in three inherited disorders, Gerodermia Osteodysplastica (GO), Motor Dysfunction, Intellectual Disability and Joint Contractures (MDIDJC) and Medial Cleft Lip (MCL) was performed with microsatellite and/or SNP markers. Two-point and multipoint lod score analyses were performed for locus identification. Candidate gene loci were investigated and gene loci were identified with additional polymorphic microsatellite markers.

Geroderma osteodysplastica (GO), a rare autosomal recessive disorder, is characterized by wrinkled skin on the dorsum of the hands and feet, droopy face, hyperextensible joints, skeletal changes such as osteoporosis and an of prematurely aged appearance. The candidate locus was identified in the study family, initially diagnosed as GO. While the thesis was in progress, the gene responsible for GO was identified as *GORAB* (1q24). In addition, some patients previously diagnosed with GO, Wrinkled Skin Syndrome or De Barsy Syndrome were found to have mutations in *PYCR1* (17q25.3), and the disease was named cutis laxa, autosomal recessive, type IIB or ARCL2B. The last disorder has similar features with GO. A previously reported *PYCR1* mutation was found in patients studied within the scope of this thesis. Further, the clinical and molecular findings of GO and ARCL2B were reviewed. Since the clinical phenotypes of patients with either *GORAB* or *PYCR1* mutations are similar to GO, it was suggested that the disorder resulting from defects in *GORAB* should be designated as GO type I (without MR) and that resulting from defects in *PYCR1* as GO type II (with MR) rather than ARCL2B.

A highly inbred family having twelve members afflicted with autosomal recessive postnatal development of multiple joint contractures, motor disability and mental disability was studied. The syndrome in the study family was assessed as novel and designated motor dysfunction, intellectual disability and joint contractures (MDIDJC). The disease loci was mapped to 8p12, and subsequently a homozygous 2-bp insertion in *ERLIN2* (endoplasmic reticulum lipid raft-associated protein 2) was identified. The mutation is predicted to lead to protein truncation.

Orofacial defects are very common congenital defects in humans. The kindred we analyzed exhibited a unique form of orofacial defects, median cleft lip (MCL): the four most affected sibs exhibited an inherited form of incomplete median clefting in upper and lower lip together, with involvement of dental dysmorphology. In addition to the affected sibs, the mother and one of the sibs had a subclinical phenotype, whereas two cousins had minimal phenotype. A homozygous intergenic novel deletion larger than 270,000 bp was identified in all affected sibs. Some of the remaining members also carried the mutation. The deletion resided between genes *TYW3* and *LHX8*. *LHX8* had been implicated in cleft palate in mouse, and a role in lip and maxilla formation. Thus, we propose that the mutation region might harbor sequences having a regulatory role in the expression of *LHX8* gene. It was concluded that a second gene likely contributes to the phenotype. Additionally, several loci that may be associated with the condition were identified.

ÖZET

ÜÇ HASTALIKTA BAĞLANTI ANALİZİ VE ADAY GEN YAKLAŞIMI

Kalıtsal hastalıklar yeni gen işlevlerinin tanımlanması açısından çok yararlıdır. Belirli bir hastalıktan sorumlu geni/genleri içeren bölgelerin tanımlanmasında genetik bağlantı analizinden yararlanılır. Sık belirteçler kullanılarak oluşturulan genotiplerin özel bilgisayar programları aracılığıyla incelenmesi genetik bağlantı analizinin temelini oluşturur. Bu tez çalışmasında üç kalıtsal hastalık, Gerodermia Osteodysplastica (GO), Motor İşlev Bozukluğu, Entelektüel Yetersizlik ve Eklem Kontraktürleri ve Orta Hat Yarık Dudak (MCL) çalışılmıştır. Bu hastalıkları taşıyan üç farklı ailede mikrosatelit ve/veya SNP belirteçler kullanılarak genom taraması yapılmıştır. İki-noktalı ve çok-noktalı lod skor hesaplamaları ile hastalıktan sorumlu geni taşıyan bölgeler aranmıştır. Aday gen bölgeleri ek polimorfik mikrosatelit belirteçler ile incelerek doğrulanmış ya da dışlanmıştır.

Geroderma osteodysplastica ellerin ve ayakların üst kısmında kırışıklık, sarkık bir yüz görünümü, aşırı esnek eklemler, kemik erimesi gibi kemik değişimleri ve cildin erken yaşlanmasıyla tanımlanan otozomal çekinik bir hastalıktır. Bu çalışmada incelenen aileye bu bulgular nedeniyle GO tanısı konmuştur ve gen bölgesi bulunmuştur. Tez sürecinde, başka araştırıcılar GO hastalığından *GORAB* geninin (1q24) sorumlu olduğunu bulmuşlardır. Ayrıca daha önce GO, Buruşuk Cilt Sendromu (Wrinkled Skin Syndrome) veya De Barsy Sendromu tanısı konulmuş bazı hastaların *PYCR1* (17q25.3) geninde mutasyon taşıdıkları da ortaya konmuş ve hastalık otozomal çekinik tip IIB kutis laksa veya ARCL2B adını almıştır. Bu nedenle *PYCR1* geni bizim çalışmadaki hastalarda da incelenmiş ve hastaların daha önce rapor edilmiş bir mutasyonu homozigot olarak taşıdıkları bulunmuştur. Tez çalışması sırasında GO ve ARCL2B hastalıklarının klinik ve moleküler bulguları gözden geçirilmiştir. *GORAB* veya *PYCR1* mutasyonu taşıyan hastaların fenotiplerinin diğer kutis laksa hastalıklarından ziyade GO'ya benzediği düşünülmüştür. Bu nedenle *GORAB* bozukluğundan kaynaklanan hastalığın Tip I GO

(zihinsel geriliğin eşlik etmediği) ve *PYCR1* bozukluğundan kaynaklanan hastalığın ARCL2B yerine Tip II GO (zeka geriliğinin eşik ettiği) adlarını almaları önerilmiştir.

İkinci olarak doğuştan gelen motor işlev bozukluğu, çoklu eklem kontraktürleri, motor ve zeka yetersizliği ile tanımlanan otozomal çekinik bir kalıtıma sahip bir hastalık çalışılmıştır. İlk kez karşılaşılan bu sendroma MDIDJC adı verilmiştir. Hastalık bölgesi 8p12'ye haritalanmış, ardından *ERLIN2* geninde 2 baz çiftlik araya girme mutasyonu saptanmıştır. Bu mutasyon son kısmı olmayan, kısa bir proteinin üretimine yol açmaktadır.

Orofasiyel bozukluklar çok yaygın görülen ve doğuştan gelen bozukluklardır. İncelediğimiz çocuklar orofasiyel bozuk yelpazesinde ilk kez tanımlanan bir orta hat yarık dudak bozukluğuna sahiptir: en çok etkilenen dört kardeş diş bozukluklarıyla beraber kısmi alt ve üst dudak yarığına sahiptir. Etkilenmiş bireylerin annesi ve bir kardeşine subklinik fenotip ve iki kuzenine minimal fenotip tanısı konmuştur. En çok etkilenen dört çocukta 270.000 baz çiftinden daha büyük bir silinme (1p31.1) tespit edilmiştir. Silinme *TYW3* ve *LHX8* genleri arasında yer almaktadır. *LHX8* geni yarık dudak/damak bozukluğu ile hayvan modellerinde ilişkilendirilmiştir ve insanlarda güçlü bir aday gen olarak öne çıkmaktadır. Bu gende mutasyon gözlenmedi. Buna dayanarak çalışmanın silinen bölgede *LHX8* geninin anlatımını düzenleyici bir işleve sahip dizilerin bulunduğu ve bu nedenle silinmenin bahsi geçen fenotipe neden olduğu ileri sürülebilir. Fenotipten sorumlu ikinci bir genin daha var olduğu sonucuna ulaşılmış ve fenotipten sorumlu birçok olası ek bölge tespit edilmiştir.

TABLE OF CONTENTS

LIST OF FIGURES

LIST OF TABLES

LIST OF ABBREVIATIONS

A	Alanine
ALDH18A1	Δ^1-pyrroline-5-carboxylate synthase gene
APS	Ammonium peroxidisulfate
AR	Autosomal recessive
ARCL1	Autosomal recessive cutis laxa type I
ARCL2A	Autosomal recessive cutis laxa type IIA
ARCL2B	Autosomal recessive cutis laxa type IIB
BMP	Bone morphogenetic protein
bp	Base pair
BSA	Bovine serum albumin
CA8	Carbonic anhydrase related protein 8
cAMP	Cyclic adenosine monophosphate
cDNA	Complementary DNA
Chr	Chromosome
CL	Cleft lip
CL/P	Cleft lip with or without cleft palate
	Cleft lip with cleft palate
CLP	CNV
cM	Centimorgan
DBS	De Barsy syndrome
dH_2O	Distilled water
DMSO	Dimethyl sulfoxide
DNA	Deoxyribonucleic acid
E	Glutamic acid
EDTA	Ethylene diaminetetraacetate
ER	Endoplasmic reticulum
ERAD	Endoplasmic reticulum-associated degradation
ERLIN2	ER lipid raft associated 2
FGF	Fibroblast growth factor

GO	Geroderma osteodysplastica
GTP	Guanosine triphosphate
HCiE	Homozygosity Comparison in Excel
HPRT1	Hypoxanthine phosphoribosyltransferase 1
IBD	Identical by descent
ITPR	Inositol 1,4,5-trisphosphate receptors
K	Lysine
kb	Kilobase
LHX8	Lim homoebox gene 8
Lod	Log of odds
Mb	Mega base
MCL	Median cleft lip
MDIDJC	Autosomal-recessive motor dysfunction, intellectual disability and multiple joint contractures
$MgCl_2$	Magnesium chloride
min	Minute
MPT	Multipoint lod score
MR	Mental retardation
MRI	Magnetic resonance imaging
mRNA	Messenger ribonucleic Acid
N	Asparagine
NA	Not Available
NCBI	National Center For Biotechnology Information
NHLBI	National Heart, Lung and Blood Institute
P	Proline
PAGE	Polyacrylamide gel electrophoresis
PAR1	Pseudoatosomal region 1
PAR2	Pseudoatosomal region 2
PCR	Polymerase chain reaction
pLOD	Parametric lod score
PYCR1	Pyrroline-5-carboxylate reductase 1
qRT-PCR	Quantitative reverse transcriptase-polymerase chain reaction
R	Arginine

Rpm	Revolution per minute
RT-PCR	Reverse transcriptase-polymerase chain reaction
SCAFUD	Scanning fluorescence detector
SDS	Sodium dodecyl sulphate
SNP	Single nucleotide polymorphism
SPFH	Stomatin, prohibitin, flotillin and HflC/K
SSCP	Single strand conformational polymorphism
TBE	Tris-boric acid-EDTA
TE	Tris-EDTA
TEMED	N, N, N, N'-Tetramethyl ethylenediamine
TGFB	Transforming growth factor
U	Unit
UTR	Untranslated region
UV	Ultraviolet
V	Valine
WWS	Wrinkly skin syndrome
X	Stop codon
Z_{max}	Maximum two-point lod score
W	Watt
µg, µl	Mikrogram, mikroliter

1. INTRODUCTION

Three families afflicted with different hereditary disorders, namely, Geroderma Osteodysplastica (GO), Autosomal-Recessive Motor Dysfunction, Intellectual Disability and Multiple Joint Contractures (MDIDJC) and Median Cleft Lip (MCL), were the subject of this thesis. Molecular genetic studies were performed with the aim of gene localization and gene identification in the disorders.

1.1. Geroderma Osteodysplastica

Geroderma osteodysplastica (GO; MIM231070), which is a rare autosomal recessive disorder, is characterized by wrinkled skin on the dorsum of the hands and feet, droopy face, hyperextensible joints, skeletal changes such as osteoporosis and an of prematurely aged appearance.

In addition to GO, progeroid appearance, wrinkled skin and cutis laxa (loose skin with reduced elasticity) are associated with other monogenic disorders, namely, De Barsy syndrome (DBS), Wrinkly Skin syndrome (WSS), autosomal recessive cutis laxa type I and type IIA and B (ARCL1, ARCL2A/B) and Autosomal Dominant Cutis Laxa (ADCL) (Morava *e*t *al*., 2009). Since the symptoms are generally indistinguishable from each other, a definite clinical diagnosis is difficult. In such a situation, molecular diagnosis becomes essential. Thus far, eight genes have been associated with such diseases. They are listed in Table 1.1, and their functions are summarized in Table 1.2.

While this thesis was in progress, the gene responsible for GO was identified as *SCYL1BP* (Hennies et *al*., 2008; Al-Dosari and Alkuraya, 2009). Additionally, some patients previously diagnosed with GO, WSS or DBS were found to have mutations in *PYCR1* (Guernsey *et al*., 2009; Reversade *et al*., 2009), and the disease was named cutis laxa, autosomal recessive, type IIB (ARCL2B; MIM 612940).

Table 1.1. The genes identified as responsible for hereditary disorders characterized with wrinkly skin and cutis laxa.

Disorder	Description	Gene	MIM	Chromosome
ARCL1	Autosomal Recessive Cutis Laxa Type I	*EFEMP2*, *FBLN5*	219100	11q13, 14q32.1
ARCL2A, WSS	Autosomal Recessive Cutis Laxa Type IIA, Wrinkly Skin Syndrome	*ATP6V0A2*	612940	12q24
GO	Geroderma Osteodysplastica	*GORAB*	31070	1q24.2
MRJHSL/MA	Mental Retardation, Joint Hypermobility and Skin Laxity, with or without Metabolic Abnormalities	*ALDH18A1*	612652	10q24.3
ARCL2B	Autosomal Recessive Cutis Laxa Type II	*PYCR1*	612940	17q25.3
ADCL	Autosomal Dominant Cutis Laxa	*ELN*, *FBLN5*	123700	7q11.23, 14q32.1

Table 1.2. Functions of the genes associated with wrinkly skin and cutis laxa and the mutational effects on phenotypes

Gene Name	MIM	Protein (Possible) Function	Molecular Effect of Gene Defects
EFEMP2 (Egf-Containing Fibulin-Like Extracellular Matrix Protein 2)	604633	Elastic fiber and vessel formation, collagen synthesis	Abnormalities in elastic fibers
FBLN5 (Fibulin 5)	604580	Interacts with integrins and the RGD motif for adhesion of endothelial cells	Abnormalities in elastin structure
ATP6V0A2 (ATPase, H+ Transporting, Lysosomal, V0 Subunit A2)	611716	Role in proton transport in Golgi Apparatus	Defects in membrane trafficking from Golgi to ER in fibroblasts
GORAB (golgin, RAB6-interacting)	607983	a GTPase, interacts with Rab6	Defects in membrane trafficking between Golgi and plasma membrane [b]
ALDH18A1 (Aldehyde Dehydrogenase 18 Family, Member A1)	138250	Involved in proline biosynthesis pathway	Probably similar effects with *PYCR1* deficiency
PYCR1 (Pyrroline-5-Carboxylate Reductase 1)	179035	Involved in proline biosynthesis pathway	Apoptosis due to defective mitochondrial function
ELN (Elastin)	130160	Component of elastic fibers	Abnormalities in elastic fibers

The clinical manifestations in the patients genetically investigated in this thesis work were similar to both GO and ARCL2B. *GORAB* (designated also as *SCYL1BP*; MIM 607983) responsible for GO consists of 394 amino acids. It is highly expressed in osteoblasts and skin. *GORAB* specifically binds to Rab6 protein. Rab6, a small G-protein, co-localizes with *GORAB* to Golgi, and it has a role in intracelluler membrane trafficking in the secretory pathway from the Golgi to the plasma membrane (Al Dosari *et al*., 2009; Short *et al*., 2005; Hennies *et al*., 2008). *PYCR1*, responsible for ARCL2B (Guernsey *et al*., 2009; Reversade *et al*., 2009), has two transcripts coding for 319 and 316 amino acids. PYCR1 protein localizes to mitochondria, and it is involved in the catalysis of proline (Phang et al., 2008). It is highly expressed in bone and skin. Proline has a protective effect against high amounts of ROS, and mammalian cell lines increase proline synthesis in oxidative stress (Krishnan *et al*., 2008). Mutations in *PYCR1* interfere with the function of mitochondria and thereby lead to apoptosis (Reversade *et al*., 2009).

In this study a large consanguineous family having four affected members was genetically investigated. The disease locus was identified. In addition, a homozygous mutation was found in the gene recently identified for ARCL2B.

1.2. Motor Dysfunction, Intellectual Disability and Joint Contractures

Genetic basis for motor learning and coordination is currently unknown. Rather than being an isolated recessively inherited disorder, intellectual disability (ID) generally occurs with other clinical findings as part of syndromes. A highly inbred family afflicted with autosomal recessive postnatal development of multiple joint contractures, motor disability and mental disability was studied. Such a syndrome combining those characteristics has never been reported. Intellectual disability, also known as mental retardation, could be associated with contractures, but then the contractures are generally congenital and limited to the distal parts of the limbs (Wortmann *et al*., 2007; Martínez-Glez *et al.*, 2006). Arthrogryposis Multiplex, in which the contractures are generalized to the whole body, is also congenital (MIM 208100, MIM 208155, MIM 162370, MIM 108110 and MIM 610001). The syndrome in the study family was assessed as novel and

designated motor dysfunction, intellectual disability and joint contractures (MDIDJC). The disorder was inherited in an autosomal recessive fashion.

In this study a large consanguineous family having twelve affected members was genetically investigated. The disease locus and subsequently the disease gene were identified.

1.3. Median Cleft Lip

1.3.1. Classification of Orofacial Clefts

Orofacial defects are very common congenital defects in humans, with a frequency of about 1.2 in 1000 births worldwide (Jugessur et al., 2009). Orofacial clefts can be classified into three types: only cleft lip (CL), cleft lip with cleft palate (CLP) or only cleft palate (CP). The first two can also be grouped into cleft lip with or without cleft palate (CL/P).

Classification of orofacial defects is also made depending on whether the cleft is part of a syndrome or is isolated. Seventy per cent of the CL/P and half of the CP cases are isolated, whereas the remaining coexists with various disorders related to morphological abnormalities (Jugessur and Murray, 2005).

In Tessier's classification system, which is a widely used anatomical system, orofacial clefts are numbered from 0 to 30 in a clockwise manner. While 0 corresponds to midline upper lip and nose cleft, 30 corresponds to a mid-mandibular cleft (Resnick and Kawamoto, 1990).

Orofacial cleftings encompassing the regions relating to mouth can be also classified as the median cleft lip (upper lip), median mandibular cleft, unilateral and bilateral cleft lip sometimes with primary palate, oblique facial cleft (from mouth to the inner canthus of the eye) and lateral facial cleft (Eppley et al., 2003). The severity of the cleftings highly varies from complete clefts to only notches. Additionally, microform

phenotypes, looking like a scar, and subepithelial (non-visible) phenotypes arise from orbicularis oris muscle defects (Marazita, 2007).

Median cleft of upper lip has an incidence of less than 1 in a million births worldwide. It is rare also among all lip clefts (Eppley et al., 2004). Other cranial malformations as well as mental retardation may accompany median clefts of the upper lip but are not common in other forms of cleft lip. On the other hand, as little as only a vermillion notch can be observed in isolated cases (Fearon, 2008; Eppley et al., 2004). Similarly, median cleft of the lower lip (Tessier No. 30) is very rare (Armstrong and Waterhouse, 1996; Seyhan and Kılınç, 2002).

1.3.2. Lip and Palate Formation

In order to understand the anatomical origins of orofacial cleftings, the development of craniofacial structures need to be overviewed. Five facial primordial structures, namely, two mandibular and two maxillary prominences and the median nasal prominence give rise to the maxillo-mandibular (relating to the upper and lower jaws) complex. The mandibular prominences fuse across the midline with each other at an early stage in embryo to produce the lower lip and jaw. The maxilla, primary palate and secondary palate are formed at later stages (Jugessur et al., 2009). The primary palate and the upper lip are derived from the merging of the medial nasal prominences with each other as well as with the bilateral maxillary processes. Additionally, the median nasal process gives rise to the midline of the upper lip and philtrum (Young, 2010). The two palatal shelves extending from maxillary prominences form the secondary palate (Jugessur and Murray, 2005).

1.3.3. Genetic Etiology of Cleft Lip and/or Palate

Simple Mendelian inheritance models can explain many of the syndromic clefts. However, complex inheritance patterns are observed for nonsyndromic types: involvement of more than one gene and dominant and recessive inheritance together as well as low penetrance (Murray, 95). In addition to genetic factors, environmental factors also play a role in the formation of clefts. Several environmental factors such as maternal exposure to

smoking, alcohol, anticonvulsant drugs, nutritional deficiency and teratogens -agents causing malformation of an embryo- have been associated with orofacial clefts (Mossey *et al*., 2009). The studies with cases having consanguineous parents have indicated that genetic background plays a more important role than environmental effects in the formation of cleftings (Sivertsen *et al*., 2008).

A list of genes that have been associated with cleft lip/palate or identified as strong candidates in humans are presented in Table 1.3.

Table 1.3. Genes associated with cleft lip and/or palate, their MIM designations and chromosomal loci.

Gene	**Gene Description**	**MIM**	**Chromosome**
ABCB1[a]	ATP-Binding Cassette, Subfamily B, Member 1	171050	7q21.1
ANKS6[b]	Ankyrin Repeat and Sterile alpha Motif Domain Containing 6	-	9q22.33
BMP4	Bone Morphogenetic Protein 4	112262	14q22-q23
CHD7	Chromodomin Helicase DNA-Binding Protein 7	608892	8q12.1-12.2
DLX1[c]	Distal-Less Homeobox 1	600029	2q32
DLX2[c]	Distal-Less Homeobox 2	126255	2q32
EGF[d]	Epidermal Growth Factor	131530	4q25
EGFR[e]	Epidermal Growth Factor Receptor	131550	7p12.3-p12.1
FGF3[f]	Fibroblast Growth Factor 3	164950	11q13
FGF7[f]	Fibroblast Growth Factor 7	148180	15q15-q21.1
FGF8	Fibroblast Growth Factor 8	600483	10q24
FGF10[f]	Fibroblast Growth Factor 10	602115	5p13-p12
FGF18[f]	Fibroblast Growth Factor 18	603726	5q34
FGFR1	Fibroblast Growth Factor Receptor 1	136350	8p11.2-p11.1
FGFR2	Fibroblast Growth Factor Receptor 2	176943	10q26
FGFR3	Fibroblast Growth Factor Receptor 3	134934	4p16.3
FOXE1	Forkhead box E1	602617	9q22
GABRB3	Gamma-Aminobutyric Acid Receptor, Beta-3	137192	15q11.2-q12
GLI2	GLI-Kruppel Family Member	165230	2q14
IRF6	Interferon Regulatory Factor 6	607199	1q32-q41
LHX8	Lim Homeobox Gene 8	604425	1p31.1
MAFB[g]	V-Maf Musculoaponeurotic Fibrosarcoma Oncogene Family, Protein B	608968	20q11.2-q13.1
MSX1	Msh Homeobox 1	142983	4p16.1
MSX2	Msh Homeobox 2	123101	5q34-q35
MTHFR	5,10-methylenetetrahydrofolate Reductase	607093	1p36.3
MYH9[h]	Myosin, Heavy Chain 9, Nonmuscle	160775	22q11.2
PAX9	Paired Box Gene 9	167416	14q12-q13
PDGFC	Platelet Derived Growth Factor C	608452	4q32
PDGFRA[i]	Platelet-Derived Growth Factor Receptor, alpha Polypeptide	173490	4q12
PTCH1	Patched Homolog 1	601309	9q22.3
PVRL1	Poliovirus Receptor-Related 1	600644	11q23-q24
RAC1[j]	Ras-Related C3 Botulinum Toxin Substrate 1	602048	7p22

Table 1.3. Genes associated with cleft lip and/or palate, their MIM designations and chromosomal loci (continued).

RARk[j]	Retinoic Acid Receptor, Alpha	180240	17q21.1
RUNXI[k]	Runt-Related Transcription Factor 1	151385	21q22.3
SHH	Sonic Hedgehog	600725	7q36
SKI	V-Ski Avian Sarcoma Viral Oncogene Homolog	164780	1p36.3
SMAD1	SMAD Family Member 1	601595	4q28
SUMO1	SMT3 Suppressor of Mif Two 3 Homolog 1	601912	2q32.2-q33
TBX1[m]	T-box 1	602054	22q11.2
TBX10	T-box 10	604648	11q13.1-q13.2
TCOF1[n,o]	Treacher Collins-Franceschetti syndrome 1	606847	5q32-q33.1
TFAP2A[p,q]	Transcription factor AP-2 alpha	107580	6p24
TGFA[r,s,t]	Transforming Growth Factor, alpha	190170	2p13
TGFB1[u]	Transforming Growth Factor, beta 1	190180	19q13.1
TGFB2	Transforming Growth Factor, beta 2	190220	1q41
TGFB3	Transforming Growth Factor, beta 3	190230	14q24
TGFBR1	Transforming Growth Factor, beta receptor I	190181	9q22
TGFBR2	Transforming Growth Factor, beta receptor I	190182	3p22
WNT9B	Wingless-type MMTV integration site family, member 9B	602864	17q21

[a]Bliek et al., 2009; [b] Vieira et. al 2008; [c]Young et al., 2010; [d] Abbott et al., 2005; [e]Miettinen et al., 1999; [f]Riley et al., 2007; [g]Beaty et al., 2010; [h]Chiquet et al., 2009; [i]Ding et al., 2004; [j]Thomas et al., 2010; [k]Mitchell et al., 2003; [l]Charoenchaikorn et al., 2009; [m]Shi et al., 2009; [n]Sull et al., 2008; [o]Dixon et al., 2006; [p]Rahimov et al., 2008; [q]Shi et al., 2009; [r]Vieira et al.,2004; [s]Sull et al., 2009; [t]Carter et al., 2010; [u]Yang and Kaartinen, 2007

Lim homoebox gene 8 (*LHX8*) encodes a transcription regulator which is composed of a DNA-binding domain and a protein binding domain (MIM 604425). During embryogenesis in mice, *Lhx8* is expressed in basal forebrain and mesenchyme of the mandible and maxilla (Grigoriou *et al*., 1998). Zhao et al. (1999) identified defects in the fusion of palatal shelves that resulted in cleft palate in *Lhx8* knock-out mice. Inoue et al. (2006) showed the involvement of TGF-b3 and Fgf-8b in high *Lhx8* expression levels in maxillary mesenchyme in chicken embryo. Mesenchyme is the mesodermal tissue that develops into bone, cartilage, connective tissue and the circulatory and lymphatic systems.

The phenotype of the family studied in this thesis work was a combination of upper and lower lip median clefts in four siblings. Such a phenotype, to our knowledge, is unique in the literature. All four patients are mentally normal and have no other congenital abnormality. The family pedigree and elaborate clinical descriptions for each individual are presented in Materials and Methods. The mother and sibling 304 were so mildly affected that they were diagnosed as subclinical. Cousins 301 and 311 displayed minimal clinical

features. The disease locus and subsequently a homozygous intergenic deletion were identified.

1.4. Genetic Linkage Analysis

Two loci that are on the same chromosome and close to each other tend to be inherited together. As the distance between the loci increases, the probability of being inherited together decreases due to crossovers that occur during meiosis. Although recombination processes can separate even two closely linked loci, the frequency of a recombination event, denoted by θ, decreases as the distance between two loci decreases. If this distance is far enough, two loci behave as if they lie on different chromosomes. In this situation, the recombination frequency is 50 per cent (θ=0.5), and the loci are unlinked. Conversely, the recombination frequency between two linked genes is always less than 50 per cent.

The unit of recombination frequency is centimorgan (cM). One cM corresponds to a distance between two loci having one per cent recombination frequency. Generally one cM is equal to approximately one megabase of DNA. However, this value varies due to recombination hotspots along the chromosomes, such as telomeres. Also, recombination events occur in sex-specific manner. Overall, the recombination frequency is greater in females than males. In females, a more uniform recombination pattern is observed across the chromosome. Generally, greatest high female:male genetic distance is observed around the centromeres, and it declines across the chromosome arm in females compared with males. On the other hand, males have a higher recombination frequency in telomeric regions (Broman *et al*., 1998; Lynn *et al*., 2000).

Recombination events are widely utilized for mapping of a disease gene. Genomes of the members of an afflicted family are genotyped using closely spaced polymorphic genetic markers spread over the entire genome. The markers that are in the vicinity of the disease gene tend to be inherited together, and if a certain allele of a marker is often passed on to offspring along with the disease trait, then it can be concluded that the responsible gene lies somewhere near the marker.

Microsatellite markers are widely used for linkage analysis. They are short sequences (two to five bp) of DNA that are repeated ten to hundred times in tandem. They are generally located within non-coding regions of the genome. They are abundant and highly polymorphic due to the high rate of mutation arising from slippage during replication. To identify alleles, primers flanking a particular microsatellite region are designed and the region is amplified by polymerase chain reaction (PCR). The products are visualized after resolution on polyacrylamide gels.

New generation polymorphic markers used for both linkage and association studies are single nucleotide polymorphisms (SNPs). SNP is a variation at a single site in DNA, which is observed in the general population at a frequency of greater than 1 per cent. Thanks to the microarray technology, efficient and dense genotyping at a low cost is possible using chips that include 10,000 to 1,000,000 SNPs.

1.5. Lod Score Analysis

Lod score (logarithm of odds) analysis, a statistical method, is used to estimate the recombination fraction between a disease locus and a marker locus. Lod score was proposed by Morton (1955), based on two alternative hypotheses: the null hypothesis of no linkage ($q = 0.5$) and the alternative hypothesis of linkage ($q < 0.5$). The LOD score is the ratio of probability of observing the distributional pattern of the two traits in a pedigree with a given linkage value to observing it with no linkage.

Lod scores are routinely calculated for 0 per cent, 5, 10, 15, 20, 30 and 40 per cent recombination values rather than only for just two basic hypotheses mentioned below. The θ value yielding the highest LOD score is considered the best estimate. A lod score of 3.0 is a threshold for accepting linkage in humans. Lod score values lower than -2.0 indicate absence of linkage, while values between -2.0 and 3.0 are inconclusive (Nyholt, 2000).

In two-point lod score the probability that a disease gene is near a particular marker is calculated. Multipoint lod score analysis calculates simultaneously linkage to the multiple, closely spaced markers in a given chromosomal region.

Lod scores are calculated with the help of sophisticated computer programs that handle pedigree and allele data introduced in certain formats. A genetic model whose components are inheritance pattern (dominant or recessive, sex-linked or autosomal), frequency of the alleles and degree of penetrance needs to be introduced to the programs. EasyLINKAGE (Hoffmann and Lindner, 2005) is a panel that merges various lod score analysis programs in one working bench, and genotypes constructed with both SNP and microsatellite markers can be utilized. The linkage analysis programs used during the study are listed in Table 1.4.

Table 1.4. List of the genetic linkage analysis programs utilized in this study.

Program	Usage Purpose
Allgero v1.2c	Two-point, multipoint and power calculations as well as construction of haplotypes in small families (bit* size ≤19)
GeneHunter v_5.05	Multipoint lod score calculations and construction of haplotypes in small families (bit size ≤19)
PedCheck v1.0	Detecting incompatibility with Mendelian inheritance due possibly to genotyping errors or deletions
SimWalk v2.91	Multipoint parametric lod score calculations in large families (bit size >19)
SuperLink v1.6	Two-point parametric lod score calculations

* Bit is a term used in computer science for a unit of information having just two possible values: digits 0 or 1.

2. PURPOSE

The purpose of this study was to localize and identify the genes responsible for three inherited disorders: Geroderma Osteodysplastica (GO), Motor Dysfunction, Intellectual Disability and Multiple Joint Contractures (MDIDJC) and Median Cleft Lip (MCL). GO and MDIDJC are autosomal recessive disorders whereas MCL displays complex inheritance. Thus, straightforward steps were followed for the first two disorders, while both autosomal and recessive models are assumed in the analysis of MCL.

3. MATERIALS

3.1. Subjects

The study was approved by the Committee on Research with Human Participants at Boğaziçi University. Informed consent was obtained from all families included in the study.

3.1.1. Gerodermia Osteodysplastica

A consanguineous family afflicted with GO was investigated (Figure 3.1). The DNA samples of the family were supplied by Dr. Beyhan Tüysüz in the Department of Medical Genetics, Cerrahpaşa Medical Faculty, İstanbul University (Figure 3.1). The clinical findings are presented in Table 3.1 and Figures 3.2 and 3.3. The clinical findings and photographs were obtained from Dr. Tüysüz.

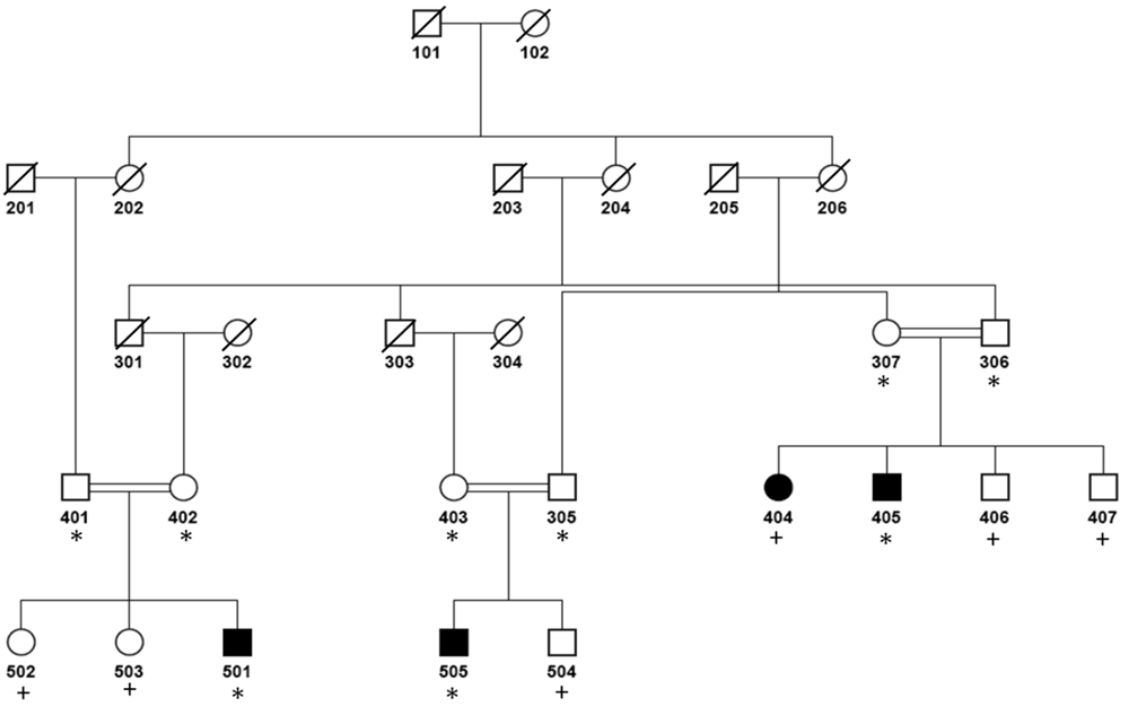

Figure 3.1. Partial pedigree of GO family. DNA available for the genome scan is marked with an asterisk and DNA available later with a plus sign.

Table 3.1. Comparison of the clinical features of GO patients investigated to those reported.

CLINICAL FEATURES	This Study (with *PYCR1* Mutations)				Reported Patients with Mutations in						
					GORAB					*PYCR1*	
						Hennies et al.					
	Patient 1	Patient 2	Patient 3	Patient 4	Newman et al.	Rajab et al. (Family B)	Hunter et al.	Picco et al.	Al-Dosari et al.	Guernsey et al.	Reversade et al.
Wrinkly skin											
at birth	+	+	+	+	10/10	4/4	4/4	1/1	7/7	5/5	16/22
over abdomen ISP*	+	+	+	+	NA	4/4	4/4	1/1	7/7	NA	22/22
on dorsum of H-F**	+	+	+	+	10/10	4/4	4/4	1/1	7/7	5/5	22/22
Translucent skin	+	+	+	+	10/10	4/4	4/4	1/1	NA	5/5	NA
Craniofacial											
Microcephaly	-	-	+	+	NA	0/4	0/4	1/1	NA	4/5	NA
Large fontanelle	+	+	-	NA	NA	0/4	1/1	NA	NA	3/5	3/6
Droopy face	+	+	+	+	2/2	4/4	4/4	1/1	7/7	4/5	22/22
Broad forehead	+	+	+	-	2/2	4/4	4/4	1/1	7/7	5/5	NA
Maxillary hypoplasia	+	+	+	+	NA	4/4	4/4	1/1	7/7	3/5	22/22
Prognathism	+	+	+	+	1/2	4/4	4/4	1/1	7/7	1/5	22/22
Large protruding ears	+	+	+	-	NA	4/4	4/4	1/1	7/7	3/3	NA
Hyperextensible joints	+	+	+	+	10/10	4/4	4/4	1/1	NA	5/5	22/22
Intrauterine growth Retardation	+	+	+	+	NA	0/4	0/4	0/1	NA	3/3	18/20
Short stature	-	-	-	-	2/10	0/4	0/4	0/1	1/7	2/2	4/13
Mental retardation	severe	mild	severe	severe	NA	3/4	0/4	0/1	0/7	5/5	21/22
Speech delay	+	+	+	+	0/4	0/4	0/4	0/1	0/7	NA	3/3
Seizures	-	-	+	+	NA	0/4	0/4	0/1	NA	NA	NA
Athetoid Movements	-	-	-	-	NA	0/4	0/4	0/1	0/7	NA	3/22
Behaviour pattern	Self mutilism	Selective mutism	Self mutilism	Self mutilism	NA	NA	NA	NA	NA	NA	NA
Hernia	-	-	+	-	0/9	0/4	1/4	0/1	NA	1/3	11/22
Skeletal findings											
Hip dislocation	+	-	-	-	4/10	0/4	4/4	1/1	2/7	0/3	14/21
Fracture	-	-	-	-	9/10	3/4	4/4	1/1	5/7	NA	4/13
Vertebral	+	+	+	+	10/10	4/4	4/4	NA	NA	NA	1/5
involvement	+	+	+	+	10/10	4/4	4/4	NA	6/7	1/2	10/12
Osteopenia	+	+	+	+	NA	0/2	NA	NA	NA	3/3	6//9
Wormian bones	+	+	+	+	NA	NA	NA	NA	NA	2/3	NA
Clasped thumbs	-	-	-	+	2/10	3/4	NA	1/1	1/7	2/3	4/7
Scoliosis											
Brain anomalies		N			NA	NA	NA	NA	N		
Colpocephaly	+										2/13
Enlarged ventricle			+							1/5	
ACC***	+									2/5	8/13
Cerebellar hypoplasia				+							

*ISP: in sitting position, **H-F: hands and feet, ***ACC: agenesis of corpus callosum, N: normal, NA: data not available

Figure 3.2. Photographs of GO patients. Patient 505 at the age of 1 year (a), patient 501 at the age of 2 years (e) and patient 405 at the age of 8 months (i), with broad and prominent forehead, droopy face, sparse hair and translucent skin. Note long triangular droopy face, bulbous nose, large ears, hypoplasia of maxilla and prognathism that became pronounced with age and wrinkling of the skin on the dorsum of the hands and feet at the age of 4 years in patient 505 (b-d), at the age of 6 years in patient 501 (f-h), at the age of 3 years and 9 months in patient 405 (j-l) and patient 404 at the age of 16 years (m-o).

Figure 3.3. Radiographs of GO patients. They revealed generalized osteopenia on long bones; at the age of 2 months in patient 505 (a), at the age of 4 months in patient 501 (b), at the age of 8 months in patient 405 (c). Note mild platyspondyly or round vertebral body at the age of 2 months in patient 505 (d), at the age of 4 months in patient 501 (e), at the age of 8 months in patient 405 (f) and wormian bones in skull at the age of 4 months in patient 2 (g,h). Cranial MRI also showed agenesis of corpus callosum and colpocephaly (i) and cerebellar hypoplasia (j) in patient 505 and patient 404, respectively.

3.1.2. Motor Dysfunction, Intellectual Disability and Multiple Joint Contractures

A consanguineous family with twelve members afflicted with MDIDJC was studied (Figure 3.4). Blood samples were collected by Aslıhan Tolun and Sibel Uğur İşeri in our department and Dr. Elif Kocasoy Orhan in the Department of Neurology, Istanbul University Istanbul Medical School. Clinical findings are presented in Table 3.2. Examples of joint contractures in patient autopods are presented in Figure 3.5. Clinical examinations were performed by Elif Kocasoy and Dr. Piraye Serdaroğlu in the the Department of Neurology, Istanbul University Istanbul Medical School and Dr. Bülent Kara in the Department of Neurology, Kocaeli University Medical School.

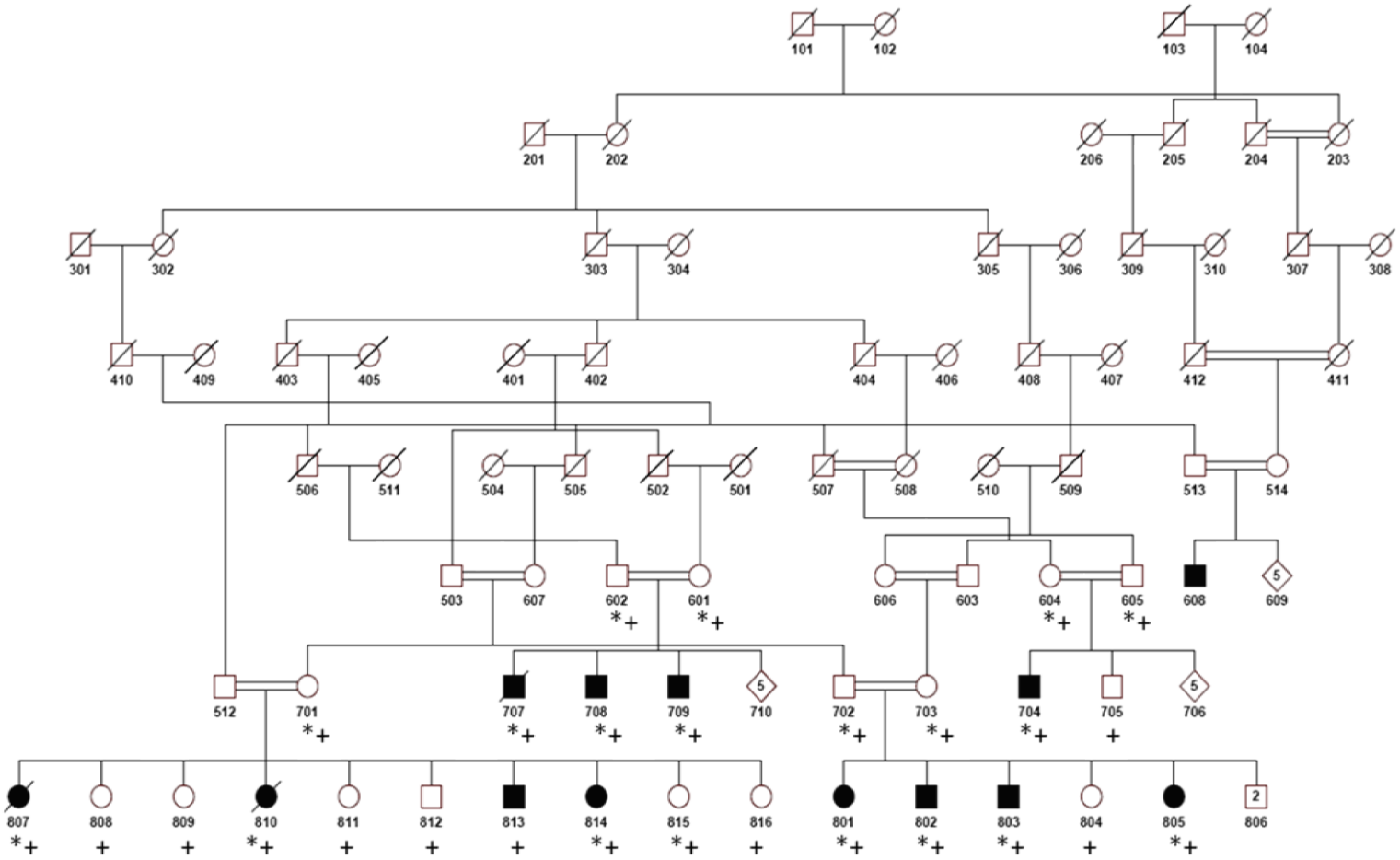

Figure 3.4. Partial pedigree diagram for MDIDJC family. Samples available for microsatellite genome scan are marked with a plus sign, and those for SNP genome scan marked with an asterisk.

Table 3.2. Clinical findings for MDIDJC Family

		Age (yrs) at		Clinical Features						
ID	**Sex**	**Exam.**	**Onset**	**Ability to walk/sit**	**Intellectual disability**	**FC[a]**	**CrCT[b]**	**EMG[c]**	**Dysphagia**	**Muscle Biopsy**
608	M	20	1	never walked/sat	moderate to severe	no	-	-	no	-
704	M	19	0.5	never walked	mild to moderate	yes	-	-	yes	-
708	M	22	2	never walked	mild	no	normal	normal	no	normal
709	M	18	1	never walked	mild	no	-	-	no	-
801	F	20	1	never walked	mild to moderate	yes	-	-	yes	-
802	M	17	1	never walked	mild	yes	-	-	no	-
803	M	6	1	never walked	mild	yes	-	-	no	-
805	F	4	2	never walked	mild	yes	-	-	no	-
807	F	22	2	never walked	moderate	yes	-	-	yes	-
810	F	15	1	never walked	mild	yes	-	-	yes	-
813	M	8	2	never walked/sat	moderate to severe	yes	-	-	no	-
814	F	10	2	never walked	mild	yes	-	-	no	-

[a]FC: Febrile Convulsion, [b]CrCT: Cranial computer tomography, [c]EMG: Electromyography.

Figure 3.5. Examples of joint contractures in MDIDJC patients. Age in years are indicated in brackets: **A.** Left 709 (18), right 708 (22) **B.** 805 (4), **C.** 805 (10)

3.1.3. Median Cleft Lip

A consanguineous family afflicted with median cleft lip was investigated. Blood samples from 17 family members were supplied by Dr. Metin Kerem (Figure 3.6).

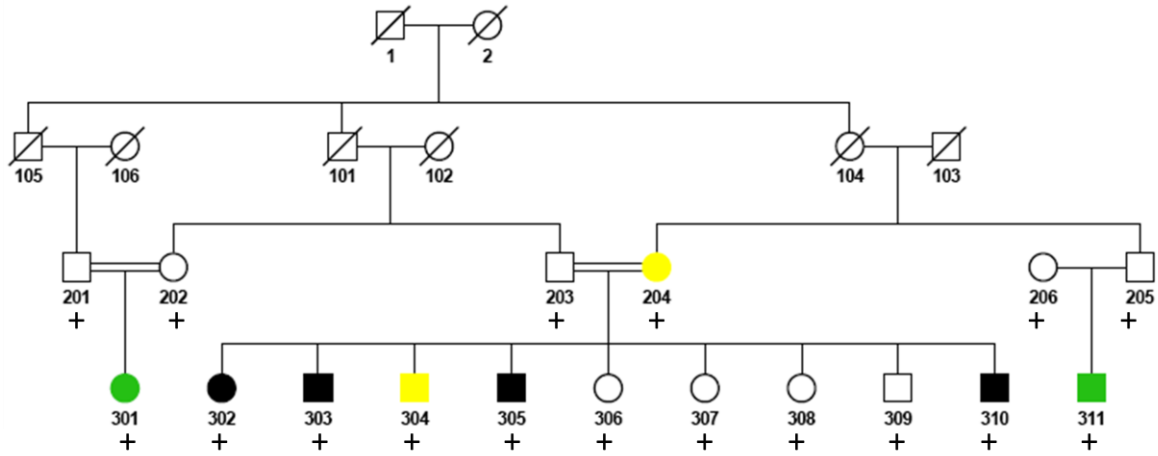

Figure 3.6. Partial pedigree of Median Cleft Lip family. Each color indicates a different clinical status: Black for affected phenotype, green minimal phenotype and yellow subclinical phenotype. DNAs available for the genome scan are marked with asterisk.

All affected individuals share the same phenotype: incomplete median clefting in upper lips (Tessier No:0) where muscle M. Orbicularis oris integrity is disrupted in the Cupid's Bow area, absence of philtral complex and median clefting in lower lips (Tessier No:30). The clefting in lower lip was limited to the vermilion, without significant muscle involvement. All affected sibs had a double labial frenulum between the lower lips and lower gingiva across the vestibular fold. (Labial frenulum is the small band of tissue that connects the underside of the tongue to the floor of the mouth, and gingival is the tissue of the jaws surrounding the bases of the teeth). In the upper lips, fusion of the labial mucosa with upper gingival was observed, resulting in a shallow or totally erased upper vestibular fold. The interdental distance between the upper incisors was increased. The same distance was even more increased in the lower incisors. Anterior teeth alignment was poor in individuals 302, 303 (Figure 3.7.A and B) and 305. Dental architecture of 310 was because of having less alteration of the interdental distances between incisors, as he was not in the age of permanent dentition yet. Palatal cleft involvement was not present in any of the members. A complete cranial CT scan performed for all four patients indicated no other cranial or maxillofacial abnormality. Mental status of all family members were normal, and no accompanying medical condition was detected. Minimal individual 311 (Figure 3.7.C) had an increased interdental distance between the lower incisors. Other minimal individual

301 (Figure 3.7.D) had a notch in her lower lip, similar to mother 204. Individuals 204 and 304 had the mildest form of cleft lip, and they were diagnosed as subclinical phenotype.

Figure 3.7. Examples of clefting patterns in MCL patients. Age in years are indicated in brackets: **A** and **B.** 303 (18), **C.** 311 (3), **D**. 301 (24).

3.2. Chemicals

All solid and liquid chemicals used in this study were purchased from Merck (Germany), Sigma (USA), Riedel de-Häen (Germany), Carlo Erba (Italy) or Biochrom (Germany), unless stated otherwise in the text.

3.3. Buffers and Solutions

All buffers and solutions were prepared in dH_2O unless stated otherwise.

3.3.1. DNA Extraction from Whole Blood

Cell Lysis Buffer	:	155 mM NH_4Cl, 10 mM $KHCO_3$ 0.1 mM Na_2EDTA (pH 7.4)
Nucleus Lysis Buffer	:	400 mM NaCl, 2 mM Na_2EDTA, 10 mM Tris (pH 8.2)
Proteinase K	:	20 mg/ml proteinase K
Sodium dodecylsulfate (SDS)	:	10 per cent SDS (w/v)
Ammonium Acetate	:	7.5 M CH_3COONH_4
Ethanol	:	Absolute ethanol
TE buffer	:	1 mM EDTA, 20 mM Tris-HCl (pH 8.0)

3.3.2. Polymerase Chain Reaction (PCR)

10X PCR Buffer A	:	20 mM $MgCl_2$, 500 mM KCl, 100 mM Tris-HCl (pH 8.3)
10X PCR Buffer B	:	20 mM $MgSO_4$, 100 mM KCl, 200 mM Tris-HCl (pH 8.8), 100 mM $(NH_4)_2SO_4$, 1 per cent Triton X-100
10X PCR Buffer C	:	20 mM $MgSO_4$, 100 mM KCl, 200 mM Tris-HCl (pH 8.8), 100 Mm

		$(NH_4)_2SO_4$, 1 per cent Triton X-100
5X Combinatorial Enhancer Solution (CES)	:	1 mg/ml BSA 2.7 M betaine, 6.7 mM dithiothreitol (DTT), 6.7 per cent dimethyl sulfoxide (DMSO)
$MgCl_2$	:	25 mM $MgCl_2$ (Roche, Germany)
dNTP	:	12.5 mM each of dATP, dCTP, dGTP and dTTP in dH_2O (Roche, Germany)
Betaine	:	5 M betaine (Promega, USA)

3.3.3. Agarose Gel Electrophoresis

Agarose	:	1.5 per cent agarose in 0.5X TBE buffer
NuSieve	:	2 per cent agarose-NuSieve (2:1) (FMC BioProducts, USA) in 0.5X TBE buffer
10X TBE Buffer	:	20 mM EDTA, 0.89 M boric Acid, 0.89 M trizma base (pH 8.3)
6X Loading Buffer	:	10 mM Tris-HCl (pH 7.6), 50 per cent Glycerol, 60 mM EDTA, 2.5 mg/ml bromophenol blue and/or 2.5 mg/ml xylene cyanol
Ethidium Bromide	:	10 mg/ml in dH_2O

3.3.4. Polyacrylamide Gel Electrophoresis (PAGE)

40 per cent Acrylamide (Stock)	:	40 per cent acrylamide-bisacrylamide (19:1)
8 per cent Instagel (Denaturing)	:	8 per cent acrylamide-bisacrylamide (19:1), 8.3 M urea in 1X TBE buffer
APS	:	10 per cent ammonium peroxidisulfate
TEMED	:	N,N,N,N-tetramethylethylenediamine
10X Sample Buffer	:	95 per cent formamide, 20 mM EDTA, 0.05 per cent xylene cyanol

3.3.5. Single Strand Conformational Polymorphism (SSCP) Gel Electrophoresis

40 per cent Acrylamide (Stock)	:	40 per cent acrylamide-bisacrylamide (37.5:1 or 50:1)
8 per cent Acrylamide (37.5:1, non-denaturing)	:	8 per cent acrylamide-bisacrylamide in 0.6X TBE buffer
Glycerol	:	5 or 8 per cent glycerol in gel solution

3.3.6. Silver Staining

Staining Buffer	:	0.1 per cent $AgNO_3$
Developing Buffer	:	1.5 per cent NaOH, 0.01 per cent $NaBH_4$, 0.015 per cent formaldehyde

Stop Buffer : 0.75 per cent $NaCO_3$

3.4. Kits

Table 3.3. Kits used, descriptions and manufacturing companies

Name	Used for	Company
Qiagen Taq PCR Core Kit with Q solution	Amplification of difficult DNA templates	Qiagen, USA
Dream Taq PCR Kit	Amplification of DNA templates	Fermantas, Canada
GC-Rich PCR System	Amplification of DNA templates with high GC content	Roche, Germany
QIAquick PCR Purification Kit	Purification of PCR products	Qiagen, USA
LightCycler 480 High Resolution Melting Kit	Heteroduplex analysis in LightCycler 480	Roche, Germany
LightCycler 480 ProbeMaster Kit	Relative quantification on LightCycler 480	Roche, Germany
MagNA Pure Compact RNA Isolation Kit	Isolation of RNA from a tissue	Roche, Germany
Improm-II Reverse Transcription System	Synthesis of cDNA from RNA	Promega, USA

3.5. DNA Molecular Weight Markers

pUC19 DNA/*Msp*I markers and 50 bp DNA ladder were purchased from Fermentas (Lithuania) and Roche (Germany), respectively.

3.6. Oligonucleotide Primers and Probes

Oligonuclotide primers used in this study were custom synthesized and purchased from Massachusetts General Hospital (MGH) DNA Synthesis Core (USA). Oligos were dissolved in 1000 µl dH_2O, and 10 µM dilutions were used for PCR reactions.

Intron-spanning TaqMan probes and suitable oligos for genes *HPRT* and *ERLIN2* were designed at Universal Probe Library (Roche, Germany) using software ProbeFinder

version 2.35. The oligos were purchased from MGH DNA Synthesis Core (USA) and the probes from Universal Probe Library (Roche, Germany).

3.7. Equipment

Autoclave	:	Midas 55 (Prior Clave, UK) AMB430T (Astell, UK)
Balance	:	Electronic Balance (Precisa, Switzerland)
Centrifuges	:	MiniSpin Plus (Eppendorf, Germany), Universal 16R (Hettich, Germany), Allegra X-22R (Beckman Coulter, USA) J2-MC (Beckman Coulter, USA)
Deep Freezers	:	-20^{o}C (Bosch, Germany), -20^{o}C (AEG, Turkey), -80^{o}C Ultra Freezer (Thermo Scientific, USA)
Documentation System	:	GelDoc Documentation System with Quantity One 1-D Analysis Software (BioRad, USA)
Electrophoresis Equipment	:	Horizontal DNA Electrophoresis Gel Box (Bio-Rad, USA), Primo Minicell Horizontal Gel System (Thermo Scientific, USA), Sequi-Gen Sequencing Cell (Bio-Rad, USA), DeCode Universal Mutation Detection System (Bio-Rad, USA)
Incubator	:	Orbital (Gallenkamp, Germany)
Magnetic Stirrer	:	MR3001 (Heidolph, Germany)

Micropipettes	:	Pipetman (Gilson, France)
Minishaker	:	Rotamax 120 (Heidolph, Germany)
Ovens	:	Heraus (Germany), EN 400 (Nüve, Turkey)
Power Supplies	:	Power Pac Model 3000 (Bio-Rad, USA) Fotoforce 250 Electrophoresis Power Supply (Fotodyne, USA), P250A Power Supply (Sigma-Aldrich, USA)
Refrigerator	:	4^{o}C (Arçelik, Turkey)
Spectrophotometers	:	8453 UV-Visible Spectrophotometer (Agilent, USA), NanoDrop 1000 (Thermo Scientific, USA)
Thermal Cyclers	:	MyCycler (Bio-Rad, USA) PTC-200 (MJ Research, USA) Techne (Progene, UK) LightCycler 480 (Roche, Germany)
Transilluminator	:	Fluorescent Table (Consort, Belgium)
Vortex	:	Reax vortex mixer (Heidolph, Germany) Lab Dancer Vario (Roth, Germany)
Water bath	:	Grant LTD 6G Thermostatic Water Bath (Grant, Germany)
Water Purification System	:	Ultra Pure Water Purification system (Watech, Germany)

3.8. Electronic Databases

Names, addresses and descriptions of the databases used in this study are given below.

- NCBI genome resources
  http://www.ncbi.nlm.nih.gov/genome/guide/human/
  A database for genomic maps, chromosomes and sequence information of a variety of genomes
- UCSC Genome Browser
  http://genome.ucsc.edu/
  Reference sequence data and genomic maps of a variety of genomes
- Tandem Repeats Database
  http://tandem.bu.edu/cgi-bin/trdb/trdb.exe
  A database on tandem repeats in genomic DNA and tools for analysis of tandem repeats in a particular DNA sequence
- Biology WorkBench
  http://workbench.sdsc.edu/
  Web-based tools for analysis of nucleic acids and proteins.
- OMIM-Online Mendelian Inheritance in Man
  http://www.ncbi.nlm.nih.gov/sites/entrez
  A database of human genes and phenotypes
- NetGene2 Server
  http://www.cbs.dtu.dk/services/NetGene2/
  A web-based tool for predicting splice sites in human, *C. elegans* and *A. thaliana* genomes
- Human Splicing Finder Version 2.4
  http://www.umd.be/HSF/
  A bioinformatics tool to calculate the consensus sequences of potential splice sites and to predict the possible effects of mutations on splicing process
- Optimase ProtocolWriter
  http://www.mutationdiscovery.com/md/MD.com/screens/optimase/OptimaseInput.html?action=none
  A tool to generate optimum PCR protocols

- The Biology WorkBench
  http://workbench.sdsc.edu/
  A web-based tool for storing and analyzing protein and DNA sequences.
- ExonPrimer, Institue of Human Genetics, Munich Technical University
  http://ihg2.helmholtz-muenchen.de/cgi-bin/primer/ExonPrimerUCSC.pl?db=hg18&acc=uc002uhn.1
  A tool for designing intronic primers for PCR amplification of exons using Primer3.

4. METHODS

4.1. DNA Extraction from Peripheral Blood Samples

Genomic DNA was extracted from peripheral blood samples. Blood drawn was immediately transferred into a sterile tube containing K_2EDTA as anticoagulant. Thirty ml of cell lysis buffer was added to 10 ml of blood sample, and the mixture was kept for 15 minutes (min) on ice for the plasma membrane to lyse. The samples were centrifuged at 5000 revolution per minute (rpm) for 10 min, and the supernatant containing cell debris was discarded. The pellet containing leukocyte nuclei was washed by suspending in 10 ml of cell lysis buffer and centrifuging for 10 min. The supernatant was discarded, and the nuclei were suspended in 3 ml of nucleus lysis buffer by vortexing until the pellet was entirely dissolved. After the addition of 50 µl of Proteinase K (20 mg/ml) and 80 µl of 10 per cent SDS, the sample was mixed gently and incubated either at 37°C overnight or at 56°C for 3 hours (hr) in order to allow the digestion of nuclear proteins. After the addition of 2.8 ml 9.5 M NH_4Ac, the tube was shaken gently to salt out the proteins and centrifuged at 10,000 rpm for 25 min at room temperature to get rid of them. After the transfer of the supernatant into a clean 50 ml Falcon tube, two volumes of ethanol were added for the purpose of precipitating out the DNA. DNA precipitate was fished out carefully with a micropipette tip and transferred into a 1.5 ml tube. It was air-dried to get rid of the residual ethanol before dissolving in 500 µl of TE buffer. It was stored at -20^{o}C.

4.2 Linkage Analysis

4.2.1 Genome Scan

4.2.1.1. Geroderma Osteodysplastica

Genome scan was performed at NHLBI Mammalian Genotyping Service using Marshfield Screening Set 13 (Contract Number HV48141) consisting of 405 microsatellite markers spanning both autosomal and sex chromosomes with an average spacing of 10 centimorgans (cM). The genotyping error rate in the analysis was 0.5 per cent, as estimated

by blindly typing some control DNA samples. Fifteen to 30 μg of DNA from each individual was supplied to the service for the amplification of microsatellite loci with fluorescently labeled primers. The allele sizes were detected by a custom-built **sca**nning **flu**orescence **d**etector (SCAFUD), using its own software. The genotyping results were obtained in LINKAGE file format.

4.2.1.2. Motor Dysfunction, Intellectual Disability and Multiple Joint Contractures

Initial genome scan was performed at NHLBI Mammalian Genotyping Service using Marshfield Screening Set 13 (Contract Number HV48141) with 405 microsatellite markers spanning both autosomal and sex chromosomes with an average spacing of 10 cM. The same method described in Section 4.2.1.1 was used for detecting allele sizes. The results were obtained in the same format.

A second genome wide scan was performed at deCODE Institute with Illumina Human 370-Duo Beadchip including 370,000 SNP markers at a median marker spacing of 5.0 kb.

4.2.1.3. Median Cleft Lip

The genome scan was performed at deCODE Institute with Illumina Human 370-Quad Beadchip for 17 family members.

Later, one of the affected siblings, 305 was subjected to a denser genome scan with 610K Illumina Bead Chip including approximately 610,000 SNP markers at Yale University. BeadStudio v.3.2 Genotyping Module was used to analyze this data for homozygous regions. Perl Combined_CNV program was used to analyze CNVs.

4.2.2. Linkage Analysis and Homozygosity Mapping

Marshfield Genetic Map was used in all of the linkage analysis. Illumina Genetic Map was used for the analysis of genotyping results with SNP markers. All linkage analyses were performed on easyLINKAGE package (version 5.08), which houses multiple

linkage programs. The programs and usage purposes are as follows: Pedcheck for detection of genotyping errors, SuperLink v1.6 for calculation of two-point parametric lod scores, Allegro for calculation of both two-point and multipoint parametric lod scores as well as construction of haplotypes in small families (bit size ≤19), SimWalk v2.91 for calculation of parametric lod sores and construction of haplotypes in complex families (bit size >19) and GeneHunter for calculation of parametric lod sores and construction of haplotypes in small families (bit size ≤19). For all models, equal recombination frequencies for males and females, equal frequencies of marker alleles and a disease allele frequency of one in 10,000 were assumed.

Homozygosity mapping was performed by using program Homozygosity Comparison in Excel (HCiE) developed in our laboratory (Cetinkaya, 2010).

4.2.2.1. Geroderma Osteodysplastica

SimWalk v2.91 was used for multipoint lod score calculations and haplotype construction, whereas Superlink was used for two-point lod score calculations from raw data. The assumed inheritance model was autosomal recessive with full penetrance. The physical and genetic positions of the markers were updated from the sequence tagged site (STS) map of GenBank (NCBI Build 36.3). Candidate loci were determined by either lod score analysis or haplotype inspection. Those regions were fine-mapped with additional microsatellite markers that were either flanking or located within the locus. The genome assembly of GRCh37 was utilized for marker positions for chromosome 17, which contained the final candidate locus.

4.2.2.2. Motor Dysfunction, Intellectual Disability and Multiple Joint Contractures

Prior to this work, genotypes generated using microsatellite markers had been analyzed in an attempt to identify a candidate locus. Chromosomes 6, 8, 9, 12, 20 and 22 as well as PAR regions had been investigated with additional microsatellite markers by Umut Dursun. After his work, a further analysis was performed at chromosomes 6 and PAR regions, and chromosome 10 was analyzed with additional microsatellite markers. Since a candidate region could not be identified, a whole-genome scan with SNP markers was

performed for the family for this study. A fully penetrant recessive inheritance model with equal recombination frequencies for males and females, equal frequencies of marker alleles and a disease allele frequency of 0.001 were assumed for two-point and multipoint linkage analyses. No parental consanguinity could be introduced to the program due to the limitations in its capacity.

In addition to linkage calculations, the homozygous regions shared by the affected but not the healthy siblings were determined for each chromosome by using program HCiE in order to verify homozygosity at the regions that yielded high lod scores, as well as to detect any candidate locus that had possibly escaped detection by lod score analysis. In addition, new microsatellite markers were used for genotyping to ascertain homozygosity at the regions and to narrow down the candidate locus.

After the identification of a candidate locus, lod scores were calculated by utilizing the data generated with microsatellite markers. The previous microsatellite data was also included into the analysis. This time, parental consanguinities could be introduced to the programs.

4.2.2.3. Median Cleft Lip

Multipoint lod scores were calculated assuming three different models: a recessive model with full penetrance, a dominant model with full penetrance and a dominant model with 80 per cent penetrance.

For a recessive model with full penetrance, multipoint lod scores were calculated first only for four affected siblings and their parents, because their clinical features were the most severe (Figure 4.1.a). The parents were introduced as first cousins. The loci that yielded lod scores >2 were taken into consideration, and haplotypes were constructed. In addition, two minimally affected cousins were also included in the calculations but the parents of the affected sibs were not introduced (Figure 4.12.d). For the dominant model with full penetrance, in addition to the affected sibs, unaffected sibs 308 and 309 and subclinical sib 304 were included in the linkage analysis, and the status of subclinical

mother 204 and subclinical sib 304 were introduced to the program as affected (Figure 4.1.b). Haplotypes were constructed and investigated for loci yielding lod scores >1.

For the dominant model with 80 per cent penetrance, in addition to the four affected sibs, unaffected sibs 306, 308 and 309 were included in the analysis and the father and mother were introduced to the program as unaffected (Figure 4.1.c). The parental consanguinity was not introduced to the program. For loci yielding lod scores >1, haplotypes were constructed for all family members and analyzed.

The family pedigrees utilized in lod score analysis are given in Figure 4.1.

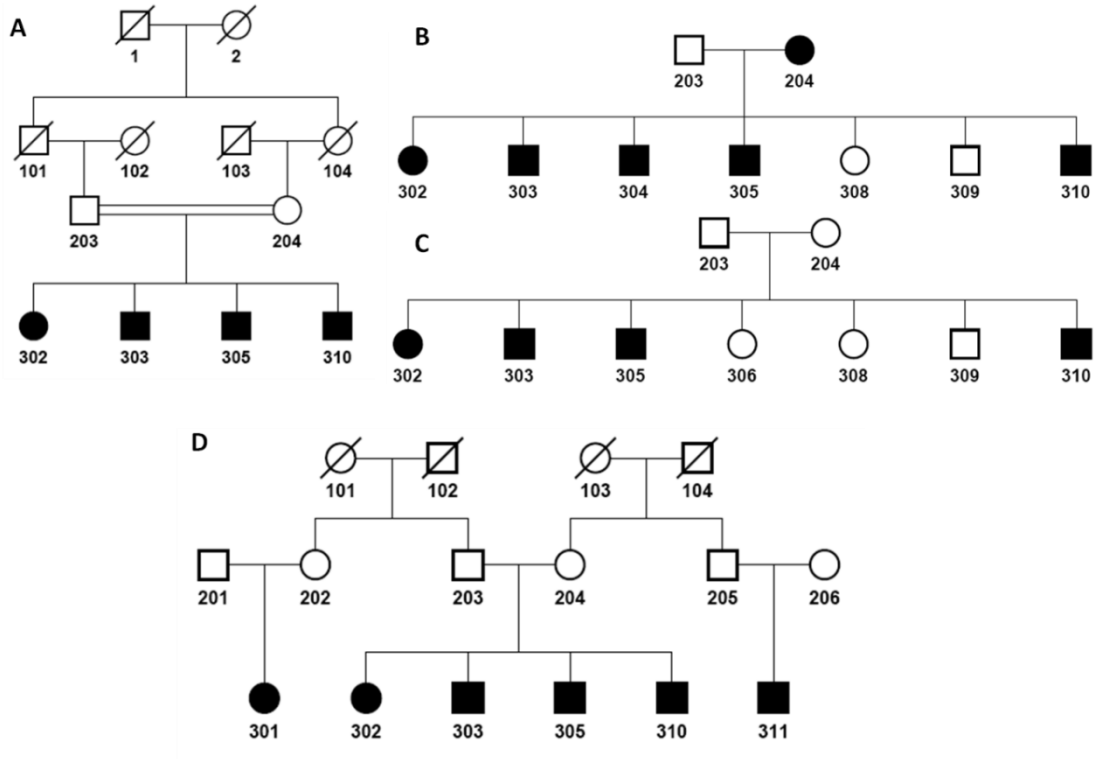

Figure 4.1. Partial MCL family pedigrees used for multipoint lod score calculations.

All the deletions and duplications detected in 305 utilizing the results of the denser SNP scan were investigated to find out whether they lied within the homozygous regions shared by all affected sibs or at any loci that yielded relatively high lod scores.

One deletion detected in all affected individuals was within a region of shared homozygosity at 1p31.1 and thus assumed to be associated with the disorder. In order to

determine its exact length, new primer pairs located both upstream and downstream of the deletion were utilized. Information on the primers is presented in Table 4.1.

Table 4.1**.** Primer pairs used for detection of the exact length of the deletion at 1p31.1 in MCL.

Marker ID	**Physical Position (Kb)**	**Product Size (bp)**	**Primer Sequence (5' → 3')**
YD_del1	75243	378	F: GCTGAATCCCCAAAATAGCA R: GGAGGAAGAGGAGCTGTGAA
YD_del2	75523	423	F: GTGCAGCTACCGATCTCACA R: TCCAAGGATATGCCCAAGAG
YD_del4	75246	183	F: CCCACTCTCTGTGCTTCTCC R: AAGGTGCTGCTGCTGGTAAT
YD_del5	75522	609	F: AGGGGAAGAAGGAAAATGGA R: CACGTTTTGTGAACCAAGGA
YD_del6	75.247	209	F: TCTCTCCCACCCTTTTACCA R: GCTTTAACTGCACCGTCCTT
YD_del7	58.62	309	F: ATGAAGGATGGAGTGAGAAGGT R: CCTGACATATTGCTGCTGTTG

4.2.3. Fine-mapping of Candidate Loci

Candidate regions determined by lod score analysis or haplotype inspection were fine-mapped by genotyping with additional microsatellite markers that either flanked the regions or were located within them (Table 4.2). The markers were either reported in databases or designed in this study, around tandem repeats found through Tandem Repeat Finder Program. The amplification conditions for the primers were determined through the guidance of website mutationdiscovery.com.

PCR for each marker was carried out in a total volume of 25 µl including 1X PCR buffer, 0.4 µM of final concentration of each primer pair, 0.2 mM of each dNTP, 20-100 ng of genomic DNA, 0.2 U Taq DNA polymerase and sufficient dH_2O to adjust the volume. The PCR conditions were as follows: an initial denaturation step at 94°C for 3 min, followed by 30-35 cycles of 30-45 sec denaturation at 94°C, 30 to 45 sec annealing at appropriate temperature and 45 sec to 2 min elongation at 72°C, and a final extension step

for 6 min at 72°C. For regions that were difficult to amplify, Betaine together with DMSO with final concentrations of 1.3 M and 1.3 per cent, respectively, were included in the reaction.

The extent of amplification and purity of PCR products were checked on 1.5 per cent agarose gels freshly prepared with 0.5X TBE buffer and 0.5-1 μg of ethidium bromide per 1 ml of agarose solution. Five μl of the product was mixed with 1 μl of 6X loading dye. The duration of electrophoresis was adjusted according to the length of the products. The products were visualized under UV light. Then they were also run on a polyacrylamide gel and visualized by silver staining in order to observe the alleles. Non-informative markers were not included in the haplotypes or in lod score analysis. Microsatellite markers used in the study are given in Table 4.2.

Table 4.2. Microsatellite markers used in this study, their positions and oligo primers. Those marked with asterisk were designed using tandem repeat database.
A) GO, B) MDIDJC, and C) MCL.

A)

Chromosome	Marker ID	Physical Position (Mb)	Product Size (bp)	Primer Sequence (5' → 3')
1	D1S168.44M*	170.18	148	F: AGCCAGCACAGTGTGTCAAT
				R: TCCTAAGAACAGCAGCTGACA
	D1S452	170.52	217-227	F: TAATGGGTTCAGTGGACCTT
				R: TGCAGTTCCATATTCCAGGT
	D1S168.82M*	170.55	211	F: GTGGGGGAATAGGGATGATT
				R: GCTGACAAATGCACGAGAGA
5	HUMUT5428	58.18	297	F: GCCTGAAACTGCTGTTCTTC
				R: GCTCCCTCCATTTTGTCCC
	D5S612	58.32	209	F: CCACAACCCAGTCTTTAGG
				R: ATGGCTGGTTGTATTTTCAGA
	D5S2091	58.62	223-241	F: GCATTTGTCATGTGCCA
				R: GGTATTTCATTCACAGCCAGTC
	D7S2474	0.98	135-151	F: GTAGGAGGATCACTTGAGCC
				R: AGGTCATGTCTCCATATTGTG
7	D7S14.18M*	14.21	138	F: CCTGGGCAACAAGAGAGAAA
				R: TTGCTGCCTCACTCAGTCAC
	D7S1810	22.71	225-226	F: CCACCTGTTAAGTGGAGGTG
				R: TCATTGGTCTGTCCTTTCGT
	D7S1791	25.14	160-184	F: GAGTTCAAGAATGCAGTGAGC
				R: GGTGGCAGGCTAACTTGTTA
	D7S26.95M	26.98	187	F: CAGCCTCCCTGCTAGTCATT
				R: CTCAGTGGCATGGGACTTTT
	D7S1808	28.04	112	F: GCAAAGTAACAAACACATC
				R: CCAAATAAGACTCAGGAC

Table 4.2. Microsatellite markers used in this study, their positions and oligo primers. Those marked with asterisk were designed using tandem repeat database. A) GO, B) MDIDJC, and C) MCL (continued).

Chromosome	Marker ID	Physical Position (Mb)	Product Size (bp)	Primer Sequence (5' → 3')
7	D7S2515	28.76	116-140	F: CACACATTCAGGACACCAG R: AGATTTATTAACTAGACCCCAGG
	D7S1830	51.75	200-228	F: GTACATGATGGGCTGTCCTC R: GATACATACTGCCAATAAATCACA
9	D9S753	96.63	286	F: ACAGAGCAAGGTTGCCCAG R: TCCACTCAGCACCAACAGT
	D9S272	101.75	195-211	F: ACTGAACTCCAGCATGGG R: CTCTCCTACAGGGAAACCG
	D9S909	105.80	186	F: TGGAAAATTGCATTTCCTGT R: AAAATGTATCATACATGGCATACG
	D9S934	121.10	206-230	F: TTTCCTAGTAGCTCAAGTAAAGAGG R: AGACTTGGACTGAATTACACTGC
10	D10S507	31.08	148	F: GGGTAATAAGAGCAAATCTGT R: CCTTCACTAAAGCAATAAGGA
14	D14S55	84.68	123-124	F: AGAGAAGTTAAAAGCATTGC R: AGAACTGTTACCTGGAGGC
	D14S86.85M*	87.78	178	F: ACAGCCTGTTGTGGGACTTC R: TCAGTGCAGTTGGGCAATAG
	D14S87.05M*	87.98	184	F: TCCACAACACATGGGGATTA R: GCAGGCAGTTATCAAGGGAC
	D14S87.22M*	88.15	140	F: TGATGTGAACCTCTCATGGC R: AGCAGCAGTCACAGTGGAAA
	D14S87.63M*	88.56	166	F: TGCAAAGGAGACTGGGAAAT R: AGGGACTGCTACCTCTTCCC
	D14S87.88M*	88.81	268	F: ACTGAAATCCCAACCAGGAA R: AGCCTGCAGTTAGCCAAGAG
	D14S543	104.59	246-272	F: ATGTGGGAAACAGACTCAG R: ATTTGGATTATTTAGAATTCCC
16	D16S3022	28.32	235-245	F: ATCTGGGGCTGCATGT R: AGCTATCGTGCCTGGC
	D16S475	34.71	160-189	F: GGTTGACAGAGTGAGACTC R: GGAACAGAAAATACTGCACG
	D16S682	49.99	292	F: TGGGTGACAGAGTAAGACCT R: ATCCACAGCCCACACTTAC
	D16S3396	51.19	138-157	F: AGAAGATTCACTTGGACCCA R: CAGAAAATGGAGGGTAGCAA
	D16S3137	53.68	217-237	F: GCAAAGAATAATTGCACATATACG R: AGTACAAAGAGATCCCCTGTAAC
	D16S673	56.96	319	F: AGGATCGCTCAAGGCCAGG R: CGAACAGGGAAGCCCAAGC
	D16S3398	63.80	190-214	F: AAGATGTGTGGGACTGCATT R: ACACCACAGGCTTACCATGT
	D16S64.94M*	66.38	162	F: TGGGCGACAGAGGTAGACTC R: GCAAATCTGGGGACATCACT
	D16S2642	74.01	198	F: CAGTGCAGGAGAGAGCCT R: GCAGCTTCAGGTGTTTTCTTT
	D16S74.70M*	76.15	191	F: TACTCAGAGGCTGAGGCAGG R: TGCAGGCATCAGAGTGTTTC
	D16S79.50M*	80.94	174	F: GCACCATTACACTCCAGCCT R: TTCATTTGGGGACAATGGAT

Table 4.2. Microsatellite markers used in this study, their positions and oligo primers. Those marked with asterisk were designed using tandem repeat database. A) GO, B) MDIDJC, and C) MCL (continued).

Chromosome	Marker ID	Physical Position (Mb)	Product Size (bp)	Primer Sequence (5' → 3')
17	D17S1290	56.33	170-210	F: GCCAACAGAGCAAGACTGTC
				R: GGAAACAGTTAAATGGCCAA
	D17S1881	65.28	216-230	F: CCCAGTTTAAGGAGTTTGGC
				R: TAGGGCAGTCAGCCTTGTG
	D17S2195	75.89	173-188	F: AAATGTCACTTTGCCAGAGG
				R: GCAAACCCTAAATGCTCAAA
	D17S674	76.31	124	F: ACACAGGGCGAGGCTCTGT
				R: CAGAAGGGATGGAAGGGCAA
	D17S74.11M*	76.60	174	F: GGAGAAGCTCTTTAGCGGGT
				R: CAGCAGGTCACAGATGCAGT
	D17S1847	77.02	144-164	F: GATCACCAGGAACACCC
				R: TCTTCAGAGCTTGCCAG
	D17S836	77.30	176	F: CTTCATGTTCCTTCCCTCAT
				R: GTACGTGTGTGTATGTACCTGC
	D17S1822	77.79	129-135	F: CAGGCATCTGTAATGGACCC
				R: AACCGAGCCTAGGACTCC
	D17S76999K*	79.39	207	F: CAAATTGATCAGGGAGGGTG
				R: AGCTCACCCGTCTTCGTG
	D17S668	80.03	151-174	F: TGACAGAGCGAGACCCTGC
				R: GAACGGGATTGGTTATACTAATGTC
	D17S78612K*	81.02	183	F: CAGGAGAATGGTGTGAACCC
				R: TCGCATCGCTATCCAGAAAT

B)

Chromosome	Marker ID	Physical Position (Mb)	Product Size (bp)	Primer Sequence (5' → 3')
6	D6S309	8.22	254-272	F: TTGCAGTGAGCCGAGATTG R: CTTGTGCGAATGAACACCG
	D6S394	26.14	108-338	F: GGCCAACATCTGAAACTCC R: GTGGTAATGGAACCTCCCA
	D6S1680	39.20	176-198	F: AAAATTCCACCCCCGC R: CCATCTCCCCAGCAGAC
	D6S1658	64.35	183-221	F: CACCATTGCACTCCAGC R: AACCTCTTTGGCCTTTGATA
8	D8S37.52M*	37.40	191	F: CAACAGAGGGAGACCCTGTC R: AGGGAGAACCAGTGGGAGTT
	D8S33.70M*	33.58	231	F: TTCTCTTGGGGTTTGGATTG R: CCCAGTTCCTGAAGAGCAAG
	D8S34.17M	34.05	235	F: CCAAGATTTCCTCCCCTCTC R: AGCCAAGTGTTGACTGGAGG
	D8S38.14M	38.02	258	F: TTTGGGGTCGTACTGGTCTC R: TTTACTGTCTGCTCCCCTCC
10	D10S1243	32.26	181-229	F: GCAATGTGGACAGTGAGACA R: CCCAGTTCCTGAAGAGCAAG
	D10S1217	36.16	159-175	F: GGGTTAAATTTGGGAGCACT R: TGGGCTGATTATTCGCATAT
PAR REGIONS	DXYS-9	X: 0.47, Y: 0.42	180	F: GTATTCCCTTTCTTGCCTGC R: ATATGGGCTACATTCACGGC
	DXYS57547K*	X: 155.03, Y:59.14	106	F: AGATCTTGCCATTGCACTCC R: TGTGACTCTGGAGTTGAGGC

C)

Chromosome	Marker ID	Physical	Product	Primer Sequence (5' → 3')
1	D1S2137	68.72	245-246	F: ACATCTTTGGTTTGGATAGATG R: CAAAACTGCACATTTTGCAC
	D1S1585	81.90	158-174	F: TAGGCAAATAATAAAATTCTAACCA R: GACCCTGTCTCAAAAAAAACA
	D1S247.135M*	249.17	232	F: AATAATGCCACAACCAACCC R: GCCAGGCCATACAGATCTCA

4.2.4. Denaturing Polyacrylamide Gels

Sequi-Gen GT (BioRad, USA) nucleic acid electrophoresis system was used to resolve the alleles of microsatellite markers. Instagel was cast in either a 21 x 40 cm or 38 x 30 cm sequencing apparatus assembled with 0.4 mm spacers. Thirty five ml of instagel solution with 250 µl of 1 per cent APS and 25 µl of TEMED was used for the first apparatus, whereas 50 ml instagel solution with 350 µl of 10 per cent APS and 35 µl of TEMED were used for the latter one. The gel was left to polymerize for at least 1 hour. Running buffer (TBE) was heated in microwave oven to heat later the gel to 40-45°C. Denaturing instagel was used for this purpose, which was initially prerun for 15 min in order to facilitate the gel temperature to rise to 40-45°C. PCR products were mixed with 10X denaturating dye in a minimum 1:2 ratio in volume and denatured at 95°C for 5 minutes. A constant power of 35 W for the shorter gel and 60W for the longer one was applied for electrophoresis. Running time was adjusted according to the size of the PCR products.

4.2.5. Silver Staining

DNA fragments/marker alleles resolved on page gels were visualized after staining with silver nitrate. The glass plates were separated carefully in order not to tear the gel. The gel was transferred to staining buffer with the help of a piece of filter paper. After allowing to stain for 10 min in the buffer, it was transferred to developing buffer and soaked until bands could be visualized. If this procedure was not sufficient to make the bands apparent, it was repeated after rinsing the gel thoroughly with distilled water.

4.3. Candidate Gene Approach

Best candidate genes residing at the candidate loci were selected on the evidence for gene function, its expression pattern and findings obtained from animal models. Moreover, the function of the genes identified for similar diseases and genes expressed in the tissues primarily affected from the disorder were taken into consideration.

Direct sequencing of PCR products, Single Strand Conformational Polymorphism (SSCP) analysis and High-Resolution Melting Curve (HRM) assay were the mutation detection methods used in this study.

4.3.1. PCR Amplifications

All regions to be analyzed were first amplified by PCR. Primers flanking exonic regions and splice junctions in candidate disease genes were designed using Primer 3 software. PCR uniqueness was checked with *in silico* PCR at UCSC database and/or NCBI.

Primers were designed for candidate genes *P4HB, RFNG, SECTM1* and *PYCR* for GO, *PROSC, BRF2, RAB11, FIP1* and *ERLIN2* for MDIDJC and *NEGR1, LHX8* and *LOC646556* for MCL. For *P4HB*, primers for amplifying a part of the predicted regulatory region were also designed. PCR protocols were described above in Section 4.2.4. Primer sequences and optimum PCR conditions are given in Table 4.3.

Additionally, after the identification a deletion for MCL in affected siblings, new primers were designed to identify deletion break points. The sequences of the primers are given in Table 4.4. Primers YDdel_6-F and YDdel-7 were used together to amplify across the deletion breakpoints in one of the patients. Then the product was sequenced, and the deletion breakpoints were identified. For a population scan, a primer pair flanking the deletion was designed: YD_DEL_POP (F:AAGGATAGTCAAGTTTCACCAGAA and R:TGTTTGTTTTGTCATCTGTTTCA). The region was amplified by PCR in all MCL family members.

Table 4.3. Sequences, PCR product sizes and PCR conditions for primer pairs designed to amplify candidate genes.

Region	Primer Name	Primer Sequence (5' → 3')	Product Size (bp)	Buffer and Additives	Annealing Temperatures (°C)
GO					
P4HB					
Exon 1	P4HB17ex1	F: AGGAGCGTTTCCGAATCC R: TGCCTGCGTCCCAAGAG	472	Buffer A + 1.3M Betain + 1.3 per cent DMSO	Touchdown 65 →55
Exon 2	P4HB17ex2	F: GCACTGCTGAGGGATCAAG R: GCTCAGACAGCTGCCCC	360	Buffer A + 12 per cent DMSO	59
Exon 3	P4HB17ex3	F: CTGGCAGAGAGCAGAGACG R: CAGGCTGTGGACCCCTC	286	Buffer A	56.2
Exon 4	P4HB17ex4	F: TACAGGGTCTGCCCTACTGC R: ATAAGGAGAGCAACGCCAC	281	Buffer A	56.2
Exon 5	P4HB17ex5	F: CCCACGTCCAGGGAGAC R: GCAGTGGTGACCGGGAG	264	Buffer B	59
Exon 6	P4HB17ex6	F: CAGCGTCTGACATTGGAGG R: ACACTTGTCACCTCGGGAAG	285	Buffer A	56.2
Exon 7	P4HB17ex7	F: GTCTGCTTCCGAGCAAAGTC R: CACTGAGAGCCCAGAGACC	355	Buffer A	56.2
Exon 8	P4HB17ex8	F: GGTTGGGGAGCTCTGTGG R: CAGGAGTCTGCCTACCTTGC	253	Buffer A	56.2
Exon 9	P4HB17ex9	F: TCCTGGGGAAGCGTCTG R: CTCCTTCCAGAGAGGCACC	333	Buffer B	59
Exon 10	P4HB17ex10	F: TTCTCTAGGGAGGAGGAGCC R: AGTGGGCATGTCCCGTG	237	Buffer A	Touchdown 65 →55
Exon 11.1	P4HB17ex11.1	F: GTGTGAGCAGTGTGGGGTG R: GAGACTCCGAACACGGTAG	476	Buffer B	59
Exon 11.2	P4HB17ex11.2	F: CCCCGTCTCTTCCTTCTG R: CCACCAGCTCCTCTTCCAG	422	Buffer A	59
Exon 11.3	P4HB17ex11.3	F: TGACTGATCATGGCTCTTGC R: TAACCCCACTAAGGCCTGG	448	Buffer A	Touchdown 65 →55
Promoter_1	P4HB_PRO1	F: GGCAAGGATCTCCCCTAGAC R: TGAAGGGCTCCCTTGCTG	521	Buffer A	Touchdown 65 →55
Promoter_2	P4HB_PRO2	F: GTCGATCCTGTTCTTCTCGC R: GATTTATAAAGGCGAGGCCG	498	Could not be sequenced	-
Promoter_3	P4HB_PRO3	F: CATGTCGGACACGGATCA R: TAAACTGGGAACTCCTCCCC	518	GC Rich Kit	Touchdown 65 →55
Promoter_4	P4HB_PRO4	F: TTCTAATTGGTGGCTTTCGC R: AGCCCCATTCTCCTAACCAC	500	Buffer A	58
Promoter_5	P4HB_PRO5	F: GTCACGCGAGACACTCACC R: CAGGTGGACTGGCCATATTT	485	Buffer A	Touchdown 65 →55
RFNG					
Exon 1-2	RFNG_EX1/2	F: CCGCTGCGTTCTTAAAGG R: GCTTCGGAGCGAGAAAGG	621	Q-Solution	Touchdown 65 →55
Exon 3-4	RFNG_EX3/4	F: ACAGGCCTTACCCCAACC R: TTCTCAAGCCAGCTTTCCAC	518	Buffer A	Touchdown 65 →55
Exon 5-6	RFNG_EX5/6	F: CCTGGGTGGGATCTCCTAAG R: AATCCCACCTGCCTGCTC	553	Buffer A	Touchdown 65 →55
Exon 7	RFNG_EX7	F: TTTCCAAGCCTGGCCTC R: GGGTAGAGGGAGCTGATGC	288	Buffer A	Touchdown 65 →55
Exon 8.1	RFNG_EX8_1	F: CCCCGCTTCTCTCTCCG R: GGGCCTGAGTCCCACTG	641	Buffer A	Touchdown 65 →55
Exon 8.2	RFNG_EX8_2	F: GGCTCCATTACCTGTTGCTG R: GAGCCTTCCTGGGGTAGAAG	583	Buffer A	Touchdown 65 →55
SECTM1					
Exon 1	SECTM1 _EX1	F: *GGGTCCAGCTCACTCTGC* R: AACCCCAGTGCACCAAGAG	634	Could not be sequenced	60
Exon 1	SECTM1 _EX1.2	F: GTGCACCAAGAGGCCCTAAC R: GGGACATCACTCCTCTGCTC	682	Buffer B	61.3

Table 4.3. Sequences, PCR product sizes and PCR conditions for primer pairs designed to amplify candidate genes (continued).

Exon 2	SECTM1 _EX2	F: CAGGTGACAGCCGCTCC R: ACCTGGACCCAACCTCAGTC	314	Buffer A	Touchdown 65 →55
Exon 3	SECTM1_ EX3	F: ACTGTGTCCCTTAGAGGCCC R: TCCCTCTCAGTCTCAGCCC	520	Buffer A	Touchdown 65 →55
Exon 4	SECTM1_ EX4	F: GAGCTACACGGAGGAGGTAGG R: GCAGGACAGTAAGGCTGACC	290	Buffer A	Touchdown 65 →55
Exon 5.1	SECTM1_ EX5_1	F: GTATGCCCGTGAGTGTGAAC R: GTCTGTGGGTTTGATGAGGG	586	Buffer A	Touchdown 65 →55
Exon 5.2	SECTM1_ EX5_2	F: GTCTTCCAAGCTCTGCTTCC R: CGCAGTGACGAAGACAAAAG	561	Q-Solution	Touchdown 65 →55
Exon 5.3	SECTM1_ EX5_3	F: CTCAGTCCCTCGGCCAC R: AAGACACGCCAATGCTCTTC	586	Buffer A	Touchdown 65 →55
PSCD					
Exon 1	PSCD_ EX1	F: AGGAGCCTCGGGTGGAC R: GACCCTCATCCCTCAAAACC	500	GC Rich Kit	Touchdown 65 →55
Exon 2	PSCD_ EX2	F: GGCCTCTGGATCTTCCTTG R: CCCTTTCATACAAATGGAACTG	221	Buffer B	Touchdown 65 →55
Exon 3	PSCD_ EX3	F: TTGTCATATTTTGTTTCATTTTGC R: CTTCAATGTGCCACGTAAGC	278	Buffer A	Touchdown 65 →55
Exon 4/5	PSCD_EX4/5	F: TCTTTCAAGCCTTTCCGATG R: TGGGAGTTTGTTTCTTTGTGTC	612	Buffer A	Touchdown 65 →55
Exon 6	PSCD_EX6	F: GTGTAGGAGACATGGCCTGG R: AGGACAGACTCATGATCAAAGG	235	Buffer A	Touchdown 65 →55
Exon 7	PSCD_EX7	F: GAGAAATAAATTGCCTCCCC R: TCTGGTGCCAAGAAAATAATCC	233	Buffer A	Touchdown 65 →55
Exon 8	PSCD_EX8	F: GATACCACTCTTGCTCTTGCG R: CAAAAGACGATCCTGTTCCC	300	Buffer A	Touchdown 65 →55
Exon 9	PSCD_EX9	F: CACATGAATGCTTGTGGAATG R: ACACGCACAAACACGCAC	314	Buffer A	Touchdown 65 →55
Exon 10	PSCD_EX10	F: TGATGTCAATGTTGTGGGCT R: ACGGTCTCCTCAACCATGTC	307	Buffer A	Touchdown 65 →55
Exon 11	PSCD_EX11	F: CAGGAAAGTTCGGCTGAGTC R: GAGTCTCATCTTTGGCTTGAAC	319	Buffer A	Touchdown 65 →55
Exon 12	PSCD_EX12	F: GGGTTTTGGGGAAAGAAATC R: GCGGCATGTTTAACCACTAAG	326	Buffer A	Touchdown 65 →55
Exon 13.1	PSCD EX13_1	F: CTGCCTGGGTGTGTTTCTTC R: GGCTTCTCTTCCTTTCCACC	574	Buffer A	Touchdown 65 →55
Exon 13.2	PSCD EX13_2	F: TAGCAGAGCTCAGAGCCAAC R: AACGTAAGCGTCCAGTCAGC	534	Buffer A	Touchdown 65 →55
Exon 13.3	PSCD EX13_3	F: GCACAGTCAGAGTCGGGG R: TGTCACGGCTCCCTTCATAC	573	Buffer B	53
Exon 13.4	PSCD EX13_4	F: GATGGGCCTTTATCTGCTCC R: CAGCCTGGACCCTCTTCTG	541	Buffer A	Touchdown 65 →55
Exon 13.5	PSCD EX13_5	F: CCCCGCCACTTTGTGTAG R: ACAAGTGTCCGGTCAGCAC	548	Buffer A	Touchdown 65 →55
GORAB					
Exon 1	SCYL1BP1 EX1	F: TTTGTCAGGCACTGCTGAAG R: CCGCTAACACAAACGTAGCC	363	Buffer A	Touchdown 65 →55
Exon 2	SCYL1BP1 EX2	F: GAGAATGGGGTAGGAGAACCA R: CTTAAAGCCCATTGGGAAAA	550	Buffer A	Touchdown 65 →55
Exon 3	SCYL1BP1 EX3	F: TGAACTGCAGATGGGTTTCTT R: AACAGCCTCTCCTGGTTCAG	296	Buffer A	Touchdown 65 →55
Exon 4	SCYL1BP1 EX4	F: GGAAAGCTCTGTTGAATGTTTC R: CTGGAACAGCTGGCAATAAA	541	Buffer A	Touchdown 65 →55
Exon 5.1	SCYL1BP1 EX5.1	F: TTTCCCAATTTTGGAGTTGAG R: TGATTTGGGCAGTTTGGAC	510	Buffer A	Touchdown 65 →55
Exon 5.2	SCYL1BP1 EX5.2	F: CAGTGGTTCGTTTAGAGAGGC R: TCTCCCAGGAGAAGTGAAATG	580	Buffer A	Touchdown 65 →55
Exon 5.3	SCYL1BP1 EX5.3	F: CGGTTCTTTCAGTGTTCCG R: TCAATTCATCGATTAAAGGAAAG	495	Buffer A	Touchdown 65 →55

Table 4.3. Sequences, PCR product sizes and PCR conditions for primer pairs designed to amplify candidate genes (continued).

Exon 5.4	SCYL1BP1 EX5.4	F: CCAAACAACTTAAACCAGCATC R: CAGGATGTCCCTAAGTTTTTCA	597	Buffer A	Touchdown 65 →55
PYCR1					
Exon 1	PYR1_EX1	F: GCGACGGTAGCCCAGTTC R: CCCTGCAGAAGTGGAAAGAG	505	Buffer A	Touchdown 65 →55
Exon 2	PYR1_EX2	F: CAGGAGCATGGCGTGAAC R: ACACTCCTGCCTCTCACACC	284	Buffer A	Touchdown 65 →55
Exon 3/4	PYR1_EX3-4	F: CTACCTGTGGGGCTCTTGG R: GACAGATGTGCCCGGTG	731	Buffer A	Touchdown 65 →55
Exon 4*	PYCR1 EX4-ter	F: ACCGTGTATGCCACAGGC R: AGATGTGCCCGGTGGTC	204	Buffer A	55
Exon 5/6	PYR1_EX5-6	F: GGAACTGGAGCTTGCCC R: AGTGCGTGAATGAGCAGATG	578	Buffer A	Touchdown 65 →55
Exon 7.1	PYR1_EX7.1	F: TGGGCTTCACTCCCTCTTC R: CCCACCTCTGCTGAGCC	561	Buffer A	Touchdown 65 →55
Exon 7.2	PYR1_EX7.2	F: GAGGGTCTTCACCCACTCC R: TATTCTGTTTCTGGCAGGGG	611	Buffer A	Touchdown 65 →55
MDIDJC					
ERLIN2					
Exon 1	ERLIN2_EX1	F: CATTGACCGCTGGGAGC R: GAAAGTGACGGGTCAGCC	259	Buffer B	Touchdown 65 →55
Exon 2	ERLIN2_EX2	F: GAGGTCCTCTCGCTGTTGTG R: AAAGCAATGACCAGGAAAGG	262	Buffer A	60
Exon 3	ERLIN2_EX3	F: GGGCTGAAGGGAAAGTTGAC R: GCATTTTACTCATCCAATGGC	271	Buffer A	60
Exon 4*	ERLIN2_EX4	F:CCAGGACAAAGGCATTTAGG R: CTCTTCCTGCAACCAGCC	207	Buffer A	Touchdown 65 →55
Exon 4*	ERLIN2_Ex4-2	F: GCCATGCTCAACCCAAAC R: TAGGGAGCTACGAGACAGGG	287	Buffer A	Touchdown 65 →55
Exon 5-6	ERLIN2_EX5/6	F: CCACATCTTACGCCATCACC R: AGGCTTTAGGCAGTGGAGAG	501	Buffer B	Touchdown 65 →55
Exon 7-8	ERLIN2_EX7/8	F: GCACTTTACCTCATCCTGCC R: GCAGCTTTGGTTACCTCTGG	453	Buffer B	Touchdown 65 →55
Exon 9	ERLIN2_EX9	F: AGAATTCGACTTACCTGGGG R: TTAGCCTCCTTGCATCTTCC	241	Buffer B	Touchdown 65 →55
Exon 10	ERLIN2_EX10	F: TCGGGTGAAAGGTGAAATTAG R: GTTAAAGGGCAAAGGCAATG	248	Buffer B	Touchdown 65 →55
Exon 11	ERLIN2_EX11	F: TCCCATAGCCTCTGCACTTC R: CAACACTGGAAACTCTCCTGC	232	Buffer B	Touchdown 65 →55
Exon 12.1	ERLIN2_ EX12_1	F: AATTGAAGGGGCACCACTC R: GGAAGGTCAAATGTTCTCTGC	783	Buffer A	Touchdown 65 →55
Exon 12.2	ERLIN2_ EX12_2	F: TGCCTCCAAGGTAGGAGATG R: TGGGCATGAACTCTGATTTG	754	Buffer A	Touchdown 65 →55
Exon 12.3	ERLIN2_ EX12_3	F: GGGAGTGGGTCTGACTTAGTG R: CAAGGGAAATGACCACCTTC	795	Buffer A	55
Exon 12.4	ERLIN2_ EX12_4	F: CTGACTCCTGGGACTTCTGG R: TGATAGAAACTTGGGGTGGG	761	Buffer A	Touchdown 65 →55
Exon 12.5	ERLIN2_ EX12_5	F: AGGGCCTCTCCGGTACTAAC R: GGTTACATTCACAGACACAGTAGC	836	Q-Solution	60
Exon 12.6	ERLIN2_ EX12_6	F: TTGATTCAGGAAAAGGAGCTG R: TTTGGAGCAGAATTGCAGTG	809	Buffer A	Touchdown 65 →55
PROSC					
Exon 1	PROSC_EX1	F: TCTTGGACAGCAGTGGTCTG R: GTGACGACCCATTCCCAC	752	Buffer B	Touchdown 65 →55
Exon 2-3	PROSC_EX2/3	F: TCAATGCCTGTCTATCCTACAG R: CACCAGGATGGGTCTAATTTTC	390	Buffer A	Touchdown 65 →55
Exon 4	PROSC_EX4	F: ATGTGAAAGGTGACAGGGAG R: GCTCTCTCTTCCACAAAGGG	244	Buffer B	Touchdown 68 →58
Exon 5	PROSC_EX5	F: TCAGAGGAACTGAGATTTAACTGTG R: TTATCCATCAGACACTTGGGC	361	Buffer A	Touchdown 65 →55

Table 4.3. Sequences, PCR product sizes and PCR conditions for primer pairs designed to amplify candidate genes (continued).

Exon 6	PROSC_EX6	F: AAGGGAGGAAAATGGAGCC R: GATGACTCTGCAATCCCCAC	312	Buffer A	Touchdown 65 →55
Exon 7	PROSC_EX7	F: AACCGTTGTCAGAGAAGTTCAG R: CAAAGATCTGCTCTTGTGTCAG	268	Buffer A	Touchdown 65 →55
Exon 8.1	PROSC_ EX8_1	F: ACAGCTTCAGCACTGGCTC R: ACACTGCCATTCCACAGTTG	721	Buffer B	Touchdown 65 →55
Exon 8.2	PROSC_ EX8_2	F: CGTCGTCTAAATTGCTGCTC R: TTCTCATCACTGTAGGTCCCAG	694	Buffer B	Touchdown 65 →55
Exon 8.3	PROSC_ EX8_3	F:CCCTGAAATTAAAGGATAACATAAGG R: GCCAAGGCACCAGCATAG	729	Buffer A	54
BRF2					
Exon 1	BRF2_EX1	F: AGGCACAGACCGGAAGTG R: GCGTTACAGTTAGGAGTATGGGG	434	Buffer B	Touchdown 65 →55
Exon 2	BRF2_EX2	F: CACCATGCCCAGCTAATTTT R: AATTTTGCGTCCTGGTTTTG	346	Buffer B	Touchdown 65 →55
Exon 3	BRF2_EX3	F: AGAATTTTCTAGGAGTTGCACG R: GGCCAAAGGTCAAAGGATTC	461	Buffer B	Touchdown 65 →55
Exon 4_1	BRF2_EX4_1	F: TGGGCTGTCTTTCCTCACTG R: CCTAAGGAATTATTTCCCACCTC	569	Buffer B	Touchdown 65 →55
Exon 4_2	BRF2_EX4_2	F: CAGTCACTGGTCCGCTCTG R: CCAAGGGATGGGAATCTCTC	558	Buffer B	Touchdown 65 →55
Exon 4_3	BRF2_EX4_3	F: AAGAGGGGCTCTGCCATTAG R: CCAATGCCTTAGCACTGGAG	572	Buffer B	Touchdown 65 →55
RAB11BPI1					
Exon 1	RAB11BPI1 EX1	F: GCAGCAGGTGGAGCAGG R: TTACTCTCGAAGGGTCCAGC	627	Q-Solution	63
Exon 2	RAB11BPI1 EX2	F: CATGGGGATTGTGAACATTG R: TCTCTCAGAACGAAGCATGG	576	Buffer A	Touchdown 65 →55
Exon 3	RAB11BPI1 EX3	F: ACGTTGACAGATGCCCCTAC R: AAGCCTGAAAACCACCAATG	945	Buffer A	Touchdown 65 →55
Exon 4.1	RAB11BPI1 EX4_1	F: CTCCCCTGGTGAATGACTTG R: ATGGAAGGGACTGATGCTCC	822	Buffer A	Touchdown 65 →55
Exon 4.2	RAB11BPI1 EX4_2	F: TCACTCAGCAGTGATGGAGC R: TGATCTCCGTCATCTTCAACC	752	Buffer A	Touchdown 65 →55
Exon 4.3	RAB11BPI1 EX4_3	F: TAAATCTCCAATCATGGCCG R: GCCGTAACCTCTGCAGGTAG	759	Buffer A	Touchdown 65 →55
Exon 5	RAB11BPI1 EX5	F: GCAGTTGCTCAGTTTTGCC R: ATGGAAACGGGTGTTCTGTC	227	Buffer B	Touchdown 65 →55
Exon 6.1	RAB11BPI1 EX6_1	F:TTTTCCTCCTTTGTACTTCTTTTAGG R: AATCGCATGGTCCTTTTCTC	739	Buffer A	Touchdown 65 →55
Exon 6.2	RAB11BPI1 EX6_2	F: CACTGGGGTTTTCTTTCTTTC R: ACCACGACTGGCCTGAAG	692	Buffer A	51
Exon 6.3	RAB11BPI1 EX6_3	F: GTGCTCTGGTTTCCTCAGC R: GGGGTAAAATGCTGGTGAGTC	692	Buffer A	Touchdown 65 →55
Exon 6.4	RAB11BPI1 EX6_4	F: GTGGGATACTGGGGAAATTG R: ACCGCGTCCAGCCATAC	787	Buffer A	Touchdown 65 →55
Exon 6.5	RAB11BPI1 EX6_5	F: ATCTGAAGGATGATACTGTAACTTG R: CAGGAATTTACTCCTCCACCC	754	Buffer A	Touchdown 65 →55
Exon 6.6	RAB11BPI1 EX6_6	F: TCACAAGGATGTTGGTTTGG R: CAGTATGGCAAAGGGCAGAC	697	Buffer A	Touchdown 65 →55
Exon 6.7	RAB11BPI1 EX6_7	F: CTCAGGCTTTGGCAGGTATC R: ACCAAGAGAGGTTTTCCAGG	723	Buffer A	Touchdown 65 →55
CL					
NEGR1					
Exon 1 (CDS)*	NEGR1_EX1	F: AAGACTCGCCAGCACCAG R: GGCAAAGAGGGTTCAAAGAG	319	Buffer A	63
Exon 1 (UTR + CDS)*	NEGR1-5'UTR	F: GCAACCGAGAGGAGGTGTAG R: GGCAAAGAGGGTTCAAAGAG	548	Buffer C	Touchdown 65 →55

Table 4.3. Sequences, PCR product sizes and PCR conditions for primer pairs designed to amplify candidate genes (continued).

Exon 2	NEGR1_EX2	F: GTTTGCATTTGATGCTGTGC R: TGCTTCCTAGTCATTTTGATACC	431	Buffer A	Touchdown 65 →55
Exon 3	NEGR1_EX3	F: ACATTTCACCCTCATACCTTTC R: AAGTTCTGAACAAGTGAGGTTAGTG	314	Buffer A	Touchdown 65 →55
Exon 4[a]	NEGR1_EX4	F: AATTCCCCAGTTTCATTTGG R: TTCAACATCTACACGTCTTCAGTG	403	Buffer A	Touchdown 65 →55
Exon 4	NEGR1_EX4.2	F: ATACCTCGTTCTGCTTCTGC R: TTTACTTGGGACAATTGTTGTTAC	515	Buffer A	Touchdown 65 →55
Exon 5	NEGR1_EX5	F: GCGTTGGTCTATCAGGCATAAG R: GCTGAGAATCATTCAAGCCAG	355	Buffer A	Touchdown 65 →55
Exon 6[b]	NEGR1_EX6	F: TGCCATGACAACCCCAG R: ATGGATAGGGGCCCAGAG	290	Buffer A	Touchdown 65 →55
Exon 6	NEGR1_EX6.TER	F: TACCAACGTGACACAGGAGC R: AAAATGAACGTACTCCATTCTTAGG	183	Buffer A	Touchdown 65 →55
Exon 7 (CDS)	NEGR1_EX7	F: ATGCACCTGGCTACCTTTTG R: TCCAGCCATCAGCACTTTC	265	Buffer A	Touchdown 65 →55
Exon 7.1 (UTR)	NEGR1_EX7.1	F: CCTGGCTACCTTTTGATTATTG R: AAAGAGAAGCAGAGCTGCAC	794	Buffer A	Touchdown 65 →55
Exon 7.2 (UTR)	NEGR1_EX7.2	F: TCAATCCACATTTACAAAGATGC R: CTTGTTTGCACTGAAATGGC	897	Buffer A	Touchdown 65 →55
Exon 7.3 (UTR)	NEGR1_EX7.3	F: GGGCACAAAGTCCTATCACC R: TTTTGTGGTAGCACCACTATTTC	1085	Buffer A	Touchdown 65 →55
Exon 7.4 (UTR)	NEGR1_EX7.4	F: AAATGAATCTTAAATGAGGGGAC R: TCAGGACTGATAAAATGGGG	804	Buffer A	Touchdown 65 →55
Exon 7.5 (UTR)	NEGR1_EX7.5	F: CCCTCGGACAGAGTGAAATC R: TGGGTAATTTTCTCAGTTCTCC	812	Buffer A	Touchdown 65 →55
7 Exon.6 (UTR)	NEGR1_EX7.6	F: TGAGACACTAAAAGATTTGAGAGGG R: GAATATAGTGTGGAGTCATTTGAAAC	779	Buffer A	Touchdown 65 →55
Exon 7.7 (UTR)	NEGR1_EX7.7	F: ATGTTGTACTGTTTCCAATAGGTG R: TGAAGCATCTATGTTTTGCCC	1002	Buffer A	Touchdown 65 →55
LHX8					
Exon 1 (UTR)	LHX8 EX1	F: AACCTCAGCAAGAGTAGGCG R: AATGGCAGTAATCATAGCTGTTG	358	Buffer C	Touchdown 65 →55
2 (5'UTR + CDS)	LHX8 EX2	F: GATGGACTTTAGCGTTTCGC R:TTCAGGGTTAGGAGACCGTG	733	Buffer C	Touchdown 65 →55
Exon 3-4	LHX8 EX3/4	F: CATTAGCTCGCTCCCCG R:CTTTTCCCAGAGCTCCCAC	818	Could not be amplified	
Exon 3	LHX8-EX3	F: CTGAGGGCCTTCATTAGCTC R: CCCGTCCTCTGTCTGCTG	318	Buffer C	Touchdown 65 →55
Exon 4	LHX8-EX4	F: GTAGCCAGAGCTTGGACTCG R: GCCTACAACCTTCACCCAGA	457	Buffer C	Touchdown 65 →55
Exon 5	LHX8 EX5	F: CATCTTTTGGATGAAAACATTCAG R:TCTCAAACAGGAAAGCACCC	408	Buffer C	Touchdown 65 →55
Exon 6	LHX8 EX6	F:TGTGCTGGTTTAATATTCGACTG R:TGCATTAAGATGACCTTAGGAAAAG	386	Buffer C	Touchdown 65 →55
Exon 7	LHX8 EX7	F: GAAACCTGTTATTGTAAGATGGGTG R: TGGGCAGCATGGAGGTTAC	252	Buffer C	Touchdown 65 →55
Exon 8	LHX8 EX8	F: TCCCCATACCGATTTTCAAG R: GCCAGGTACAGTGGCTCATC	388	Buffer C	Touchdown 65 →55
Exon 9	LHX8 EX9	F: ACATTTATGCGGTGCTTGTG R: TGGATAATTTTGCTCTCTACTGC	460	Buffer C	55
Exon 10 (CDS + 3'UTR)	LHX8 EX10	F: ATGAGTGTAGCTTGGTGCCC R:TCTTTCACATTGATTTTATTAGCTGG	1058	Buffer C	Touchdown 65 →55
LOC646556					
Exon 1	LOC646556 EX1	F: CATCTTTTGGATGAAAACATTCAG R: TCTCAAACAGGAAAGCACCC	408	Buffer C	Touchdown 65 →55
Exon 2-3	LOC646556 EX2/3	F: ATGTGTGGCAAACTTCACGA R: TAGGGCAAAACAAGGTGCTC	922	Buffer C	Touchdown 65 →55

*CDS: Coding sequences, UTR: untranslated regions

[b]NEGR1_EX4-F and NEGR1_EX4-2-R; [b]NEGR1_EX6-F and NEGR1_EX6.TER-R were used together for further amplifications, since amplification with NEGR1_EX 4 and NEGR1_EX6 did not give a high yield.

Table 4.4. Primers used to identify the breakpoints of the deletion at 1p31.1 in MCL.

Marker ID	Amplified Region	Product Size (bp)	Primer Sequence (5' → 3')
YD_del1	75243323-75243700	378	F: GCTGAATCCCCAAAATAGCA R: GGAGGAAGAGGAGCTGTGAA
YD_del2	75522954-75523376	423	F: GTGCAGCTACCGATCTCACA R: TCCAAGGATATGCCCAAGAG
YD_del3	75529897-75530293	397	F: TGGGCATCCTTTTCTTGTTC R: ACAGGCCAATATCCCTGATG
YD_del4	75246432-75246614	183	F: CCCACTCTCTGTGCTTCTCC R: AAGGTGCTGCTGCTGGTAAT
YD_del5	75521988-75522596	609	F: AGGGGAAGAAGGAAAATGGA R: CACGTTTTGTGAACCAAGGA
YD_del6	75247021-7524749	477	F: TCTCTCCCACCCTTTTACCA R: GCTTTAACTGCACCGTCCTT
YD_del7	75521160-75521468	309	F: ATGAAGGATGGAGTGAGAAGGT R: CCTGACATATTGCTGCTGTTG

4.3.2. DNA Sequence Analysis

Fragments of all candidate genes to be analyzed for mutations were PCR-amplified in tubes containing 50 µl reaction mix each; the total volume of the product was 100-200 µl. PCR products were purified from primers, nucleotides, polymerases and salt using QIAquick PCR Purification Kit (QIAGEN). Sequence analysis was performed at Iontek (Istanbul, Turkey), Refgen (Ankara, Turkey), Massachusetts General Hospital DNAcore Facility (MA, USA) and Macrogen Inc (South Korea).

4.3.3. SSCP Analysis

Gel plates 20 cm x 20 cm in size were assembled using 0.75 mm spacers. Six ml of 40 per cent acrylamide:bisacrylamide stock (37.5:1) was mixed with 1.8 ml of 10X TBE, the volume was adjusted to 30 ml with dH_2O and 250 µl of 10 per cent APS and 25 µl of TEMED were added. After gently mixing, the solution was poured between the glass plates. For gels desired to contain 5 per cent or 8 per cent glycerol, 1.5 or 2.4 ml, respectively, glycerol was added before adjusting the volume with dH_2O. A 20-well comb was inserted, and the gel was left to polymerize for at least an hour. After polymerization, the gel was cooled to 4°C before use, and electrophoresis was performed at the same temperature. PCR products to be run were mixed with equal volumes of denaturing buffer

and denatured at 95°C for 5 min before chilling on ice. Nine to 12 µl of each sample was loaded onto the gel, and electrophoresis was performed at a constant power (10-30 Watts) in 0.6X TBE buffer at 4°C. Running time was adjusted according to the lengths of the products. DeCode Universal Mutation Detection System or Protean IIxi Cell was the apparatus used for SSCP analysis. The gel was stained with silver nitrate to visualize DNA bands, as described in section 4.2.5.

GO family members and population controls were screened by SSCP for the variant that was identified in *PYCR1* exon 4 in a patient. The templates were amplified by primer pairs PYCR1 EX4-ter (Table 4.3).

4.3.4. High-Resolution Melting Curve Analysis

Population DNA samples were screened for *ERLIN2* mutation c.812_813insAC identified in MDIDJC Family, by high-resolution melting curve analysis using LightCycler 480 system. The reaction mix contained 10 µl of High Resolution Melting Master Mix, 200 nM of each primer pair (Table 4.3 ERLIN2_EX11-2), 3 mM $MgCl_2$, 20 ng of total genomic DNA and sufficient dH_2O to adjust the volume to 20 µl. PCR was performed in 96-well plates under the following conditions: 95°C for 10 minutes for initial denaturation, followed by 45 cycles of 95°C for 10 seconds, annealing at 57°C for 16 seconds and elongation at 72°C for 15 seconds. High-resolution melting curve data were obtained at a rate of 25 acquisitions per °C. The fluorescence data was normalized, adjusted using temperature-shifting and then analyzed using the LightCycler 480 Gene Scanning Software. A total of 64 control DNA samples were scanned by this method. In addition, a total of 44 control DNAs were analyzed using denaturing polyacrylamide gel electrophoresis.

4.3.5. Assessment of Relative *ERLIN2* Transcript Levels

Blood samples from individuals 512, 514, 608, 701, 813 and 814 (Figure 3.3) were collected for RNA study. Blood samples of two female and two male control individuals were also used for RNA isolation. Total RNA was extracted from whole blood using MagNA Pure Compact RNA Isolation Kit (Roche, Germany). Control RNAs that had been

extracted in Kommagene Laboratory (Dursun et al., 2009) were also included in the RNA study. High Fidelity cDNA Synthesis Kit (Roche, Germany) was used to synthesize first strand cDNA from total RNA using Random Hexamer primers. Real time quantitative RT-PCR was performed to analyze the relative transcript amounts of *ERLIN2*. *HPRT1* was used as the control gene. Intron-spanning TaqMan assays were designed and purchased from Universal Probe Library (Roche Applied Science, Germany). The reaction was performed in 96-well plates using 10 µl of LightCycler 480 ProbeMaster Mix, 100 nM of appropriate hydrolysis probe, 200 nM of each primer pair, 5 µl of cDNA and dH_2O to adjust the total volume to 20 µl. It was important to preheat the primer-probe mix to 95°C for one minute before starting the reaction to avoid possible primer interactions. All reactions were performed using three replicates per sample under the following conditions: 95°C for 10 minutes, and 40 cycles of 95°C 10 seconds, 55°C for 30 seconds and 72°C for one second. LightCycler 480 relative quantification software was used to calculate relative transcript levels.

5. RESULTS

In this section the results of the linkage analysis and candidate gene approach for diseases Geroderma Osteodysplastica, Motor Dysfunction, Intellectual disability and Joint Contractures and Midline Cleft Lip are presented.

5.1. Geroderma Osteodysplastica

5.1.1. Linkage Analysis

Genome scan data generated by microsatellite markers were analyzed with SuperLink and SimWalk v2.91 to obtain two–point and multipoint lod scores, respectively. A fully penetrant, recessive model was assumed. Five loci (9q21, 10p13, 10q11.1, 12q12 and 17q25.3) yielded multipoint LOD scores >1.5, and again five loci (3p20.2, 7p15.1, 9q31.2, 10q22.1 and 17q25.3) yielded two–point LOD scores >1.75. Among them, locus 17q25.3 yielded the highest multipoint and two–point lod scores of 3.42 and 2.88, respectively (Figure 5.1). In addition, haplotypes were constructed.

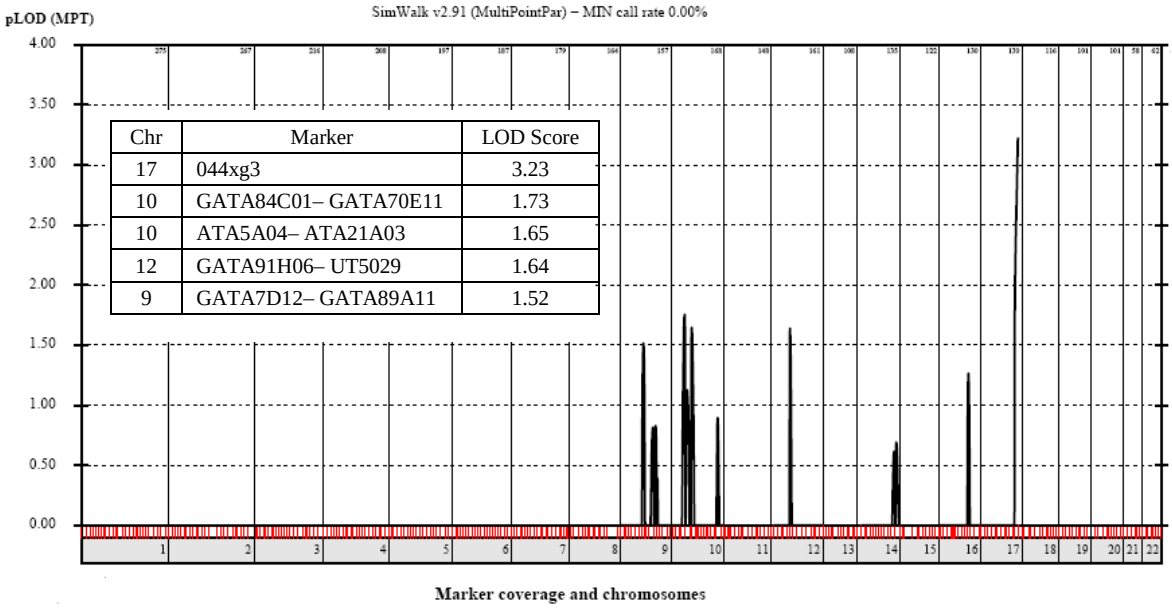

Chr	Marker	LOD Score
17	044xg3	3.23
10	GATA84C01– GATA70E11	1.73
10	ATA5A04– ATA21A03	1.65
12	GATA91H06– UT5029	1.64
9	GATA7D12– GATA89A11	1.52

Figure 5.1. Multipoint lod scores of the total data set generated by the genome scan in GO family. Loci having >1.5 lod scores are marked with asterisks and given in the insert.

Analysis of haplotype segregation for autosomal chromosomes and PAR regions pointed to possible identity by descent for a few loci. Five of those loci (5q11.2, 9q22.32-q31.1, 10p11.23, 14q31.3-q32.2 and 16p13.3) together with two others (7p15.1-p22.2 and 17q25.3) that yielded high lod scores were analyzed with additional microsatellite markers (Table 4.2). Consequently, all loci except 17q25.3 were excluded. For that candidate locus, final two-point LOD scores were 2.59-4.09 at markers D17S1847 to D17S78612k at zero recombination frequency (Table 5.1), and multipoint LOD scores were >5.6 at a maximum 18.76-cM region (111.22-129.98 cM) and 4.18-Mb region (77.02-81.20 Mb or 17qter) (Figure 5.2). All affected individuals shared the same homozygous haplotype descending from the same ancestor. This homozygous genotype delineated centromerically by D17S674. A parental crossover in unaffected individual 406 narrowed down the candidate locus, since it resulted in his sharing the homozygous genotype with the patients for markers D17S674, D17S74.11M and D17S1847 (Figure 5.3). Thus, the maximum gene locus was identified as D17S1847-qter, the most telomeric 4.18-Mb and 18.76-cM region of the long arm.

Table 5.1. Markers used at 17q25.3, their physical and genetic map positions and two-point LOD scores for GO.

Locus	Mb	cM	LOD Score at θ [a] =						Z_{max} [b]	θ at max
			0.00	0.05	0.10	0.20	0.30	0.40		
300XA5P	65.49	88.06	–10.12	1.20	1.37	1.16	0.74	0.32	1.37	0.35
GATA28D11	72.68	100.00	–2.47	0.71	0.74	0.52	0.26	0.08	0.74	0.10
TTCA006M	75.60	106.10	–1.41	1.43	1.42	1.09	0.66	0.28	1.43	0.05
D17S2195	75.89	106.80	2.10	1.86	1.61	1.13	0.67	0.28	2.10	0.00
D17S674	76.31	108.69	–4.77	0.91	1.12	0.95	0.60	0.27	1.12	0.10
D17S74.11M	76.60	109.71	4.35	3.90	3.44	2.51	1.59	0.73	4.35	0.00
D17S1847	77.02	111.22	2.59	2.29	1.99	1.37	0.80	0.32	2.59	0.00
044XG3	77.80	116.88	4.09	3.65	3.20	2.29	1.39	0.58	4.08	0.00
D17S76999K	79.39	123.75	3.63	3.24	2.85	2.05	1.27	0.56	3.63	0.00
D17S668	80.03	126.46	4.04	3.60	3.15	2.24	1.35	0.55	4.04	0.00
D17S78612K	81.02	129.98	3.55	3.12	2.69	1.82	1.02	0.38	3.55	0.00

[a] Recombination fraction, [b] Maximum two–point LOD score

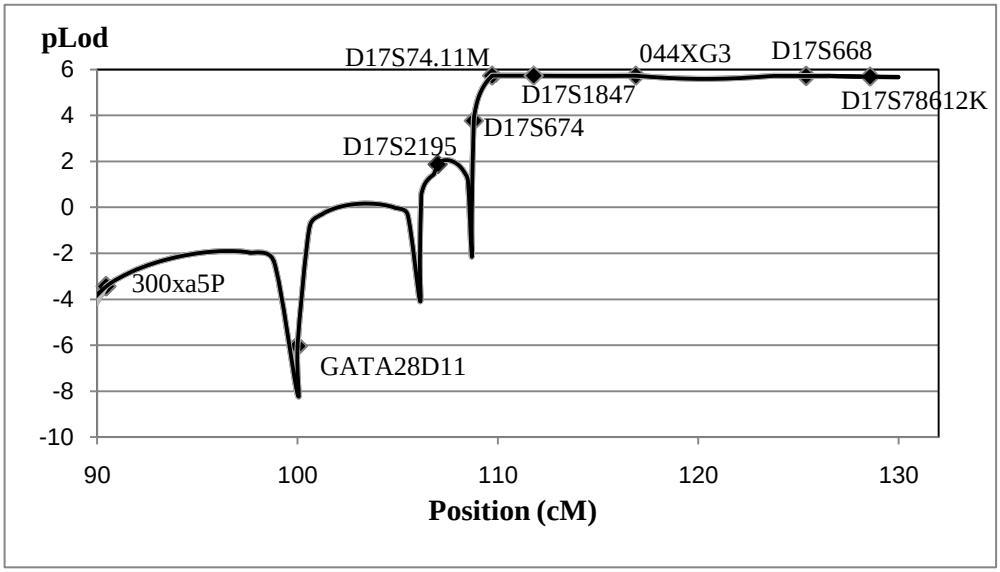

Figure 5.2. Multipoint LOD score curve of the final genotype data at chromosome 17q25.3 for GO family. Eleven markers were used.

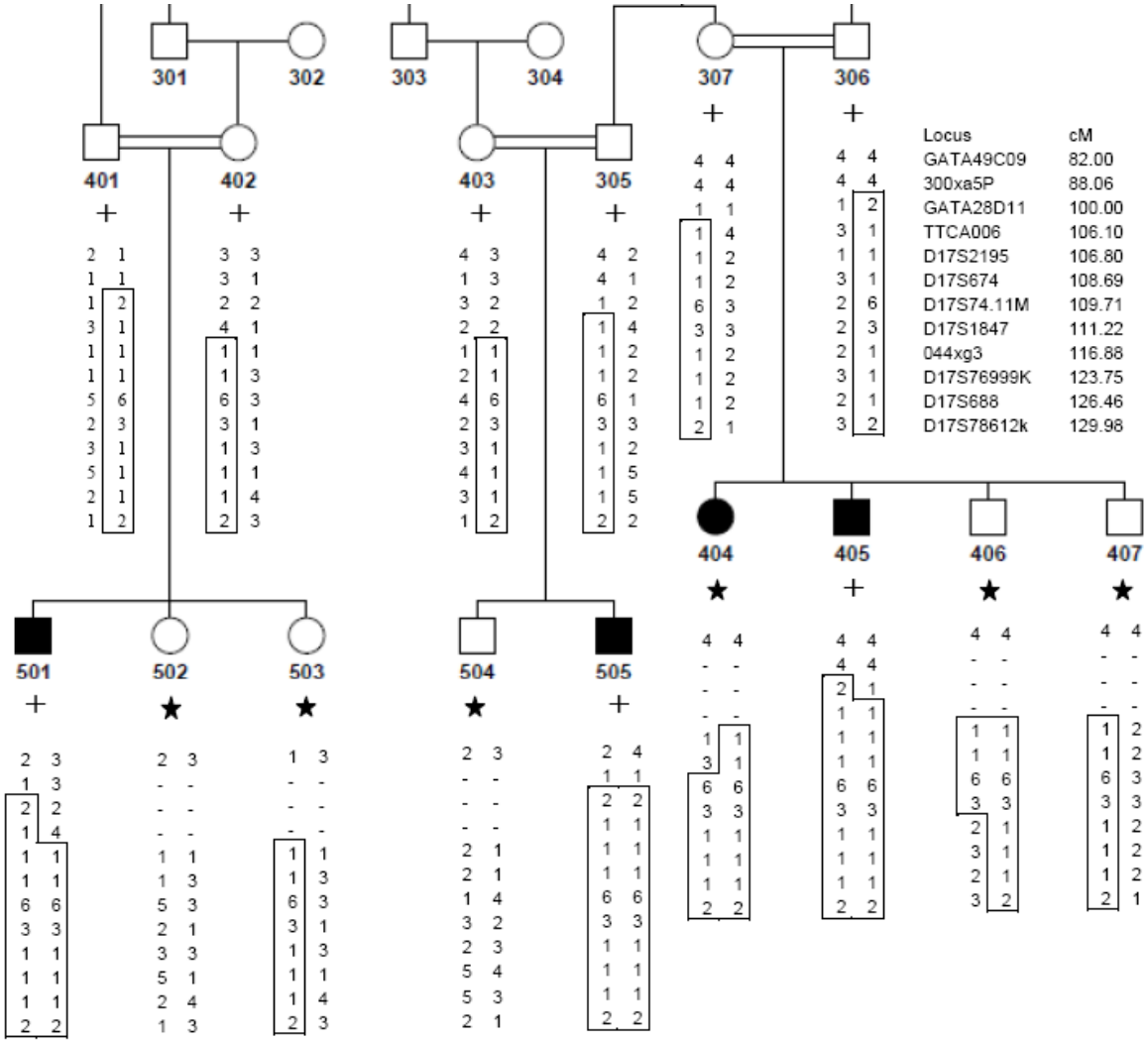

Figure 5.3. Partial pedigree and haplotypes for GO family at 17q25.3. Disease haplotype is boxed. DNA available for the genome scan is marked with a plus sign and DNA available later with an asterisk.

5.1.2. Candidate Gene Approach

While this study was in progress, *GORAB* (1q24) was identified as responsible for GO by Hennies et al. (2008). In the family studied in this thesis, investigation of linkage to 1q24 by flanking markers revealed that there was no homozygosity or shared genotype among the patients. Additionally, analysis of all exons and flanking sequences of *GORAB* by direct resequencing in a patient did not result in the detection of a novel variant. The extent of the resequencing is presented in Table 5.2.

Candidate locus 17q25.3-qter contained 123 genes, according to NCBI Mapviewer (Build GRCh37). *P4HB*, *RFNG* and *SECTM1* at the locus were assessed as strong candidates and analyzed for mutations in a patient. All exons and flanking sequences were resequenced, and no novel variant was detected. During candidate gene analysis, a novel cutis laxa gene, *PYCR1* was reported at the locus. Cutis laxa has similar clinical features as GO. That gene was analyzed by resequencing in an affected individual, and homozygous mutation c.540+1G>A, which had been previously reported (Reversade et al. 2009), was detected (Figure 5.4).

Table 5.2. Extent of resequencing in GO candidate genes *P4HB, RFNG, SECTM1* and *GORAB*

Gene Region	Sequence Read
GORAB	
Exon 1	–83 to +44
Exon 2	–82 to +69
Exon 3	–100 to +20
Exon 4	–265 to +60
Exon 5	–38 to +93
PYCR1	
Exon 1	–44 to +65
Exon 2	–11 to +25
Exon 3–4	–37 to +48
Exon 5–6	–62 to +38
Exon 7	–20 to +60

Gene Region	Sequence Read
P4HB	
Exon 1	–33 to +63
Exon 2	–70 to + 50
Exon 3	87 to +65
Exon 4	–68 to +16
Exon 5	–79 to +46
Exon 6	–34 to +52
Exon 7	–80 to +74
Exon 8	–64 to +30
Exon 9	–65 to +38
Exon 10	–41 to +69
Exon 11	–34 to+44

Gene Region	Sequence Read
RFNG	
Exon 1–2	–17 to +55
Exon 3–4	–43 to +29
Exon 5–6	–127 to +57
Exon 7	–135 to +20
SECTM1	
Exon 1	–77 to +77
Exon 2	–70 to +35
Exon 3	–50 to + 87
Exon 4	–67 to +31
Exon 5	–39 to +43

DNA samples of all family members were screened for the mutation by SSCP analysis, and the mutation was found to segregate with GO (Figure 5.5). Also, mutation screening in a random sample of 109 unrelated individuals from Turkish population was performed with the same method, but no mutation was found.

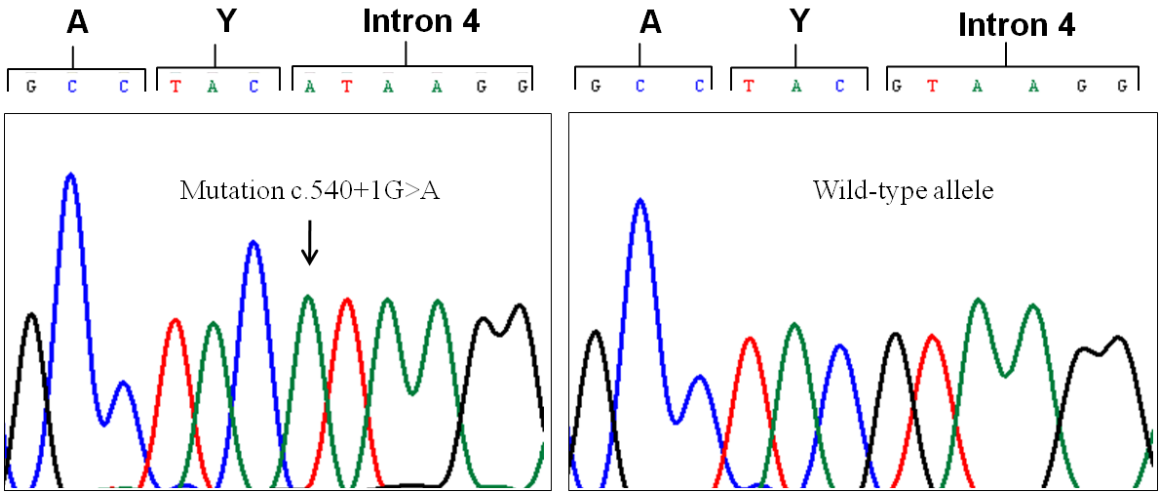

Figure 5.4. Partial chromatogram showing mutation c.540+1G>A identified in GO patients.

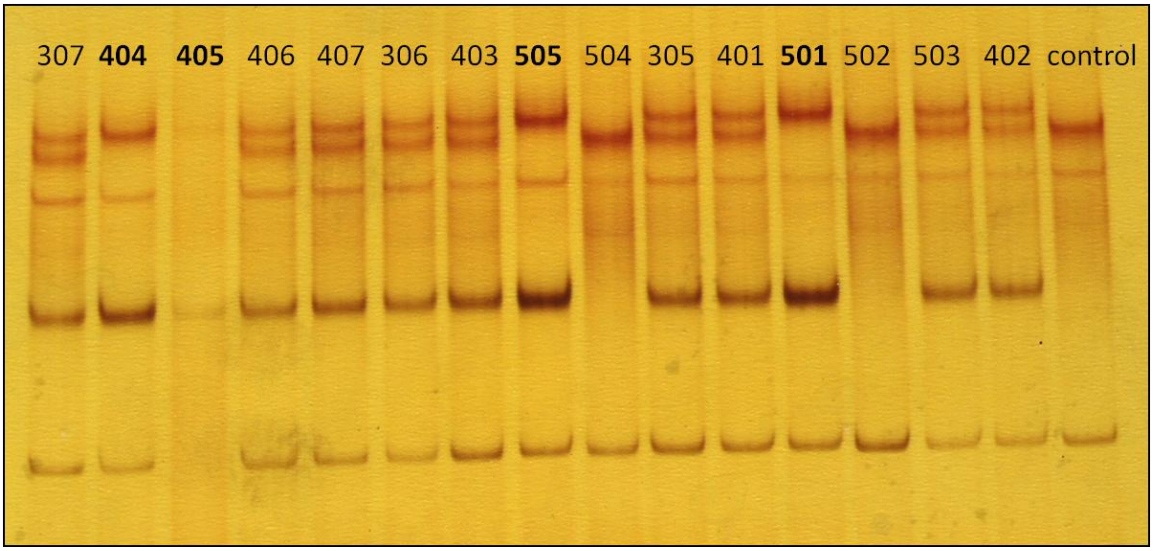

Figure 5.5. SSCP results showing the segregation of c.540+1G>A in GO family. The individuals given in bold are affected.

5.2. Motor Dysfunction, Intellectual Disability and Multiple Joint Contractures

Firstly, genome scan data generated by microsatellite markers were analyzed for linkage to identify a gene locus, assuming an autosomal recessive inheritance model, but no locus was found. A second genome scan with SNP markers was performed, and the gene locus was identified.

5.2.1. Linkage Analysis with Microsatellite Markers

Multipoint linkage performed using the genome scan data did not yield a significant lod score. By haplotype inspection, possible identity by descent was detected at ten loci, namely, 6p22.3, 6p 24.3, 8p21.3, 9p24.2, 10p11.23–10p11.21, 12q24.33, 20p13, 22q13.31, PAR1 and PAR2. Analysis with additional microsatellite markers indicated that none harbored the gene responsible for the disease.

Considering that one of the patient's DNA sample could have been mixed up with that of a healthy sib, a new set of linkage analysis was performed. In each analysis, a different patient was left out. Again, no significant lod score value was obtained. A denser genome scan with SNP markers seemed essential.

5.2.2 Linkage Analysis with SNP Markers

Five loci 6p21.1, 7p11.1, 8p12 – 8p11.3, 10p12.1 and 13q13.2 (Figure A.1 in Appendix) yielded multipoint lod scores >3 in linkage analysis. Inspection of genotypes at those loci through homozygosity mapping using HCiE (Cetinkaya, 2010) excluded all loci except 8p12, where maximum two-point and multipoint lod scores were 3.68 and 4.34, respectively. The homozygous genotypes shared by patients were disrupted by a heterozygous region.

One of the two identified homozygous loci lied between markers rs2732316 and rs7832148 (33,314,105-33,958,412 bp), whereas the other lied between rs474620 and rs6474491 (37,000,273-38,013,848 bp). Genotyping all family members available with microsatellite markers revealed that the homozygosity at the second locus but not the first one was shared by all affected members of the family. Moreover, all unaffected members were heterozygous. The disease gene was thus mapped to an approximately 1 Mb region between rs474620 and rs6474491. The haplotypes constructed using microsatellite alleles are shown in Table 5.3. The first region was excluded because homozygosity was broken in patients 704, 708 and 709. Two-point lod scores >3 (Table 5.4) and a multipoint LOD score > 11 (Figure 5.6) were obtained between markers D8S33.70M and D8S38.14M.

Table 5.3. Microsatellite haplotypes at 8p12 for MDIDJC.

		Family A				Family B									
		601	602	708	709	512	701	807	810	811	812	813	814	815	816
Marker ID	Position (Mb)	M	F	P1	P2	F	M	P1	P2	S1	S2	P3	P4	S3	S4
D8S136	22.43	1 3	3 3	1 3	3 3	3 1	3 1	1 1	1 1	1 1	3 1	1 1	1 1	3 1	1 1
D8S1048	26.81	– –	– –	1 3	– –	– –	– –	– –	– –	– –	– –	1 1	– –	– –	– –
GGAA20C10	32.07	– –	– –	1 2	– –	– –	– –	– –	– –	– –	– –	1 1	– –	– –	– –
D8S33.70M	33.58	2 4	1 4	2 4	2 4	3 2	3 2	2 2	2 2	2 3	3 2	2 2	2 2	3 2	2 3
D8S34.17M	34.05	1 2	1 2	1 2	1 2	3 1	5 1	1 1	1 1	1 5	3 1	1 1	1 1	3 1	1 5
D8S37.52M	37.40	2 2	2 2	2 2	2 2	2 2	3 2	2 2	2 2	2 3	2 2	2 2	2 2	2 2	2 3
D8S37.71M	37.59	2 3	3 1	3 3	3 3	1 3	3 3	3 3	3 3	3 3	1 3	3 3	3 3	1 3	3 3
D8S38.14M	38.06	3 3	3 4	3 3	3 3	1 3	3 3	3 3	3 3	3 3	1 3	3 3	3 3	1 3	3 3
D8S1110	53.18	– –	– –	2 2	– –	– –	– –	– –	– –	– –	– –	3 4	– –	– –	– –
D8S1113	59.71	– –	– –	3 3	– –	– –	– –	– –	– –	– –	– –	3 3	– –	– –	– –
D1S1136	66.07	– –	– –	2 3	– –	– –	– –	– –	– –	– –	– –	3 2	– –	– –	– –

		Family C				Family D						
		605	604	704	705	702	703	801	802	803	804	805
Marker ID	Position (Mb)	F	M	P	S	F	M	P1	P2	P3	S	P4
D8S136	22.43	2 1	3 1	1 3	2 3	1 3	1 3	1 3	1 1	1 3	3 3	3 1
D8S1048	26.81	– –	– –	1 3	– –	1 1	2 1	1 1	1 1	1 1	1 1	1 2
GGAA20C10	32.07	– –	– –	1 2	– –	1 3	3 1	1 1	1 1	1 1	3 1	1 3
D8S33.70M	33.58	2 2	4 3	2 4	2 4	2 3	3 2	2 2	2 2	2 2	3 2	2 2
D8S34.17M	34.05	4 1	2 2	1 2	4 2	1 5	2 1	1 1	1 1	1 1	5 1	1 1
D8S37.52M	37.40	1 2	2 2	2 2	1 2	2 3	2 2	2 2	2 2	2 2	3 2	2 2
D8S37.71M	37.59	4 3	3 3	3 3	4 3	3 3	3 3	3 3	3 3	3 3	3 3	3 3
D8S38.14M	38.06	2 3	3 3	3 3	2 3	3 3	3 3	3 3	3 3	3 3	3 3	3 3
D8S1110	53.18	– –	– –	4 2	– –	2 4	1 1	2 1	2 1	2 1	4 1	2 1
D8S1113	59.71	– –	– –	1 3	– –	3 3	2 4	3 2	3 4	3 4	3 4	3 2
D1S1136	66.07	– –	– –	3 3	– –	3 2	1 2	3 1	3 2	3 1	2 2	3 1

M: mother, F: father, P: patient, S: sibling

Table 5.4. Microsatellite markers used for the verification of 8p12 as gene locus for MDIDJC and for calculation of two-point LOD scores. Their physical and genetic map positions and the LOD scores are given.

			LOD Score at Θ [a] =							
Locus	Mb	cM	0.00	0.05	0.10	0.20	0.30	0.40	Z_{max} [b]	Θ at max
D8S136	22.43	43.96	-4.89	0.19	0.74	0.96	0.70	0.29	0.96	0.20
D8S1048	26.81	54.28	-5.82	0.26	0.62	0.60	0.35	0.13	0.67	0.15
GGAA20C10	32.07	60.34	-4.23	1.51	1.69	1.33	0.75	0.24	1.69	0.10
D8S33.70M	33.58	60.87	4.58	4.97	4.53	3.35	2.04	0.80	4.97	0.05
D8S34.17M	34.05	61.00	4.58	4.97	4.53	3.35	2.04	0.80	4.97	0.05
D8S37.52M	37.40	62.47	4.82	4.34	3.84	2.78	1.70	0.68	4.82	0.00
D8S37.71M	37.59	62.50	4.21	3.79	3.36	2.44	1.52	0.67	4.21	0.00
D8S38.14M	38.06	63.00	3.82	3.44	3.04	2.20	1.36	0.59	3.82	0.00
D8S1110	53.18	67.27	-6.14	-0.19	0.35	0.51	0.32	0.11	0.51	0.15
D8S1113	59.71	77.89	-9.23	-0.77	-0.01	0.34	0.28	0.13	0.34	0.20
D8S1136	66.07	82.26	-6.55	0.16	0.77	0.85	0.54	0.20	0.90	0.15

Markers in italics were designed in this study. [a] Recombination fraction,

[b] Maximum two-point LOD.

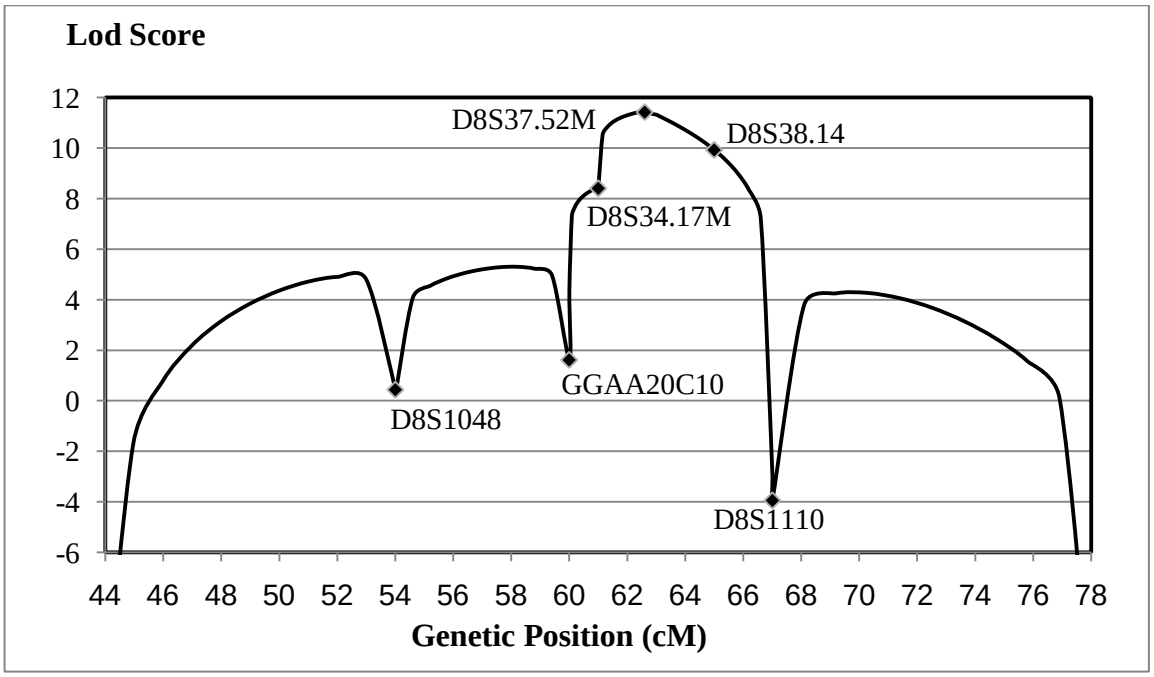

Figure 5.6. Multipoint lod score curve for MDIDJC using 10 microsatellite markers at 8p12.

5.2.3. Candidate Gene Approach

The gene locus harbored 12 genes. Four genes were selected as strongest candidates, and all exons and flanking sequences of *PROSC*, *BRF2* and *RAB11FIP1* as well as all coding exons of *ERLIN2* were resequenced in an affected individual. The extent of the resequencing is presented in Table 5.5. A homozygous 2-bp insertion in *ERLIN2* exon 11 that results in frameshift and a subsequent premature translational termination was identified. Three new amino acids have replaced residues 272 to 339 at the C–terminus (Figure 5.7), and the protein is truncated by about twenty per cent. The mutation (c.812_813insAC; p.Asn272ProfsX4) segregated with the disease in the family (Figure 5.8). A control panel of 109 individuals was screened using either polyacrylamide gel electrophoresis or high resolution melting analysis (Figure 5.9), and the mutation was not found in any.

Table 5.5. Extent of resequencing in MDIDJC candidate genes *PROSC, RAB11BPI1, BRF2 and ERLIN2.*

Gene Region	Sequence Read
PROSC	
Exon 1	-36 to +56
Exon 2-3	-54 to +64
Exon 4	-48 to +69
Exon 5	-97 to +90
Exon 6	-73 to +43
Exon 7	-46 to +81
Exon 8	-33 to +60

Gene Region	Sequence Read
RAB11BPI1	
Exon 1	-79 to +73
Exon 2	-24 to + 54
Exon 3	-33 to +36
Exon 4	-55 to +32
Exon 5	-18 to +60
Exon 6	-43 to +25
BRF2	
Exon1	-65 to +41
Exon2	-126 to +82
Exon3	-67 to +29
Exon4	-33 to +38

Gene Region	Sequence Read
ERLIN2	
Exon 1	-82 to +33
Exon 2	-31 to +58
Exon 3	-45 to +45
Exon 4	-28 to +36
Exon 5-6	-33 to +61
Exon 7-8	-68 to +50
Exon 9	-33 to +68
Exon 10	-69 to +50
Exon 11	-35 to +75
Exon 12	-26 to +92

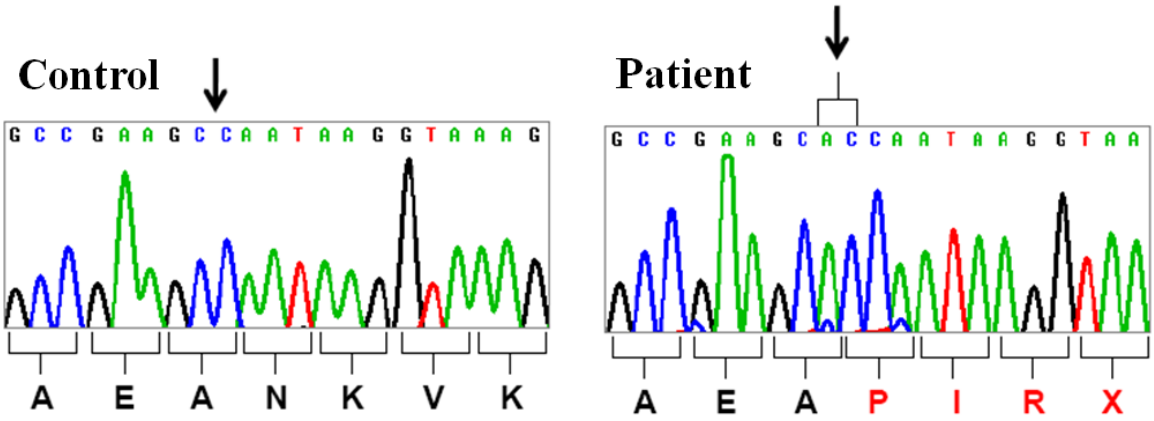

Figure 5.7. Partial chromatograms showing mutation c.812_813insAC in *ERLIN2* and the reference sequence. The insertion of 2 nucleotides results in a frameshift and premature translational termination after only 3 codons (p.Asn272ProfsX4).

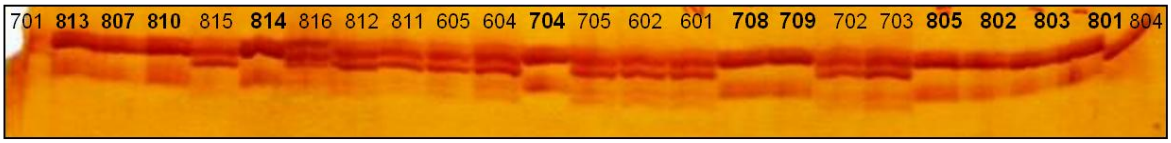

Figure 5.8. Segregation profile of c.812_813insAC in MDIDJC family. Affected individuals are indicated in bold. The larger allele with the insertion corresponds to the mutated allele.

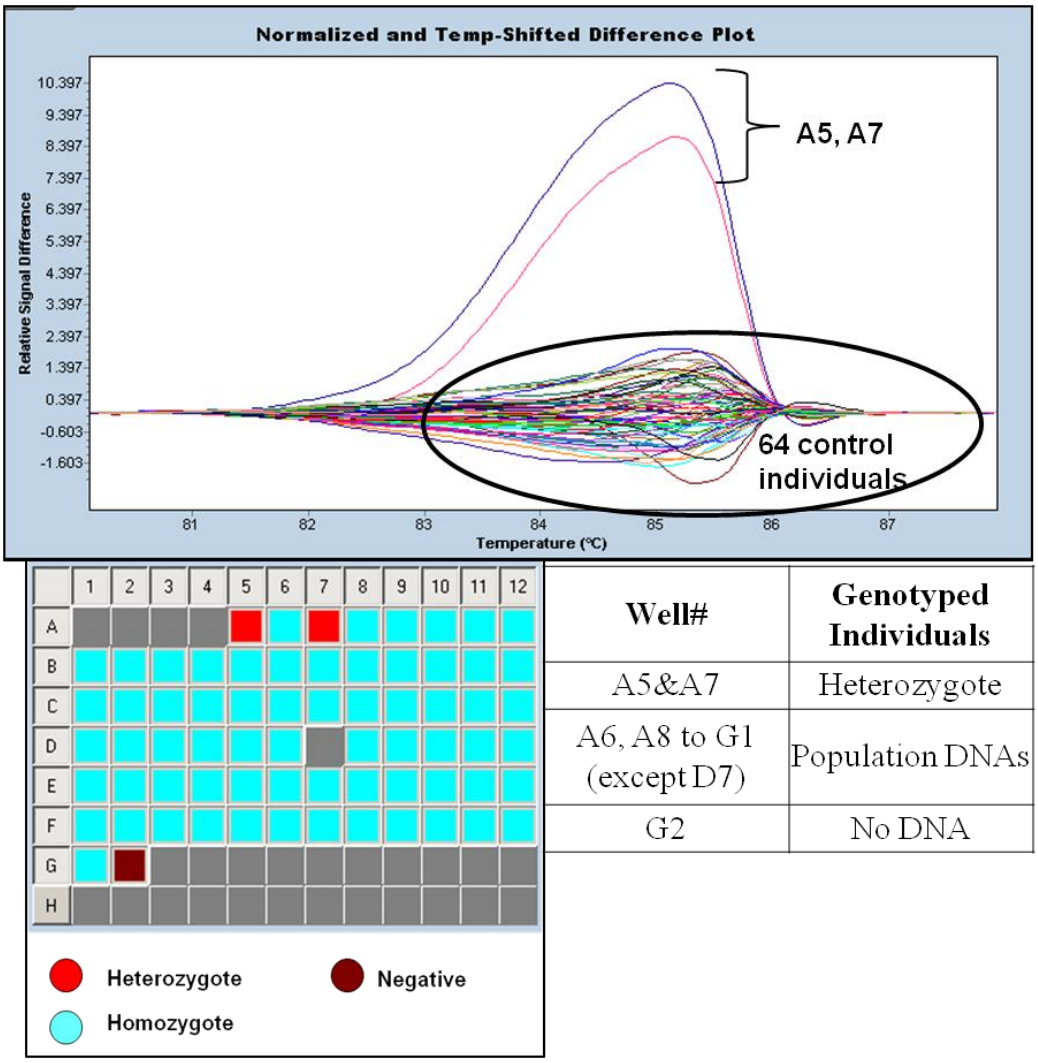

Well#	Genotyped Individuals
A5&A7	Heterozygote
A6, A8 to G1 (except D7)	Population DNAs
G2	No DNA

Figure 5.9. High Resolution Melting Curve analysis in 66 control DNAs for c.812_813insAC. Grey wells have no samples.

5.2.4. Assessment of Relative ERLIN2 Transcript Levels

ERLIN2 transcript levels were investigated relative to control individuals in three patients carrying the variant c.812_813insAC homozygously and three heterozygous carriers. The amplification efficiencies of both target and reference genes were not as desired. Standard deviations for some individuals were as high as 0.45. The results are not suitable for making a comparison between individuals (Figure 5.10). However, the results showed the absence of mRNA decay in affected individuals.

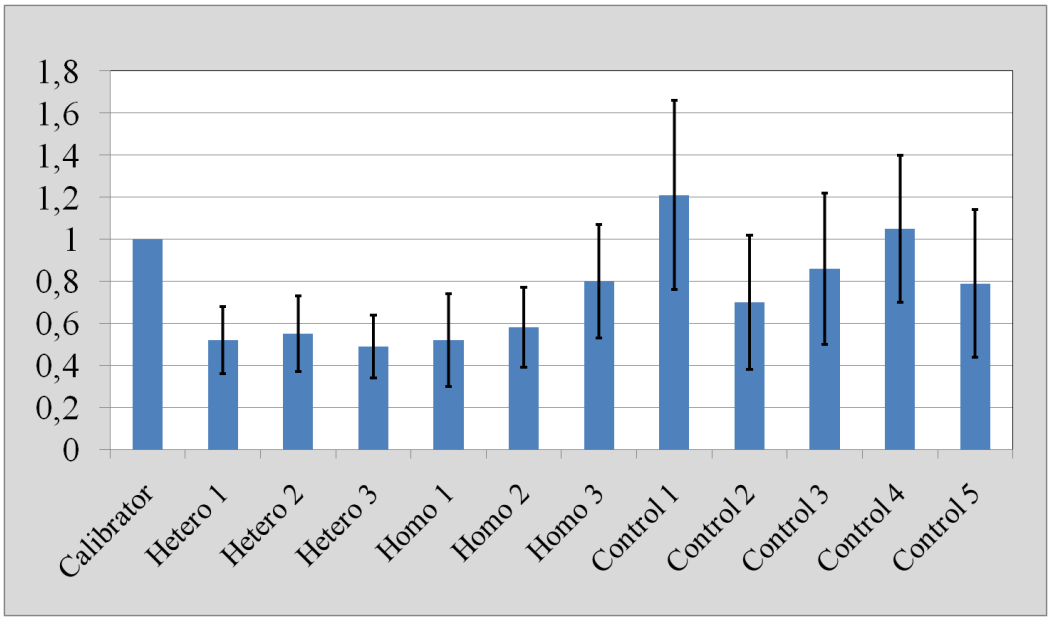

Figure 5.10. ERLIN2 transcript levels relative to HPRT1 in some MDIDJC members. Hetero: heterozygous mutation carrier, Homo: homozygous mutation carrier.

5.3. Median Cleft Lip

The family has four affected children (Fig 3.5). Mother 204 and sib 303 were described as subclinical, since their phenotype is barely noticeable. Cousins 301 and 311 are minimally affected.

5.3.1. Multipoint Linkage Analysis

5.3.1.1. Multipoint Linkage Analysis in a Fully Penetrant Autosomal Recessive Model including Only the MCL Sibs (Partial Pedigree A)

Assuming a recessive model with full penetrance, multipoint lod scores were calculated for only four affected sibs and their parents, since the four sibs were the most severely (Figure 3.4). The results for all autosomal chromosomes and PAR regions are presented in Figure A.2 in Appendix. Multipoint lod scores >2 are presented in Table 5.6.

5.3.1.2. Multipoint Linkage Analysis in a Fully Penetrant Autosomal Dominant Model Using Affected, Subclinical and Two Unaffected Sibs, and Subclinical Mother (Partial Pedigree B)

Two unaffected sibs (308 and 309) and subclinical sib 304 were also included in the linkage analysis. The status of subclinical individuals 204 and 304 were introduced to the program as affected (Figure 3.4). The results for all autosomal chromosomes and PAR regions are presented in Figure A.3 in Appendix. Multipoint lod scores >1.7 are presented in Table 5.6.

5.3.1.3. Multipoint Linkage Analysis in an Autosomal Dominant Model with 80 per cent Penetrance, Including All Affected and Three Unaffected Sibs (Partial Pedigree C)

Four affected sibs and three unaffected sibs 306, 308 and 309 were included in the analysis, and the father and mother were introduced to the program as unaffected (Figure 3.4). Penetrance was assumed 80 per cent. Multipoint lod scores for all autosomal chromosomes and PAR regions are presented in Figure A.4 in Appendix. Multipoint lod scores >1.2 are presented in Table 5.6.

Table 5.6. Multipoint lod scores obtained for MCL in fully penetrant autosomal recessive or dominant models or in an autosomal dominant model with 80 per cent penetrance using partial pedigrees A, B or C. Different combinations of sibs were included in each model: A. Only affected sibs. Their parents were introduced as cousins. Scores only >2 are presented, B. Affected, subclinical and two unaffected sibs, and subclinical mother. Scores only >1.7 are presented, C. including all affected and three unaffected sibs. Scores only >0.9 are presented.

CHROMOSOME	SNPs	GENETIC POSITION (cM)	Physical POSITION (bp)	Max. MPT
A. RECESSIVE MODEL WITH FULL PENETRANCE (Family Model A)				
1p31.1 – 31.2	rs3748705 – rs11163752	97.32 – 109.86	68624878 – 83934440	3.0
1q32.3	rs2660635 – rs2356932	215.73 – 215.94	209482201 – 209704488	2.6
1q44	rs1495942 – rs11590498	271.95 – 272.20	245075384 – 245135714	2.16
1q44–qter	rs4658713 – rs11590498	273.05 – qter	245135714 – 249250621 (qter)	3.0
12p13.1	rs7134402 – rs10772620	30.81 – 31.48	13097327 – 13256353	2.69
12p12.3	rs746690 – rs2075267	33.69 – 33.99	14783798 – 15115101	2.80
13q34	rs2075267 – qter	132.72 – qter	115008388 – 115169878 (qter)	2.8
15q.14	rs7167921 – rs955431	34.77 – 35.28	35671418 – 35984192	3.0
B. **DOMINANT MODEL WITH FULL PENETRANCE (Family Model B)**				
1q41	rs2501849 – rs2009112	219.03 – 227.60	212846609 – 218553529	1.79
2p24.3 – 2p24.2	rs1421608 – rs12621971	37.86 - 42.35	15854600 – 19066741	1.79
7p21.2	rs3801094 – rs2041556	27.16 – 29.34	13959406 – 15157688	1.79
7q34–35	rs41717 – rs10273192	151.32 – 163.86	139670417 – 149937855	1.79
9q31.3 – 33.1	rs10116353 – rs12378647	115.34 – 128.75	111950088 – 122001714	1.79
13q13.3 – 14.1	rs530240 – rs11116993	34.87 – 43.90	36256217 – 41027503	1.79
C. DOMINANT MODEL WITH 80 per cent PENETRANCE (Family Model C)				
2p24.3 – p23.2	rs12618251 – rs1581035	37.86 – 52.30	15850680 – 28686332	1.7
5p15.33	0 – rs293101	0 – 12.57	0 – 4582220	1.27
7p22.3	0 – rs28522260	0 – 4.04	0 – 1183964	1.27
7p21.2	rs3801094 – rs2041556	27.16 – 29.34	13959406 – 15157688	1.28
7p11.2 – q11.23	rs11976070 – rs1906889	137.92 – 147.30	54949471 – 75918024	1.27
8p21.2 – p12	rs1377336 – rs13278931	48.99 – 54.03	27890858 – 30879207	1.27
8q13.2 – q22.1	rs874805 – rs2466130	80.18 – 104.08	69077751 – 97182269	1.27
9q34.13 – q34.3	rs10119818 – rs7029507	142.82 – 161.71	133021887 – 138476823	1.27
13q13.3 – q14.11	rs9545074 – rs11617562	34.92 – 43.80	36273871 – 41009283	1.27
14q11.2 – q12	rs2792135 – rs17109384	4.42 – 20.96	20409258 – 25443592	1.27
19p13.3	0 – rs2074864	0 – 11.25	0 – 3155736	1.27
22p13 – q11.21	0 – rs361626	0 – 3.06	0 – 17823261	1.28

5.3.1.4. Multipoint Linkage Analysis in an Autosomal Dominant Model with 80 per cent Penetrance Using Only Affected Sibs (Partial Pedigree A)

Four affected sibs and their parents were used in the calculations. The parents were introduced to the programs as cousins (Figure 3.4). Results for all autosomal chromosomes and PAR regions are presented in Figure A.5 in Appendix. Multipoint lod scores >0.8 are presented in Table 5.7.

5.3.1.5. Multi Point Linkage Analysis in an Autosomal Dominant Model with 80 per cent Penetrance Using Affected Sibs and Minimal Cousins (Partial Pedigree D)

Results for all autosomal chromosomes and PAR regions are presented in Figure A.6 in Appendix. Multipoint lod scores >0.8 are presented in Table 5.7.

Table 5.7. Lod score results for an autosomal dominant model for MCL with 80 per cent penetrance using partial pedigrees A or D. Only scores >0.9 are given.

CHROMOSOME	SNPs	GENETIC POSITION (cM)	Max. MPT
A. DOMINANT MODEL WITH 80 PER CENT PENETRANCE (Partial Pedigree A)			
1	rs2270003 – rs1563954	78.43 – 86.94	0.97
	rs1933301 – rs2765241	89.07 – 89.77	1.08
	rs2765241 – rs11208148	89.77 – 90.90	0.86
	rs12736336 – rs6588083	90.96 – 92.49	1.16
	rs6588083 – rs3014983	92.49 – 93.26	0.92
	rs1574781 – rs1863155	184.84 – 188.54	1.08
	rs2073237 – rs10489409	189.37 – 190.34	1.08
	rs269741 – rs1171148	192.17 – 192.76	1.08
	rs6701258 – rs4657927	194.08 – 196.11	1.08
	rs4520444 – rs1471646	196.99 – 198.07	1.08
	rs880766 – rs12406229	203.55 – 206.05	1.08
	rs1160530 – rs10863725	213.02 – 214.62	1.08
	rs6689839 – rs1934619	216.38 – 217.49	1.08
	rs2211127 – rs10863310	222.53 – 226.35	1.08
	rs10495459 – rs12130718	259.62 – 260.11	1.04
	rs1000543 – rs901666	267.63 – 272.02	1.11
	rs6687026 – rs1770011	274.91 – 275.66	1.10

Table 5.7. Lod score results for an autosomal dominant model for MCL with 80 per cent penetrance using partial pedigrees A or D. Only scores >0.9 are given (continued).

2	rs13000767 – rs907169	33.86 – 35.47	1.08
	rs1829731 – rs6544021	42.93 – 47.51	1.07
	rs1541984 – rs2272417	49.30 – 51.89	1.08
	rs7421353 – rs2084336	52.96 – 54.64	1.08
6	rs150125 – rs1504281	100.54 – 100.80	1.08
	rs12202509 – rs9373790	108.66 – 110.17	1.08
	rs13202332 – rs10499099	113.21 – 122.15	1.08
	rs7750201 – rs1475143	147.19 – 153.99	1.08
	rs201202 – rs717324	109.17 – 10.02	1.08
	rs6934663–rs13214546	114.26 – 122.16	1.08
	rs7750201 – rs1475143	147.22 – 153.99	1.08
	rs2101878 – rs551444	180.92 – 181.73	1.04
	rs10946121 – rs6928843	183.99 – 193.53 (6qter)	1.08
7	rs6973935 – rs17142627	27.16 – 35.69	1.16
	rs1717942 – rs4870630	79.35 – 79.48	1.06
	rs205764 – rs9690297	135.09 – 135.89	1.07
	rs6961391 – rs10488413	142.45 – 143.46	1.08
	rs7784757 – rs2058265	144.99 – 150.89	1.08
	rs38723 – rs4236467	152.56 – 154.02	1.07
	rs11979955 – rs4725704	156.61 – 158.15	1.03
	rs975017 – rs3763422	163.25 – 163.89	1.01
8	rs11786195 – rs17571033	55.98 – 61.40	1.08
	rs11782124 – rs4433176	63.61 – 63.89	0.97
	rs4330677 – rs2272653	129.62 – 148.11	1.08
	rs2922500 – rs11996214	149.59 – 149.72	1.04
	rs4243852 – rs2873443	151.92 – 153.26	1.08
	rs7828715 – rs908843	155.56 – 156.1	1.08
9	rs10869715 – rs3905245	74.00 – 75.80	1.08
	rs10867814 – rs1898321	82.07 – 84.12	1.08
	rs1475617 – rs2183939	88.13 – 89.74	1.08
	rs1931371 – rs2026001	99.02 – 102.18	1.08
	rs518655 – rs1891218	103.48 – 106.65	1.05
	rs10979136 – rs937160	113.90 – 114.89	1.08
	rs1889326 – rs4576485	117.19 – 117.96	1.08
	rs10981621 – rs2806073	120.29 – 127.17	1.08
11	rs7936809 – rs294027	43.36 – 44.72	0.92
	rs4923583 – rs3802914	46.38 – 47.47	1.08
	rs12366193 – rs10501156	52.31 – 55.187	1.08
	rs11036320 – rs2862573	59.17 – 59.88	1.06
	rs2903517 – rs12362406	65.29 – 65.86	1.05

Table 5.7. Lod score results for an autosomal dominant model for MCL with 80 per cent penetrance using partial pedigrees A or D. Only scores >0.9 are given (continued).

11	rs618320 – rs1255453	98.48 – 99.35	0.89
	rs1532816 – rs17636424	104.59 – 105.55	1.08
	rs9667864 – rs589623	106.74 – 107.18	1.07
	rs260818 – rs524764	107.70 – 109.87	1.08
12	rs10848844 – rs609018	8.10 – 11.74	1.14
	rs609018 – rs11616092	11.74 – 24.38	>0.9
	rs10772001 – rs6488306	25.03 – 25.98	1.09
	rs2416791 – rs10772530	26.72 – 28.59	0.96
	rs10772530 – rs1061047	28.59 – 30.71	1.02
	rs7962966 – rs1550990	36.44 – 37.13	1.06
	rs1444630 – rs10743413	39.81 – 41.57	1.08
	rs2169989 – rs4964001	48.52 – 50.11	1.07
13	rs9550371 – rs9315777	27.88 – 43.86	1.08
	rs9586007 – rs3813131	100.51 – 132.80 (13qter)	1.08
16	rs8466 – rs4786169	1.15 – 20.03 (16pter)	1.08
17	rs1390247 – rs6502860	13.26 – 13.88	1.08
18	rs1442982 – rs10775449	54.84 – 55.95	1.08
	rs16963537 – rs10460048	56.33 – 56.43	1.07
21	rs2039241 – rs10482885	10.86 – 11.42	1.08
	rs1989458 – rs4818568	18.04 – 19.41	1.08
	rs2826621 – rs2828028	20.76 – 23.48	1.08
	rs2040144 – rs2212535	24.36 – 25.58 (21qter)	0.99
	rs2212535 – rs2834079	25.58 – 38.24	1.08
22	rs3954571 – rs2543958	2.88 – 8.07	1.09
PAR1	rs35193207 – rs28615667	0.00 – 7.35 (PARpter)	0.98
B. DOMINANT MODEL WITH 80 PER CENT PENETRANCE (Partial Pedigree D)			
1	rs649608 – rs2772304	91.80 – 97.35	1.22
	rs10873947 – rs4650571	104.93 – 105.02	1.16
	rs1998981 – rs2389165	108.14 – 108.72–	1.22
	rs9724933 – rs10493712	108.81 – 108.97	1.22
	rs860873 – rs259325	120.28 – 120.60	1.16
	rs680954 – rs635578	121.16 – 121.36	1.16
	rs11185392 – rs7552867	126.61 – 127.02	1.08
	rs4468120 – rs6662137	182.98 – 227.58	1.16
	rs3003542 – rs2994329	266.58 – 267.42	1.08
	rs4658749 – rs10924197	273.66 – 274.01	1.07
	rs10399672 – rs4359061	277.79 – 279.95 (1qter)	1.16

Table 5.7. Lod score results for an autosomal dominant model for MCL with 80 per cent penetrance using partial pedigrees A or D. Only scores >0.9 are given (continued).

2	rs1374459 – rs13014571	48.25 – 48.77	1.22
	rs4555301 – rs7594717	52.96 – 53.47	1.16
	rs4605324 – rs4359705	53.92 – 54.33	1.18
	rs2710605 – rs1869824	57.28 – 57.39	1.02
	rs4952277 – rs218223	57.41 – 57.48	1.06
3	rs1513299-rs2068018	114.69 – 114.75	1.22
6	rs157705 – rs1498260	100.53 – 101.66	1.22
	rs793979 – rs6928843	180.90 – 193.53 (6qter)	1.16
7	rs13223093 – rs4723505	8.73 – 8.79	1.16
	rs10269406 – rs6954805	22.11 – 22.45	1.15
	rs2290837 – rs1404966	31.35 – 31.43	1.19
	rs115063 – rs16090	41.16 – 41.47	1.21
	rs6968694 – rs11764303	55.07 – 55.22	1.15
	rs11764303 – rs12111597	55.22 – 55.45	1.16
	rs2718031 – rs1420192	57.14 – 57.33	1.15
	rs7986 – rs10499593	57.96 – 58.16	1.12
	rs4723807 – rs1404999	61.11 – 61.53	1.10
	rs7796267 – rs6974322	67.17 – 67.29	1.03
	rs2728487 – rs327649	70.75 – 95.00	1.16
	rs924368 – rs1317056	140.42 – 141.26	1.21
	rs2350451 – rs1880791	144.05 – 144.63	1.16
8	rs2116078 – rs1080333	87.80 – 88.36	1.14
	rs10955256 – rs517811	110.99 – 111.78	1.08
	rs2511748 – rs2513924	113.05 – 113.22	1.19
	rs7827275 – rs2022970	115.78 – 115.86	1.20
	rs4330677 – rs4397407	129.62 – 156.33	1.22
9	rs7875946 – rs2106804	78.35 – 78.53	1.16
	rs1538752 – rs10512091	79.24 – 79.46	1.07
	rs1867283 – rs1490400	85.45 – 85.92	1.00
	rs17742650 – rs6479028	105.39 – 105.61	1.15
	rs6479056 – rs1337707	106.87 – 107.05	1.16
	rs4743634 – rs7862239	108.43 – 128.59	1.22
	rs4240705 – rs3750508	154.89 – 164.07 (9qter)	1.22
11	rs3851576 – rs3816621	122.35 – 130.39	1.16
12	rs10774156 – rs2109112	9.34 – 11.27	1.22
	rs12422778 – rs874682	14.57 – 14.69	1.22
	rs1060619 – rs2302367	18.41-19.16	1.18
	rs3847916 – rs3852575	35.03 – 35.48	1.18
	rs10846378 – rs1513047	36.01 – 36.30	1.20
	rs725124 – rs1909355	44.59 – 45.48	1.22

Table 5.7. Lod score results for an autosomal dominant model for MCL with 80 per cent penetrance using partial pedigrees A or D. Only scores >0.9 are given (continued).

12	rs859202 – rs6487465	47.27 – 47.79	1.22
	rs2220168 – rs10843013	50.13–51.95	1.22
	rs4409923 – rs2116675	119.69 – 120.05	1.22
	rs4525299 – rs2283351	127.42 – 128.12	1.16
	rs2081587 – rs739	131.20 – 131.43	1.04
	rs7134868 – rs1318549	148.86 – 163.15	1.22
14	rs3764164 – rs2152278	16.26 – 56.72	1.22
	rs1028458 – rs4898955	60.90 – 60.99	1.13
	rs4310777 – rs1256501	66.52 – 67.08	1.10
	rs10483869 – rs8015242	76.42 – 76.70	
	rs4899579 – rs4569181	77.35 – 77.78	1.16
	rs4020115 – rs7144274	80.21 – 80.42	1.16
	rs9972219 – rs2022773	86.73 – 87.42	1.22
15	rs7167921 – rs955431	34.77 – 35.28	1.15
	rs11637130 – rs9920962	62.38 – 63.69	1.16
18	rs1442982 – rs10460048	54.84 – 56.43	1.16
19	rs740873 – rs2301843	13.57 – 13.98	1.16
	rs4807578 – rs2288932	15.66 – 16.23	1.15
	rs2967675 – rs953551	28.86 – 29.75	1.14
	rs2287802 – rs3826689	31.66 – 43.07	1.16
20	rs214831 – rs6039403	0.00 – 8.34 (20pter)	1.22
21	rs2827461 – rs2829294	22.35 – 25.64	1.16
	rs2833143 – rs11701477	33.45 – 33.81	1.15
	rs2833505 – rs11700457	34.82 – 35.0	1.15
	rs2833690 – rs2833841	35.81 – 36.67	1.15
22.	rs3954571 – rs2401081	2.88 – 3.04	1.43

5.3.1.6. Multipoint Linkage Analysis in a Fully Penetrant Autosomal Recessive Model Including the Affected Sibs and Minimal Cousins (Partial Pedigree D)

Assuming a recessive model with full penetrance, multipoint lod scores were calculated for four affected sibs, the minimal cousins and their parents. The results for autosomal loci yielding positive multipoint lod scores are presented in Figure A.7 in Appendix.

5.3.2. Homozygosity Mapping Using a Fully Penetrant Autosomal Recessive Model Including Only the Affected Sibs (Partial Pedigree A)

The results of haplotype analysis at the regions where multipoint lod scores were >1.8 using partial pedigree A are given below in the order of chromosome number and chromosomal position. The loci were later re-evaluated using the denser genome scan performed on the affected sib 305.

5.3.2.1. Chromosome 1

The data generated by SNP genome scan of the family members were analyzed on Excel sheets. In the region between rs3748705-rs11163752 (68.62-83.93 Mb) (Table 5.6), all affected sibs and minimal individual 301 were homozygous, but 301 had a different homozygosity. Minimal individual 311 and subclinical individuals 204 and 304 were heterozygous for the common haplotype. Homozygosity at the region was verified by genotyping with microsatellite markers; the haplotype segregation pattern was compatible with SNP genotype results (Table 5.8). Within this region, between markers rs10493492-rs1445591 (72500375-72960011 bp) the minimal individuals shared homozygosity with each other, but this homozygosity was different from the affected ones. All minimal and affected individuals shared the same homozygosity between markers rs2660635-rs1988163 (1q32.3, 209.48-209.58 Mb). But after a denser whole-genome scan in affected individual 305, homozygosity at this region disappeared.

In region rs1495942-rs11590498 (1q44, 245.07-245.14 Mb), the homozygosity shared by all affected sibs disappeared similarly after the denser scan.

In region rs4658713-rs1173843 (245.33-245.53 Mb) all affected individuals and unaffected sib 306 shared the same homozygosity. The parents of affected sibs were informative.

In region rs10924523-rs960227 (246.32-246.56 Mb), all affected individuals and unaffected sibling 306 had the same homozygous haplotype. However, homozygosity disappeared after the denser SNP scan.

In region rs4478844-qter (248.13-249.30 Mb), all affected sibs shared the same homozygosity. Some unaffected sibs shared the homozygous genotype in some parts. In region rs4478844-r6683472 (248.12-249.08 Mb) minimal 311 also shared the homozygosity. The parents were informative.

Table 5.8. Verification of homozygosity between 68.72 and 81.90 Mb at 1p31.1-31.2 and at 1qter using microsatellite markers.

Marker	Mb	203 M,SC	204 F,UA	309 UA	305 A	310 A	303 A	302 A	308 UA	306 UA	304 SC	307 UA
D1S2137	68.72	2,2	2,2	2,2	2,2	2,2	2,2	2,2	2,2	2,2	2,2	2,2
D1S1585	81.90	4,5	1,5	4,5	5,5	5,5	5,5	5,5	1,5	1,5	1,5	1,5

Marker	Mb	202 M,UA	201 F,UA	301 Mi	206 M,UA	205 F,UA	311 Mi
D1S2137	68.72	2,2	2,3	2,2	1,3	3,3	1,2
D1S1585	81.90	4,4	4,4	4,4	2,4	3,5	2,3

Marker	Mb	204 M,SC	203 F, UA	309 UA	305 A	310 A	303 A	302 A	308 UA	306 UA	304 SC	307 UA
D1S247.135M	249.169	1,2	1,3	1,2	1,1	1,1	1,1	2,2	2,3	1,2	2,3	1,2

Marker	Mb	202 M,UA	201 F, UA	301 Mi	206 M,UA	205 F, UA	311 Mi
D1S247.135M	249.169	2,2	1,2	2,3	2,2	1,2	1,2

M: mother, F: father, UA: unaffected, A: affected, SC: subclinical, Mi: minimal

5.3.2.2. Chromosome 12

In region rs7134402-rs10772620 (13.09-13.26 Mb), while all affected siblings shared the same homozygous haplotype, minimal 311 had a different homozygosity. After the denser SNP scan, the region was narrowed down to the interval between rs4763908 and rs10772620 (13.10 and 13.26 Mb).

In regions rs746690-rs2075267 (14.78-15.12 Mb) and rs746690-rs11614445 (14.78-14.94 Mb) all affected siblings shared same homozygous haplotype.

5.3.2.3. Chromosome 13

In region rs7331784-qter (114.99-115.20 Mb) all affected sibs, subclinical 304 and unaffected sibs 307 and 308 shared the same homozygous haplotype. However, the parents were informative.

5.3.2.4. Chromosome 15

In region rs7167921-rs955431 (35.67-35.98 Mb), all affected siblings shared the same homozygosity. The parents were informative.

5.3.3. Homozygosity Mapping Using a Fully Penetrant Autosomal Recessive Model Including the Affected Sibs and Minimal Cousins (Partial Pedigree D)

No region where all affected sibs and minimal cousins sharing the same homozygous haplotype was found.

5.3.4. Haplotype Inspection in a Fully Penetrant Dominant Model Using Affected, Subclinical and Two Unaffected Sibs, and Subclinical Mother (Partial Pedigree B)

Haplotypes were inspected at the loci yielding relatively high lod scores in a dominant model with full penetrance (for partial pedigree B: Figure 4.1.b). The regions where the same haplotype was shared by all affected sibs and minimal individuals are presented in Table 5.9.

Table 5.9. Regions where all affected and minimal individuals share the same haplotypes in chromosomes which yielded relatively high lod score using partial pedigree B.

Chromosome	SNPS	Genetic Position (cM)
1	rs4284238-rs2841616	221.40-222.39
	rs975994-qter	222.78-223.19
2	rs896609-rs16984751	41.42-41.91
7	rs4721330-rs6956840	27.97-28.31
9	rs4979030-rs1408337	118.63-119.14
	rs7042485-rs2812401	121.31-122.34
	rs2787328-rs10114562	123.58-123.87
	rs9299225-rs6478223	124.43-125.36
	rs4837514-rs4837864	126.00-126.24
	rs660234-rs10818153	127.12-127.56
	rs10818153-rs1572299	127.56-127.99
	rs10818265-rs1571903	128.26-128.75
13	rs790014-rs7988671	35.81-36.13
	rs9576460-rs6563594	39.36-39.70
	rs17298046-rs9566344	39.95-40.35
	rs2324460-rs7984035	42.19-42.40
	rs953977-rs2324591	42.40-43.11
	rs7991808-rs9315776	43.15-43.77

5.3.5. Haplotype Inspection in a Dominant Model With 80 per cent Penetrance Using All Affected and Three Unaffected Sibs (Partial Pedigree C)

The regions where the same alleles were shared by all affected sibs and minimal individuals are summarized in Table 5.10.

Table 5.10. Regions where all affected and minimal individuals share the same haplotypes in chromosomes which yielded relatively high lod score using partial pedigree C.

Chromosome	SNPs	Genetic Position (cM)
2	*rs896609-rs16984751	41.42-41.91
5	rs12520553-rs4975744	2.91-3.76
7	*rs4721330-rs6956840	27.97-28.31
	rs998827-rs2042067	140.81-141.25
	rs11769810-rs889929	141.38-141.64
	rs2350451-rs706557	144.05-144.57
8	rs7813272-rs4733224	53.51-54.08
	rs6468036-rs4733220	52.54-54.03
	rs1462441- rs1864605	90.84-91.04
	rs10103353-rs2895814	95.30-95.49
	rs1565226-rs2980372	96.35-96.78
13	rs790014-rs7988671	35.81-36.13
	rs9576460-rs6563594	39.36-39.70
	rs17298046-rs9566344	39.95-40.35
	rs2324460-rs7984035	42.19-42.40
	rs953977-rs2324591	42.40-43.11
	*rs7991808-rs9315776	43.15-43.77
14	rs4981223-rs12586536	6.51-6.89
	rs2874146-rs10483267	14.54-14.97
19	rs2074625-rs10416531	4.97-5.36
	rs758145-rs9967630	5.46-5.62
	rs4806874-rs9304900	9.29-9.81

* Same region that was indicated in section 5.3.4

5.3.6. Analysis of CNV Data

As has been mentioned, individual 305 was subjected to an additional genome scan with 610K SNP markers. CNV data were obtained and analyzed for deletions and duplications, which could be detected with the help of Perl Combined_CNV program. All the deletions and duplications within homozygous regions or at loci yielding relatively high lod scores are listed below in chromosomal order.

5.3.6.1, Chromosome 1

- rs17095902-rs6703099 (48 SNPs); 101.87-102.03 cM: Within the homozygous candidate regions, two intergenic deletions were identified at 1p31.1, within 72766085-72812440 bp and 75240211-75534319 bp. The maximum sizes of the deletions were 46353 and 294107 bp, respectively. The closest genes to the former deletion were *NEGR1* at 17808 bp upstream and *BC041341* 973,027 bp downstream. The latter deletion was 16,814 bp downstream of *TYW3* [tRNA-yW synthesizing protein 3 homolog (S. cerevisiae), MIM: 611245] and 49,149 bp upstream of *LHX8*. The former deletion was a polymorphism whereas the latter has not been reported. Additionally the former one was observed in all members regardless of their affection status. Thus, it was not considered as a candidate variation.

Haplotype inspection in all MCL family members (Figure 5.11.a and b) revealed that all affected sibs (302, 303, 305 and 310) were homozygous for this deletion. All the other sibs (304, 306, 307, 308 and 309) and the parents (203 and 204) of the affected sibs as well as 205 carried the deletion. Other members did not carry it.

Oligo primers specific to a region between the flanking SNPs that gave signals in the genome scan and the inner SNPs that did not give signals were designed to identify the breakpoints of the deletion. PCR amplification products obtained by using the primers presented in Table 4.4 were in expected lengths, as judged on agarose gels. Then primers YDdel_6-F and YDdel-7 were used to amplify across the deleted region in one of the patients. A maximum PCR product $\leq$ 1969 bp in length was expected. A band approximately 1500 bp was visualized on an agarose gel, and the product was sequenced directly. The exact length of the deletion was estimated as 273,164 bp, from 75,247,714 to 75,520,879 bp. The chromatograph showing the breakpoint is given in Figure 5.12.

Whether the other members of the MCL family carried the deletion was investigated using a new primer pair (YD_DEL_POP) that would amplify a small region in the allele with the deletion, across the deletion breakpoints. The presence of a fragment of 185 bp length would indicate that the individual carried the deletion in a homozygous or heterozygous state. Absence of an amplification product would mean the deletion-allele

was not carried at all. The optimization process was performed in an affected sib sample. The same products were obtained in all affected members but some non-specific products were also observed. Thus, new primers were designed for further amplification (YD_POP_2 and YD_POP_AMP-R).

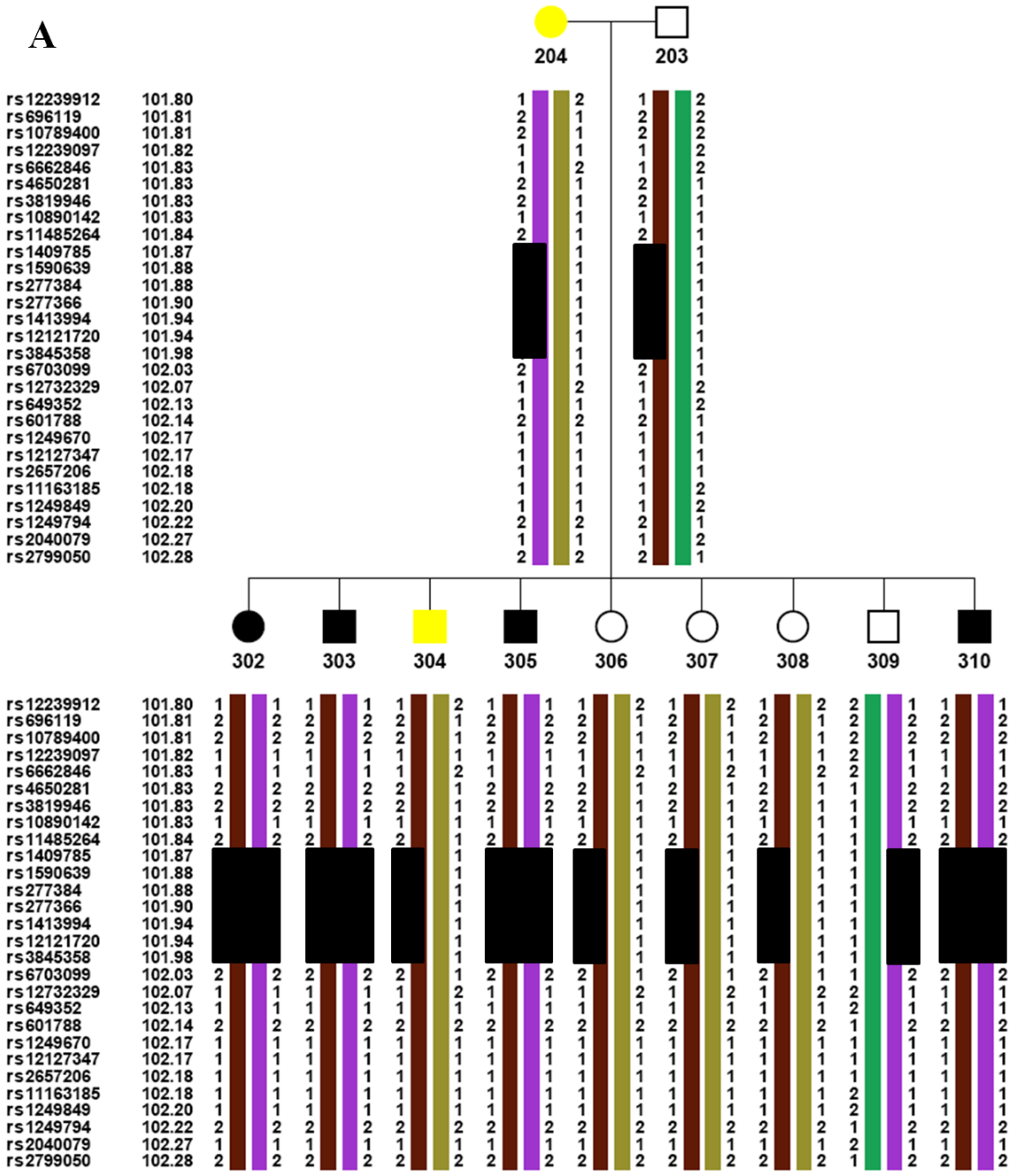

Figure 5.11. Haplotypes around the deletion at 1p31.1 for MCL family. a) The haplotypes of the core family, b) The haplotypes of the affected sibs and their parents, as well as minimals and their parents. Black rectangle represents the deletion.

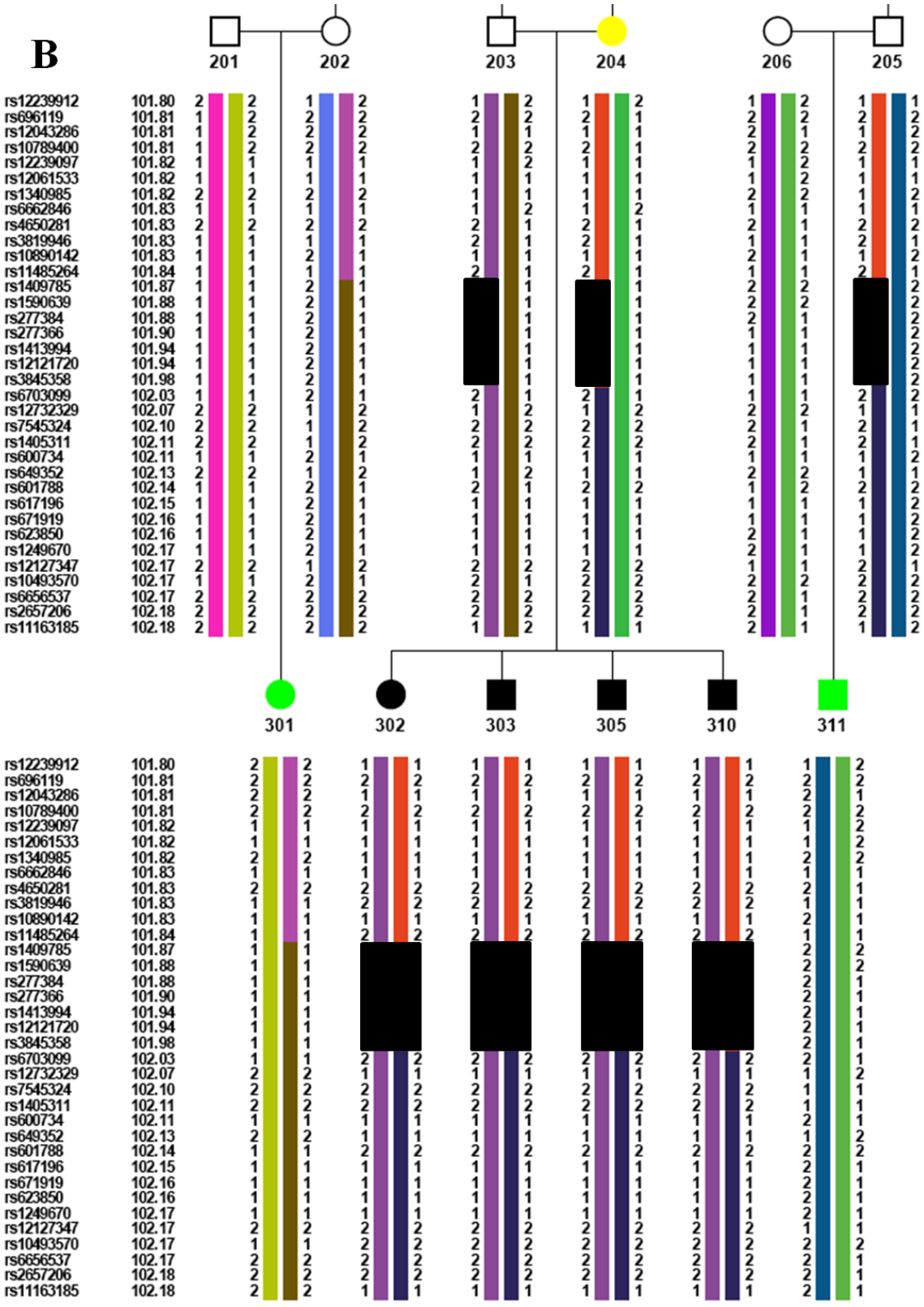

Figure 5.11. Haplotypes around the deletion at 1p31.1 for MCL family. a) The haplotypes of the core family, b) The haplotypes of the affected sibs and their parents, as well as minimals and their parents. Black rectangle represents the deletion (continued).

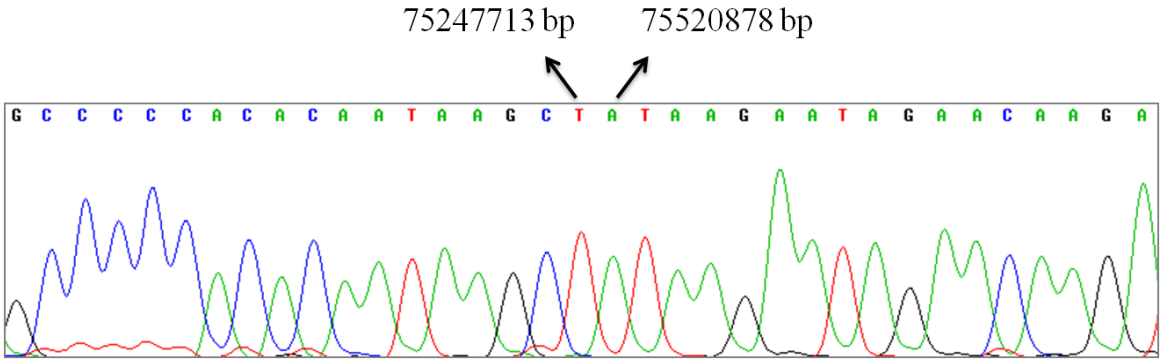

Figure 5.12. Partial chromatogram showing the breakpoints of the deletion at 1p31.1.

Figure 5.13 shows the evolutionary conservation of the sequences of the deleted region among other primates, mammals and other vertebrates.

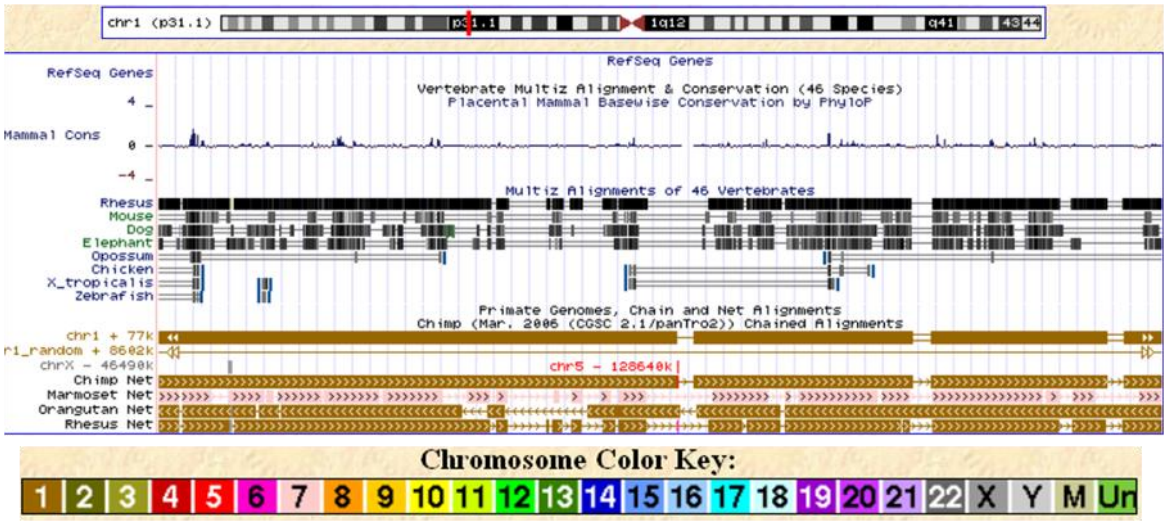

5.13. Evolutionary conservation graphic of the sequences of the deleted region among primates and other mammals and vertebrates.

- rs6661612-rs580526 (31 SNPs); 126.29-126.317 cM: Homozygous deletion and heterozygous duplication. In this locus, all affected and minimals shared the same allele. It was not a novel mutation.

- rs1439765-rs3009841 (31 SNPs); around 203.55 cM: Homozygous deletion. It lies within a region that yielded high MPT lod score (1.16) in the 80 per cent penetrant dominant model using partial pedigree D. It was not a novel mutation.

- rs2929833-rs2749172 (24 SNPs); around 144.43 cM:_Homozygous deletion. The deletion harbors the gene *NR_003377* (PDZK1P1 -PDZ domain containing 1 pseudogene 1). The genes containing PDZ domain interferes with Smad signaling pathway (Warner et al, 2003). The regions flanking the deletion are not homozygous in the affected siblings. It does not lie within a region that yielded high lod score. It was not a novel mutation.

5.3.6.2. Chromosome 6

- rs4235991-rs4235991 (5 SNPs); around 192.811 cM**:** Homozygous duplication. It lies within a region that yielded high MPT lod score (1.16) in the 80 per cent penetrant dominant model using partial pedigree D. It was not a novel mutation.

5.3.6.3. Chromosome 7

- rs1406527-rs1729824 (5 SNPs); 76.17-76.209cM: Homozygous and heterozygous duplications. It lies within a region that yielded high MPT lod score (1.16) in the 80 per cent penetrant dominant model partial pedigree D. It was not a novel mutation.

- rs12674132-rs1598411 (26 SNPs); around 79.89 cM:_Heterozygous duplication. It lies within a region that yielded high MPT lod score (1.16) in the 80 per cent penetrant dominant model using partial pedigree D. It was not a novel mutation.

- rs1574986-rs6956675 (2 SNPs); around 79.897 cM:_Homozygous duplication. It lies within a region that yielded high MPT lod score (1.16) in the 80 per cent penetrant dominant model using partial pedigree D. It was not a novel mutation.

5.3.6.4. Chromosome 8

- rs8175350-rs6997669 (9 SNPs); 63.029-63.503 cM: Heterozygous duplication. It lies near a region that yielded high MPT lod score (0.97) in the 80 per cent penetrant dominant model using partial pedigree A. *POTEA* gene (POTE ankyrin domain family, member A) resides downstream of the duplication. *ANKS6* includes ankyrin repeats. A

SNP in *ANKS6* with cleftings and dental morphology has been associated with cleftings and dental morphology (Vieira et. al 2008). The duplication was not a novel mutation.

- rs16904092-rs1897683 (5 SNPs); 142.191-142.205 cM: Homozygous duplication. It lies within a region that yielded high MPT lod score in the 80 per cent penetrant dominant model using partial pedigrees both A and D (1.08 and 1.22, respectively). It has not been reported.

5.3.6.5. Chromosome 11

- cnvi0005120-rs35834377 (2 SNPs); 59.68 cM: Homozygous deletion. Any signal could not be detected in some of the family members. (The individuals from which a signal could be detected might carry a heterozygous deletion.) It lies within a region that yielded high MPT lod score (1.06) in the 80 per cent penetrant dominant model using partial pedigree A. It was not a novel mutation.

- rs1588069-rs4441015 (48 SNPs); 65.417 cM: Homozygous and heterozygous deletions. It lies within a region that yielded high MPT lod score (1.05) in the 80 per cent penetrant dominant model using partial pedigree A. It was not a novel mutation.

5.3.6.6. Chromosome 14

- rs28796940-rs1937746 (91 SNPs); 4.1-4.18 cM: Heterozygous duplication. It resides near the region that yielded high MPT lod score (1.27) in the 80 per cent penetrant dominant model using partial pedigree C. It was not a novel mutation.

- rs4502127-rs1778370 (7 SNPs); 45.04-45.06 cM: Heterozygous deletion. It lies within a region that yielded high MPT lod score (1.22) in the 80 per cent penetrant dominant model using partial pedigree D. It was not a novel mutation.

5.3.6.7. PAR1

- cnv13984PP1-cnv13027PP9 (7 SNPs); 1.182-1.185 cM: Heterozygous duplication. It lies within a region that yielded high MPT lod score (0.98) in the 80 per cent penetrant dominant model using partial pedigree A. It has not been reported.

5.3.7. Candidate Gene Approach

Among the 85 genes at 1p31.1–p31.2 (68,624,878-83,934,440 bp), *NEGR1*, *LHX8* and *LOC646556* were assessed as best candidates. All exons and flanking regions were sequenced in an affected individual; no novel mutation was detected (Table 5.11).

Table 5.11. Extent of resequencing in MCL candidate genes *NEGR1*, *LHX8* and *LOC64655*.

Gene Region	Sequence Read
NEGR1	
Exon 1	–31 to +71
Exon 2	–71 to +74
Exon 3	–71 to +79
Exon 4	–136 to +171
Exon 5	–77 to +98
Exon 6	–33 to +47
Exon 7	–39 to +133
LOC646556	
Exon 1	–31, +135
Exon 2	–185 to +100
Exon 3	–85, +72

Gene Region	Sequence Read
LHX8	
Exon 1	–70 to + 42
Exon 2	–101 to + 76
Exon 3	–74 to +126
Exon 4	–139 to +121
Exon 5	–111 to +106
Exon 6	–31 to + 86
Exon 7	–71 to +42
Exon 6	–34 to +52
Exon 7	–80 to +74
Exon 8	–106 to +111
Exon 9	–117 to +106
Exon 10	–92 to +105

5.3.8. Loci of Genes Associated with Cleft Lip and/or Palate

The genes that are associated with cleft lip and/or palate are listed in Table 1.3 in Introduction. Whether any of them or some other genes belonging to the same gene families were located within any region that yielded high multipoint lod score was investigated. The genes, their locations, assumed penetrance level and partial pedigrees

that yielded relatively high lod score and the maximum MPT lod scores obtained are presented in Table 5.12

Table 5.12. Genes associated with clefts or their paralogs that are located within regions that yielded high MPT in dominant models.

Gene ID	**MIM**	**Chromosome**	**PHYSICAL POSITION (Mb)**	**Max. MPT**	**Penetrance**	**Partial Pedigre**
ANKS6	-	9q22.33	101,558,794-101,494,291	1.05	80	A
BMP4	112262	14q22-23	54,416,454-54,423,554	1.22	80	D
EGFR	131550	7p12	55,086,725-55,275,031	1.16	80	D
FGF10	602115	5p13-p12	44,305,097-44,388,784	1.27	80	C
FGFR1	136350	8p11.2-p11.1	38,268,656-38,326,352	1.08	80	A
GDF6	-	8q22.1	97,154,558-97,173,020	1.27	80	C
GDF7	-	2p24.1	20,866,424-20,871,250	1.7	80	A, C
FOXB1	-	15q21-q26	60,296,42-60,298,142	1.16	80	D
FOXE1	602617	9q22	100,615,537-00,618,997*	0.83	80	A
IRF6	607199	1q32.3-q41	209,961,262-209,979,479	1.79	80	D
NANOGP5	-	9q31	102,937,281-102,939,278	1.05	80	A
NANOG	607937	12p13.31	7,941,995-7,948,655	0.90	80	A
PAX9	167416	14q12-q13	37,126,782-37,147,012	1.22	80	D
PTCH1	601309	9q22.3	98,279,247-98,205,264	1.08	80	A
PVRL1	600644	11q23.3	119,508,808-119,599,435	1.16	80	D
SMAD9[b]	603295	13q12-q14	37,422,207-37,494,409	1.79; 1.08, 1.27	Full; 80	B; A, C
TGFB2[c]	190220	1q41	218,519,391-218,617,961	1.79	80	B
TGFBR1	190181	9q22	101,867,412-101,916,474	1.05	80	A
TMEFF1	603421	9q31	103,235,717-103,339,914	0.95	80	A

*This region was not included in Table 5.7.

6. DISCUSSION

In the framework of this study, the gene responsible for Autosomal-Recessive Motor Dysfunction, Intellectual Disability and Multiple Joint Contractures was identified, a mutation in Geroderma Osteodysplastica family was found, and the disease locus for MCL and subsequently a homozygous intergenic novel deletion were identified.

6.1. Geroderma Osteodysplastica

The disease in the family studied here exhibited autosomal recessive inheritance, and it had been initially diagnosed as GO. While the thesis was in progress, the gene responsible for GO was identified as *SCYL1BP* (Hennies et *al*., 2008; Al-Dosari and Alkuraya, 2009) residing at 1q24. Additionally, some patients previously diagnosed with GO, WSS or DBS were found to have mutations in *PYCR1* (Guernsey *et al*., 2009; Reversade *et al*., 2009), and the disease was named cutis laxa, autosomal recessive, type IIB (ARCL2B). We had already mapped the disease locus, so *PYCR1* gene was analyzed in study patients, and homozygous mutation c.540+1G>A was detected. The mutation was reported in an Austrian patient and two Turkish patients (Reversade *et al*., 2009). Any consanguinity between those families and ours is not known.

Although c.540+1G>A had been reported as a mutation, no population screen had been performed. Therefore, 109 unrelated individuals representative of the Anatolian population were screened for this mutation to achieve at least 80 per cent power to distinguish a normal sequence variant (Collins and Schwartz, 2002). The mutation was not found in any, which indicates that this variant is not a polymorphism. The mutation is predicted to lead to the loss of the splice donor in intron 5 and thus the retention of the intron, although the potential aberrant splice products were not assayed. We observed that the substituted nucleotide is conserved in all U2-type GT–AG splice sites (Sheth *et al*., 2006) and accessed via bioinformatics tools that the effect of the mutation is potentially harmful.

PYCR1 catalyzes the conversion of Δ^1-pyrroline-5-carboxylic acid to L-proline. Proline is a stress substrate, and the enzymes involved in proline metabolism respond to mutagenic, inflammatory and nutritional stress (Phang *et al*., 2008). PYCR1 is localized to mitocohdria (Reversade *et al*., 2009). Reversade *et al*. (2009) showed that H_2O_2 treatment of skin fibroblast cells derived from *PYCR1* deficient individuals resulted in the collapse of the mitochondrial network and elevated cell death due to apoptosis. This data is in concordance with the findings that have demonstrated the protective effects of proline against reactive oxygen species and apoptosis (Krishnan *et al.*, 2008).

Twenty five per cent of collagen is hydroxyproline and proline (Dixit *et* al., 1977). Collagen is the main component of the extracellular matrix, connective tissue and the organic part of bone (Liu *et al*., 2005), which can explain the phenomenon that the primarily affected tissues in ARCL2B are skin and bones.

Deficiencies in Δ^1-pyrroline-5-carboxylate synthase gene (*ALDH18A1*), which is another enzyme participating in proline biosynthesis pathway, give rise to autosomal recessive neurocutaneous syndrome deficiencies. *ALDH18A1* also localizes to mitochondria. This disorder has many overlapping phenotypes with ARCL2B, such as neurodegeneration, lax skin and joint dislocations (Baumgartner *et al*., 2005; Bicknell *et al*., 2008). These data demonstrate that defects in proline pathway result in similar clinical features.

Using the results of this study, Dr. Beyhan Tüysüz reviewed the clinical features of all reported cases with mutations in either *PYCR1* or *GORAB*. In the patients with GORAB mutations, mental development was mostly normal. Only three patients described by Rajab *et al*. (2008) had mild learning disabilities. As for the patients reported here, one (Patient 2, 501) had apparently mild cognitive impairment and his cranial MRI was normal. The cognitive impairment in the other three was severe, and various findings were detected in their cranial MRI: agenesis of corpus callosum and dilatation of posterior horns of lateral ventricles (colpocephaly) (Patient 1, 504), enlarged ventricles (Patient 3, 405) and hypoplasia of cerebellum (Patient 4, 404). Interestingly, the cranial MRI findings of patient 1 were similar to those of two patients with *PYCR1* mutations (Reversade *et al*., 2009), described previously as GO both by Al-Gazali *et al*. (2001) and Nanda *et al*. (2008). The

three patients reported here with apparently severe cognitive impairment also displayed self-mutilation and had seizures. Seizures had been reported for other GO patients with cranial findings (Al-Gazali *et al*., 2001), whereas self-mutilation has not been reported. Selective mutism displayed by patient 2 (with mild cognitive impairment) has been reported in another GO patient (Al-Gazali *et al*., 2001).

To sum up, patients with *PYCR1* mutations have brain malformation and cognitive impairment whereas, patients with *GORAB* mutations generally do not have cognitive impairment. Also, seizures and behavior abnormalities such as selective mutism and self-mutilation are associated with *PYCR1* mutations. The patients reported with *GORAB* mutations had more severe osteopenia than in the patients reported here. While fractures were reported in 22 of the 26 patients with *GORAB* mutations, none of the present patients or other patients reported with *PYCR1* mutations had fractures (Table 3.1).

In Reversade et al. (2009), the clinical findings of the patients with *PYCR1* mutations were notably similar to GO. Remarkably, 8/22 families had been initially diagnosed with GO and 3/22 families with GO or WSS (Reversade *et al*., 2009). After molecular analysis, they were grouped as cutis laxa with progeroid features. The Turkish family we studied also was initially diagnosed with GO. The disorder ARCL2A, also known as cutis laxa with growth and developmental delay, shares many features with WSS. Generalized wrinkled skin and distinct facial features including frontal bossing, hypertelorism, long philtrum and downslanted palpebral fissures are associated with these disorders. Deficiencies within the same gene, *ATP6V0A2*, can cause either WSS or ARCL2A, due to phenotypic heterogeneity (Kornak *et al*., 2008). Patients with either *GORAB* or *PYCR1* mutation share several clinical features that distinguish them from WSS and ARCL1/2A. These are the limitation of skin wrinkling to the dorsum of hands and feet, hyperextensible joints and distinct facial appearance including droopy, long and triangular face, hypoplastic maxilla, prognathism and large protruding ears, together with skeletal changes (Hunter *et al*., 1978; Picco *et al*., 1993; Rajab *et al*., 2008; Al-Dosari *et al*., 2009). Based on these clinical features, the patients studied here were initially diagnosed as GO (Table 3.1).

In conclusion, clinical phenotypes of patients with either *GORAB* or *PYCR1* mutations are similar to GO. It was suggested that the disorder resulting from defects in *GORAB* should be re-designated as GO type I (without MR) and that resulting from defects in *PYCR1* as GO type II (with MR) rather than ARCL2B. The findings and the proposal have been submitted for publication (Yildirim *et al*., 2010).

6.2. Motor Dysfunction, Intellectual Disability and Joint Contractures

In this study, a highly inbred family diagnosed with autosomal recessive multiple joint contractures, motor disability and mental disability was studied. This condition was unique since motor dysfunction, intellectual disability and postnatal development of multiple joint contractures together in a single syndrome have not been reported previously. We designated the syndrome as motor dysfunction, intellectual disability and joint contractures (MDIDJC). We identified a homozygous 2-bp insertion in *ERLIN2* exon 11 segregating with the disease in the family.

The protein in the patients is predicted to be truncated by about twenty per cent due to the mutation, c.812_813insAC or p.Asn272ProfsX4. Three new amino acids have replaced residues 272 to 339. The deletion covers the protein regions that are essential for the association of the protein with detergent-resistant membranes and the oligomerization into large complexes. Hoegg *et al*. (2009) showed that residues 228-305 lying downstream of the SPFH domain and upstream of the non-conserved C terminus are required for protein's proper activity, or more specifically, the assembling properties. This finding is compatible with the deleterious effect of the deletion identified in this study.

Endoplasmic reticulum is responsible for the folding of the secretory and membrane proteins as well as for the quality control of the folding process. About thirty per cent of newly synthesized proteins are degraded immediately due to the folding errors they carry (Schubert *et al.,* 2000), in order to prevent any possible negative effects of the misfolded proteins (Hirsch *et al*., 2009). In addition to this quality control, normal proteins are also subject to degradation through endoplasmic reticulum-associated degradation (ERAD) pathway to maintain the regulation of various cellular pathways (Hampton, 2002).

In ERAD pathway, after the proteins to be degraded are transported from ER into cytosol, they are ubiquitinated and transferred to proteasome for degradation (Vembar and Brodsky, 2008).

ERLIN2 is involved in ER-associated degradation of activated inositol 1,4,5-trisphosphate receptors (ITPRs) and other substrates in mammalian cells (Pearce *et al*., 2007; Pearce *et al*., 2009). ERLIN1 and ERLIN2, which are paralogs, share ~80% homology in amino acid sequence. Both proteins are identical between human and chimpanzee. Additionally the human, mouse and rat ERLIN2 orthologs are about 97 per cent identical. ERLIN1 and ERLIN2 are also named SPFH1 and SPFH2, respectively, since they share homology with a protein family having a stomatin, prohibitin, flotillin and HflC/K (SPFH) domain (Browman *et al*., 2006). They assemble into ~2 MDa complexes in an approximately 1:2 ratio (Pearce *et al*., 2009). They are localized to endoplasmic reticulum (ER) and nuclear envelope (Ikegawa *et al*., 1999). ERLIN1/ERLIN2 complex is involved in the early stages of ITPR-associated ERAD pathway, associating with each other just upon activation of the channels. The subsequent steps of the ERAD pathway, polyubiquitination and degradation, follow the association (Pearce *et al*., 2007).

ITPRs are specific intracellular ligand-gated calcium release channels localized mostly in the membrane of ER (Ferreri-Jacobia *et al*., 2004). Upon binding of inositol 1,4,5-trisphosphate (ITP), which is an intracellular second messenger in the inositol trisphosphate signaling pathway, to ITPRs, the channels open and Ca^{2+} diffuses from the ER lumen to cytoplasm (Foskett *et al*., 2007). In vertebrates there are three types of ITPRs -ITPR1, ITPR2 and ITPR3- encoded by three different genes (Blondel *et al*., 1993), and each of them are 2700 amino acids in length. The amino acid sequences of these proteins share 60–80% homology. The proteins form homomeric or heteromeric tetramer channels (Taylor *et al*., 1999). ITPRs are expressed ubiquitously, and most cells express more than one type, whereas some neurons express only ITPR1. The expression pattern is dynamic and may change during development and differentiation as well as during cellular activities (Taylor *et al*., 1999; Foskett *et al*., 2007).

Futatsugi *et al.* (2005) showed that mice deficient of ITPR2 and ITPR3 displayed undernourished phenotype, and they lost weight. This finding indicated the role of ITPR2

in energy metabolism and animal growth. *ITPR1* gene is expressed in neuronal tissues, predominantly in cerebellar Purkinje cells, but neurons in the hippocampal CA1 region, caudate-putamen and cerebral cortex also have high *ITPR1* expression (Matsumoto *et al*., 1996; Dent *et al*, 1996; Takei *et al*., 1998; Jordan *et el*., 2005). The channels are localized to dendrites, and their local translation is essential for the induction of long-term depression in cerebellar Purkinje neurons, which is thought to be required for synaptic plasticity, motor learning and motor coordination in cerebellum (Iijima *et al*., 2005).

Nagase *et al.* (2003) found that although ITPR1 activity is not essential for induction of long-term potentiation or long term depression, the intracellular Ca^{2+} levels are adjusted through ITPR1 channels. Ca^{2+} amount modifies the activities of Ca^{2+} kinases and phosphatase, which are involved in learning processes. They proposed that ITPR1 involves in stabilization of cell excitability. Thus, high cellular calcium levels expected in ERLIN2 deficiency may interfere with motor learning and motor coordination.

ERLIN2 expression is high also in skeletal muscle, and the role of *ITPR1* activity has been associated with the regulation of muscle fiber phenotype (Jordan *et al*., 2005). MDIDJC patients displayed atrophy in all skeletal muscles. The contractures and muscle atrophy might stem from either structural deformities or from the absence of motor learning.

Despite the fact that an ERLIN2 knock-out animal model has not been created yet, the effects of ITPR1 deficiencies have been studied. Ogura *et al.* (2001) has shown that ITPR1+/− mice have impairment in motor coordination, whereas homozygous null mutants could not be utilized because either they died in utero or before the weaning period, and most of the latter developed ataxia and convulsions. This motor coordination impairment was more severe in males than females. This finding coincides with the phenotypes of the patients studied here since males were more severely affected than females.

In humans ITPR1 haploinsufficiency leads to spinocerebellar ataxia 15 (SCA15; MIM 606658), which is an autosomal dominant pure form of spinocerebellar ataxia (loss of muscular coordination) with cerebellar atrophy. Human carbonic anhydrase related protein 8 (CA8, MIM 114815), which is highly expressed in cerebellar Purkinje cells,

binds to ITPR1 and inhibits ITP binding to ITPR1, acting in an antagonistic manner. Turkmen et al. (2009) identified a homozygous mutation in *CA8* leading to mild intellectual disability and congenital ataxia. Although ataxia is not a feature of the disease describe here, the association of ITPR1 with motor activities is outstanding. However, a point of caution is that ERLIN2 deficiency is predicted to lead not to ITPR deficiency but to high levels of activated ITPRs, which is the opposite situation of CA8 deficiency.

Neither any animal model nor any human diseases associated with defective or inactivated *ERLIN2* or *ERLIN1* have been reported so far. This study is an indicator of importance of ERLIN2 in motor learning and coordination. However, it is important to emphasize the probability that the functions of ERLIN2 may not depend on its interaction with ITPR1. Future molecular studies focusing on the clarification of ERLIN2 substrates in neurons as well as on the other main players in motor learning and coordination is important. Although *ERLIN2* is expressed ubiquitously in human tissues, its deficiency leads to a primary pathology only in the brain and joints. Elucidating the function of the protein would help to find the molecular basis of this dilemma.

6.3. Median Cleft Lip

The kindred we analyzed exhibited a unique form of Median Cleft Lip: the most affected four sibs exhibited incomplete median clefting in upper and lower lips together, with the involvement of dental dysmorphology. In addition to affected sibs, the mother and one of the sibs had the subclinical phenotype while two cousins had a minimal phenotype (Figure 3.5). The presence of heterogeneous phenotypes among the family members pointed out complex inheritance.

Lod score analysis performed using a fully penetrant homozygous inheritance model and including only the affected individuals pointed out to several candidate loci (Table 5.6). However, haplotype inspection eliminated most of them, and loci 1p31.1 – 31.2 stood out as the strongest candidate. All the affected sibs shared the same homozygous haplotype. The remaining members did not share the homozygosity. Minimal 301 had also a homozygous haplotype there, but the genotype was different. Subsequently, a homozygous intergenic deletion larger than 270,000 bp at 1p31.1 was identified in all

affected sibs. While their parents and all other sibs as well as individual 205 carried the deletion, the others did not.

Most of the deletion carriers, except the subclinical ones, did not exhibit the phenotype. Moreover, minimal 301, whose phenotype resembled subclinical mother 204 and other minimal 311 did not carry the mutation. These findings indicated the contribution of a second locus to the development of the phenotype. Another gene associated with developmental processes might result in the clefts and the homozygous deletion might worsen the phenotype, acting as a modifier. A homozygous mutation in a second locus is plausible, since none of the minimal individuals' parents were affected. However, a region where all affected sibs and minimals have the same homozygous haplotype could not be identified. In such situation, two explanations are plausible: either incomplete penetrance in a dominant model or a very small homozygous region escaped detection.

Lod score calculations and haplotype analysis were performed assuming a full or an 80 per cent penetrant autosomal dominant model. Several regions with relatively high lod scores were obtained, which makes handling of data difficult. Genes that have been associated with cleftings (Table 1.3) and their paralogs were taken into consideration, and were investigated whether they were located within regions that yielded high lod scores. *ANKS, BMP4, EGFR, FGF10, FGFR1, GDF6, GDF7, FOXB1, FOXE1, IRF6, NANOG, NANOGP5, PAX9, PTCH1, PVRL1, SMAD9, TGFB2, TGFB3, TGFBR1* and *TMEFF1* were found to lie within such regions.

TYW3 lies ~16,400 bp upstream of the deletion at 1p31.1, whereas *LHX8* (Lim homoebox Gene 8*)* lies ~73,200 bp downstream of it. Chicken and mouse gene knock-out models with clefts ordered *LHX8* a good candidate (Grigoriou *et al*., 1998; Zhao *et al*., 1999; Zhao *et al*., 2003; Inoue *et al*. 2006). Exons of the gene were resequenced in one affected individual, and no sequence variation was found. The gene encodes a transcription regulator that is composed of a DNA-binding domain and a protein binding domain (MIM 604425). It is expressed during embryogenesis in basal forebrain and the mesenchyme of the mandible and maxilla (Grigoriou *et al*., 1998; Inoue *et al*. 2006). In addition, the effects of TGF-b3 and Fgf-8b on *LHX8* expression levels in maxillary mesenchyme in chicken

embryo are noteworthy. *TGFB3* has been associated with palate development (Proetzel *et al*., 1995), and *FGF8* with nonsyndromic cleft lip or palate (Riley *et al*., 2007).

Evolutionary conservation of the sequences in the deletion region among primates and other mammals and vertebrates was investigated. The sequences are highly conserved among primates, and homologous regions are present among other vertebrates (Figure 5.17). This fact indicates that the region perhaps has a regulatory role in the expression of *LHX8.*

Although several environmental factors are related to orofacial clefts (Mossey *et al*., 2009), we do not know whether there is an environmental involvement in the formation of the phenotype studied here.

This study revealed the advantage of the high density SNP scan over sparse markers in the identification of candidate loci. False-positive regions disappeared after a dense scan in MCL family since some informative SNP markers interspersed within non-informative regions eliminated those areas. Additionally, some other homozygous regions turned to be heterozygous after the denser scan.

To sum up, the phenotype of the family studied seems to be unique in the literature. The identified deletion is likely associated with the phenotype. Even though nor polymorphic deletion within that region has been reported so far, a sample of Turkish population should be screened to make sure that it is a novel deletion. If its effect in cleft lip formation in the family is verified, it would be the first demonstration that *LHX8* is associated with orofacial clefts in humans. Contribution of another gene(s) is obvious in this family. Resequencing of the possible genes given in Table 5.12 might reveal those genes.

7. APPENDIX

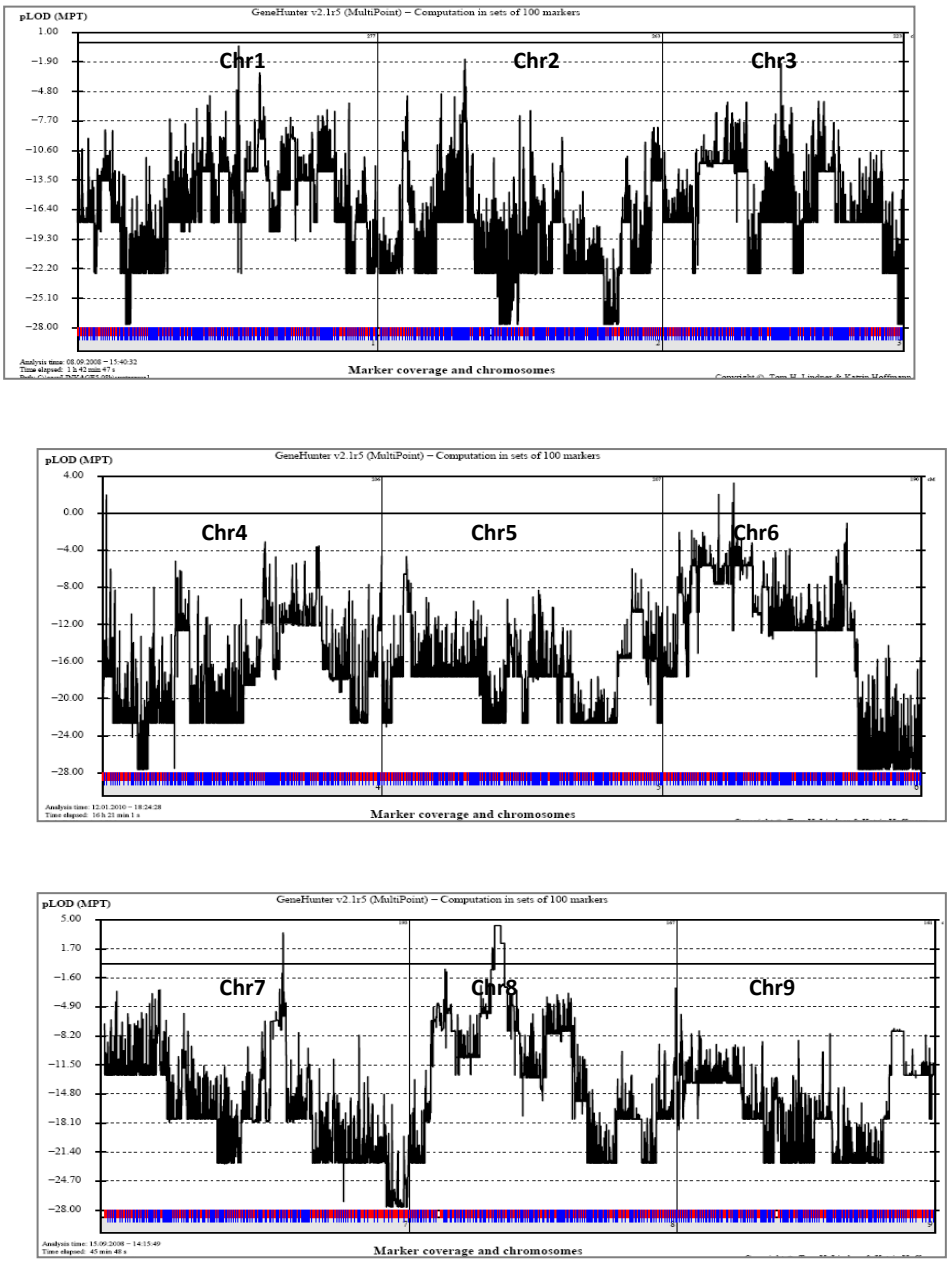

Figure A.1. Multipoint lod scores of SNP scan data for autosomal chromosomes and pseudoautosomal regions (PAR1 and PAR2).

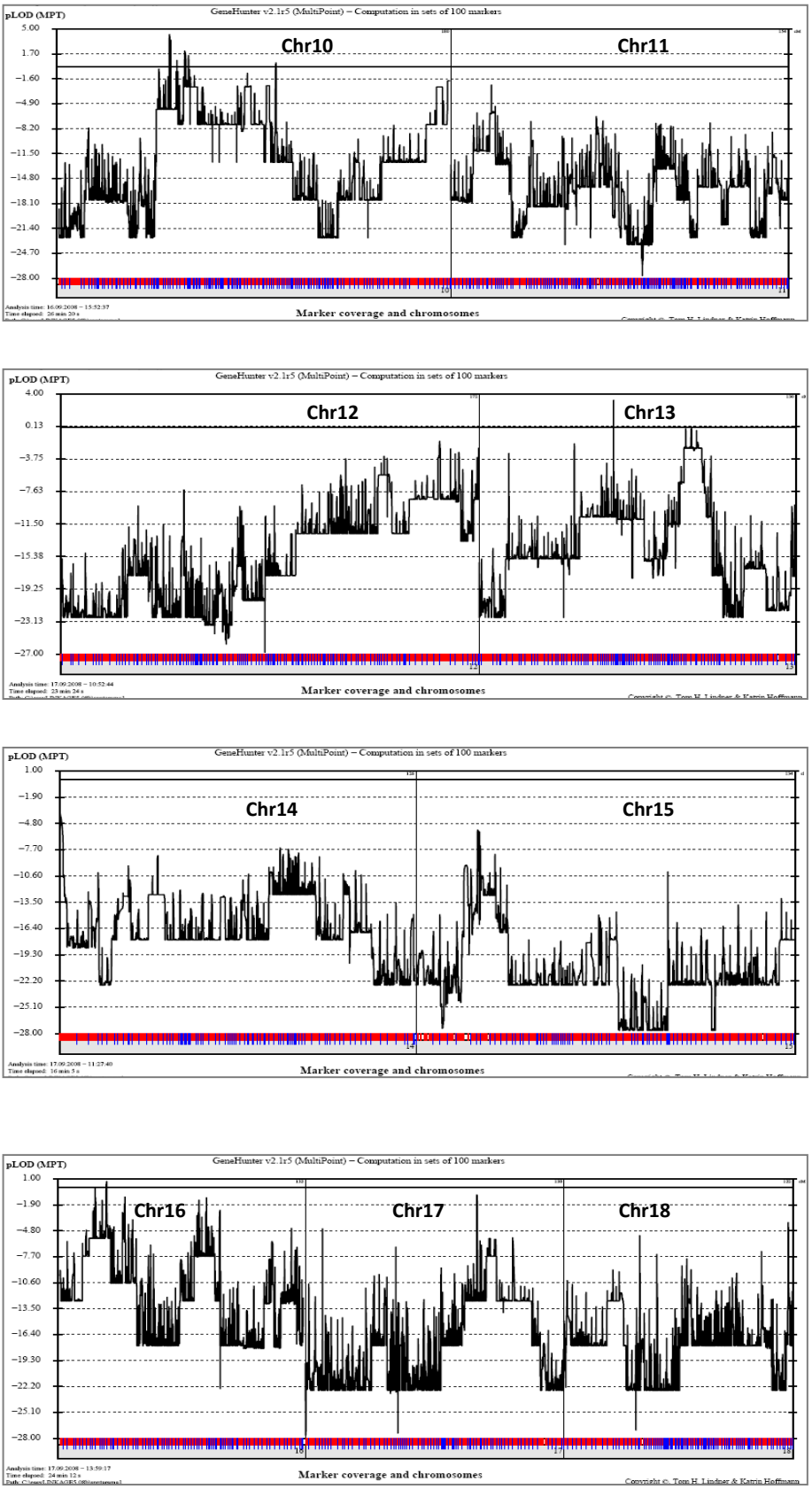

Figure A.1. Multipoint lod scores of SNP scan data for autosomal chromosomes and pseudoautosomal regions (PAR1 and PAR2) (continued).

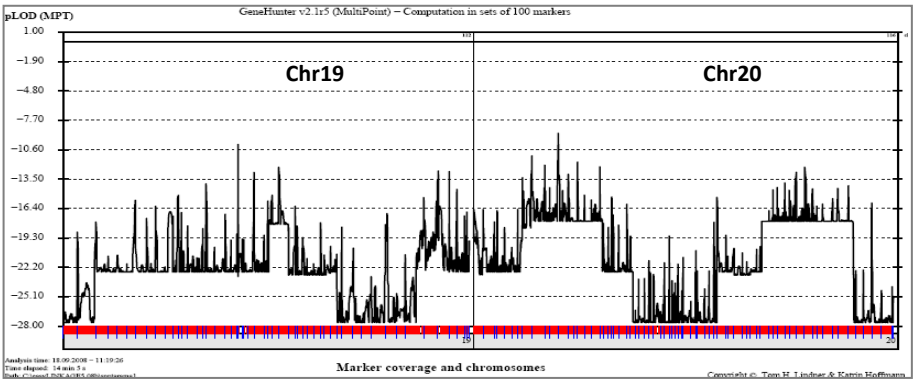

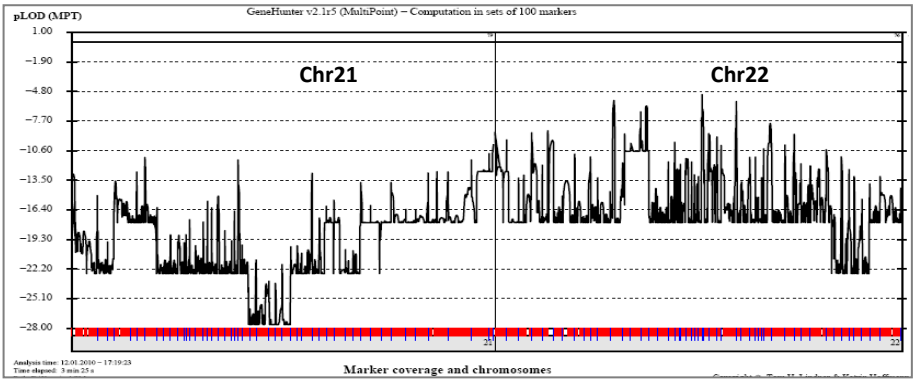

Figure A.1. Multipoint lod scores of SNP scan data for autosomal chromosomes and pseudoautosomal regions (PAR1 and PAR2) (continued).

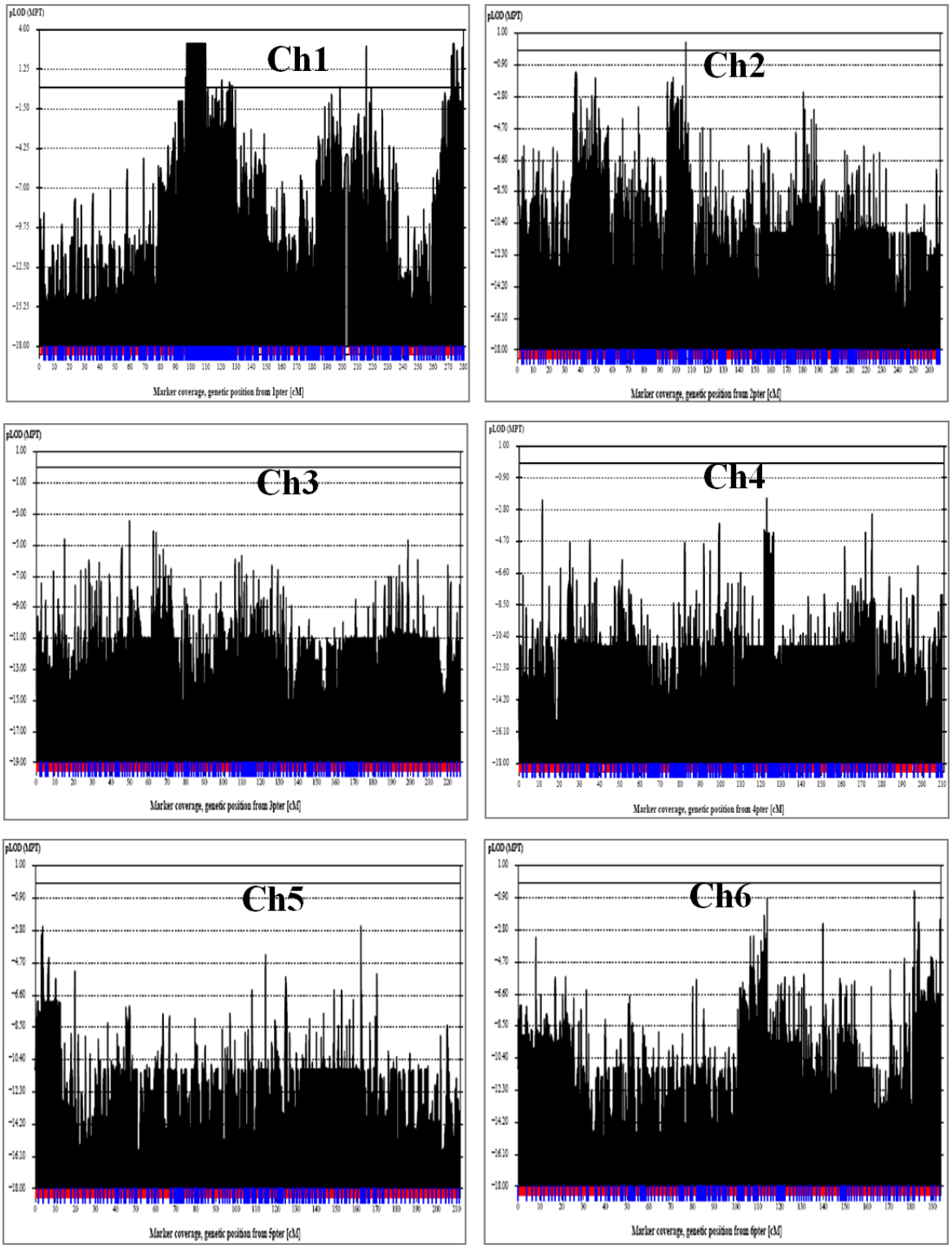

Figure A.2. Multipoint lod score results in a fully penetrant recessive model for MCL using only the affected sibs. Results for all autosomal chromosomes and PAR regions are given.

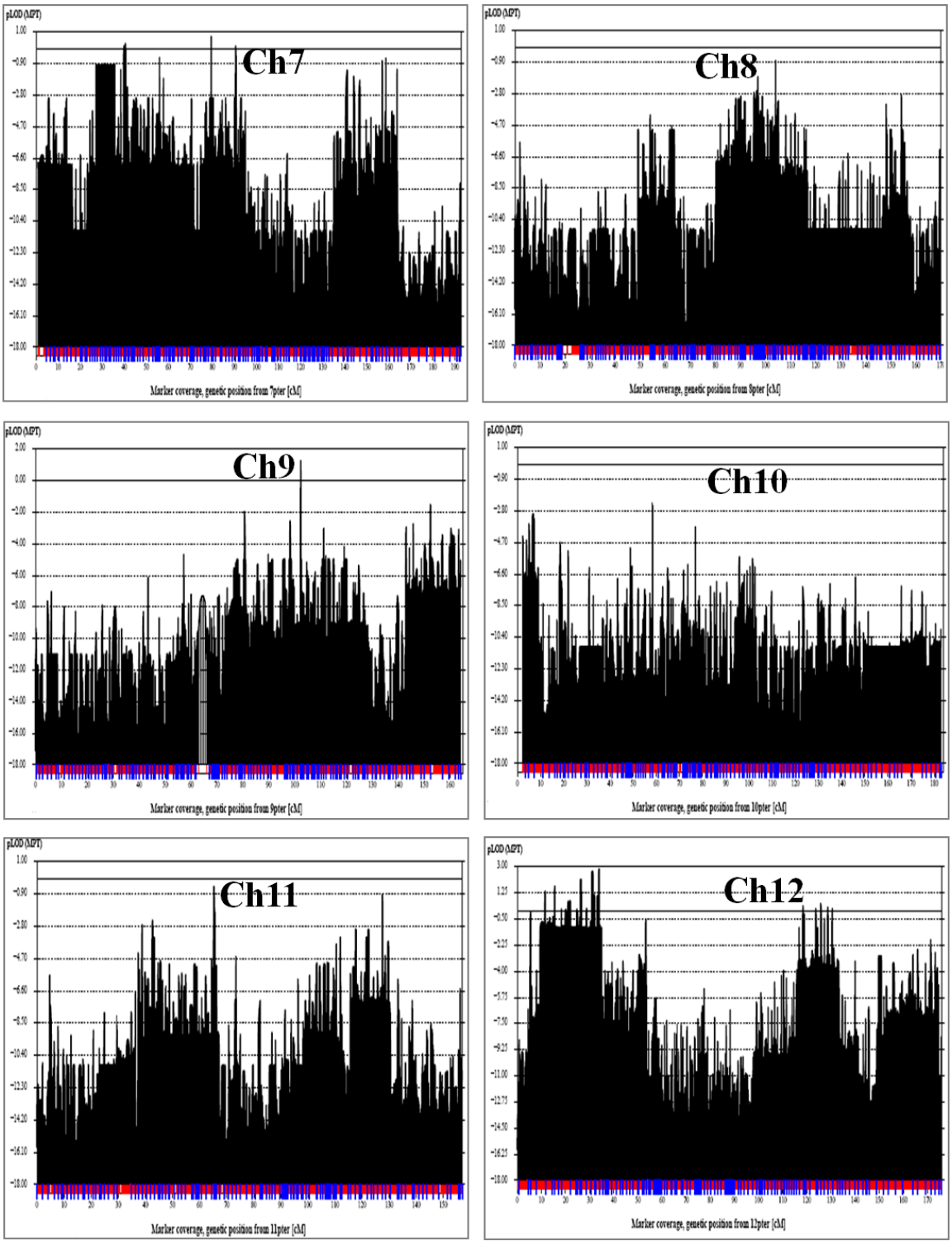

Figure A.2. Multipoint lod score results in a fully penetrant recessive model for MCL using only the affected sibs. Results for all autosomal chromosomes and PAR regions are given (continued).

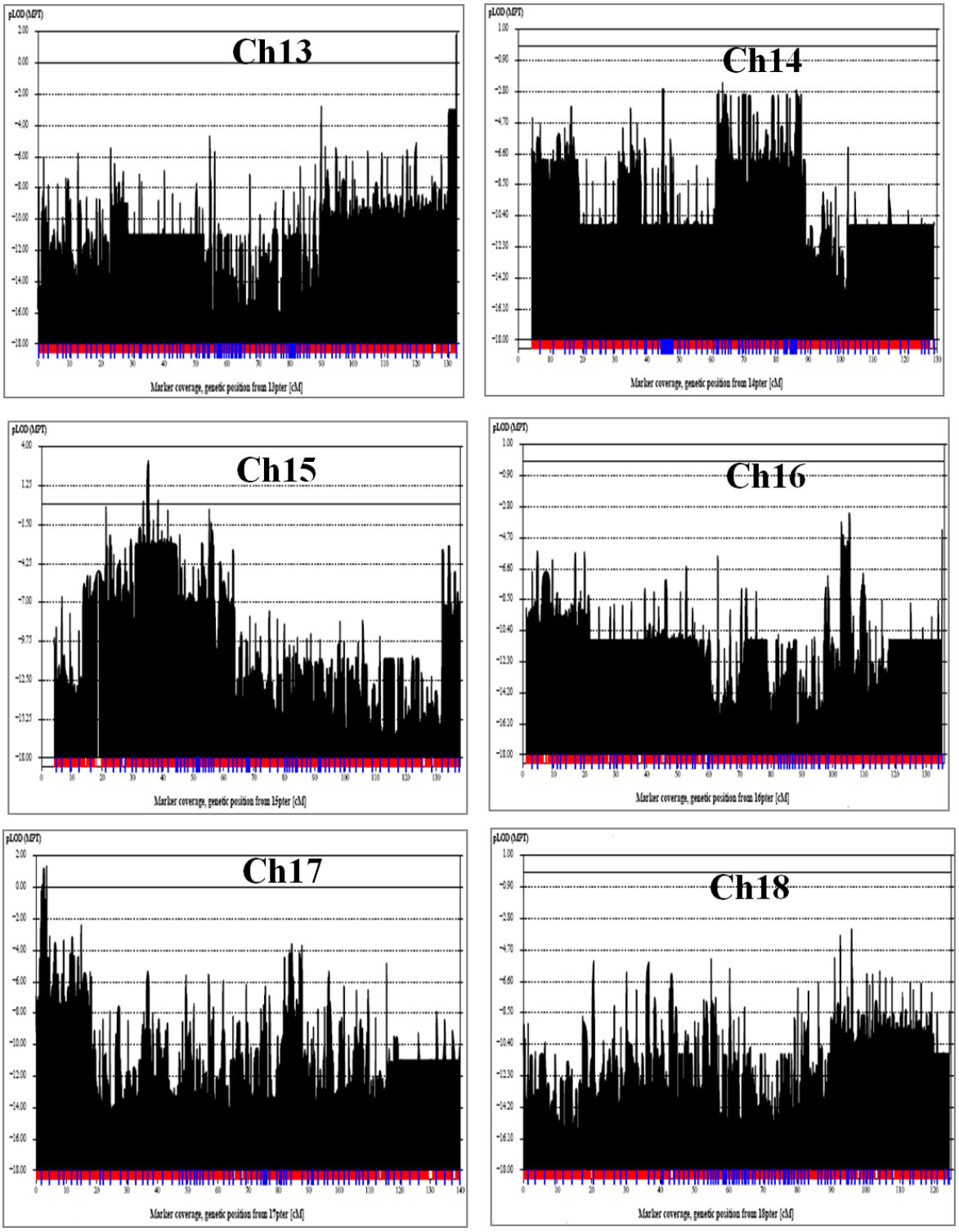

Figure A.2. Multipoint lod score results in a fully penetrant recessive model for MCL using only the affected sibs. Results for all autosomal chromosomes and PAR regions are given (continued).

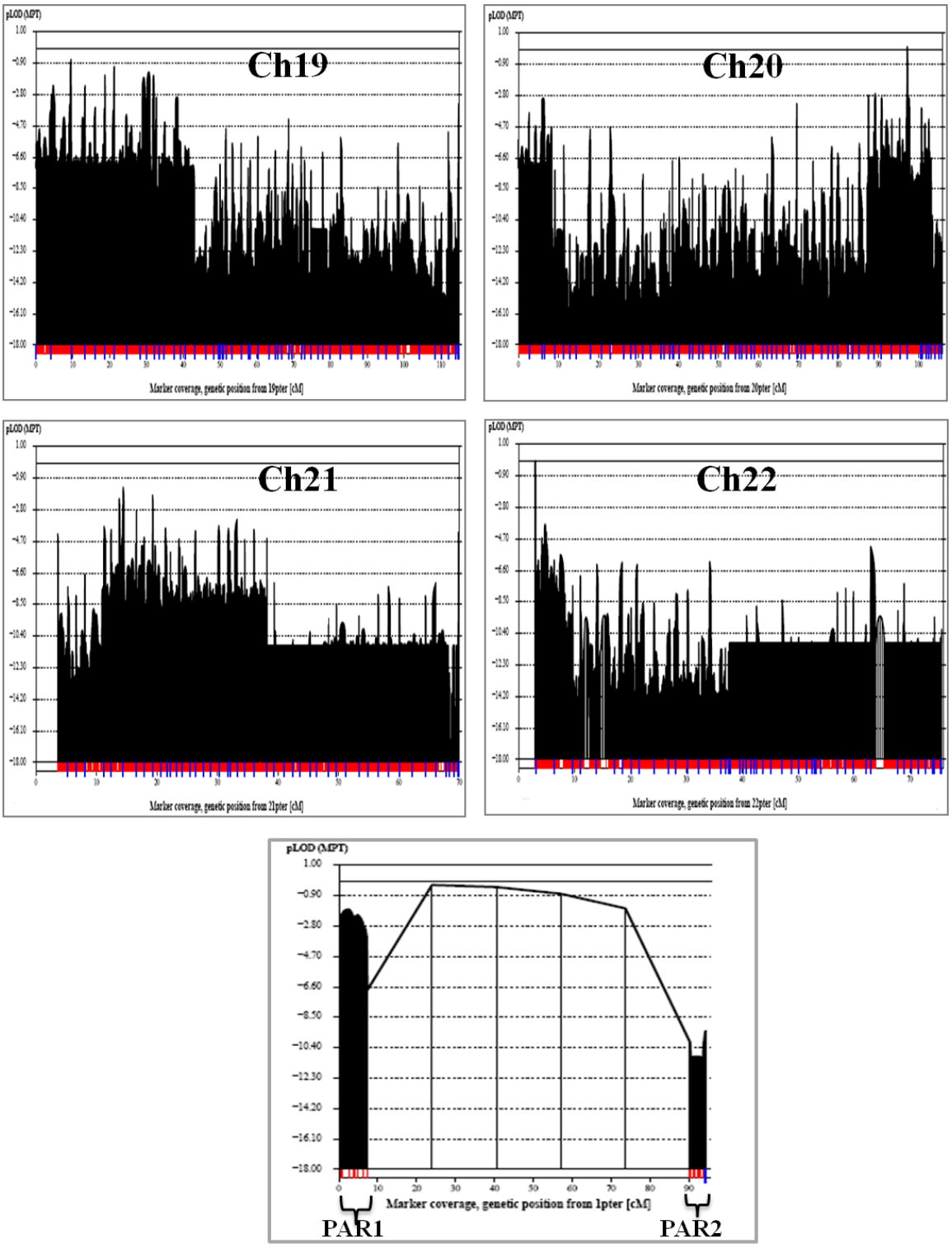

Figure A.2. Multipoint lod score results in a fully penetrant recessive model for MCL using only the affected sibs. Results for all autosomal chromosomes and PAR regions are given (continued).

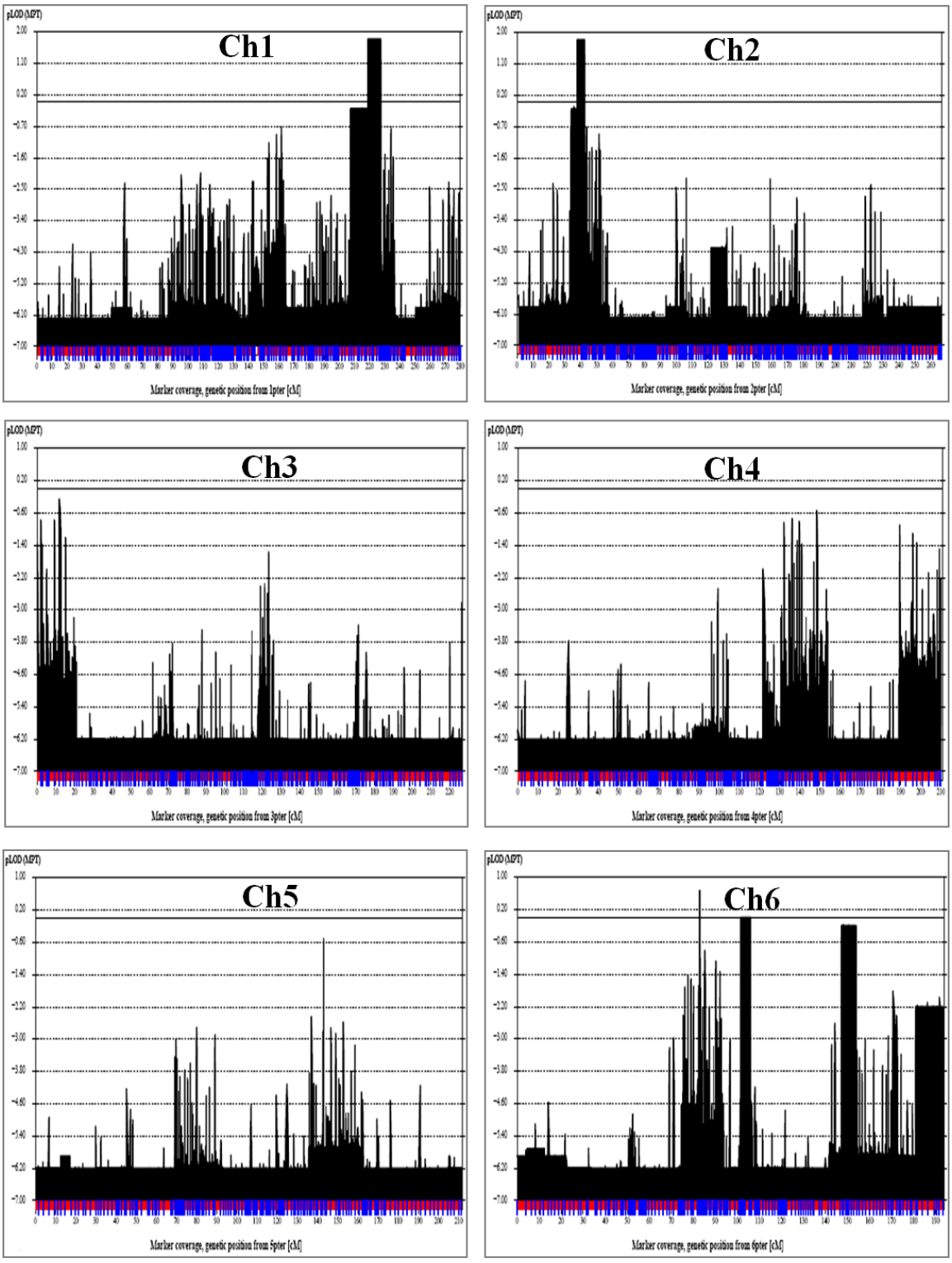

Figure A.3. Multipoint lod scores in a fully penetrant dominant model for MCL. Affected, subclinical and two unaffected sibs and subclinical mother are included. The results for all autosomal chromosomes and PAR regions are given.

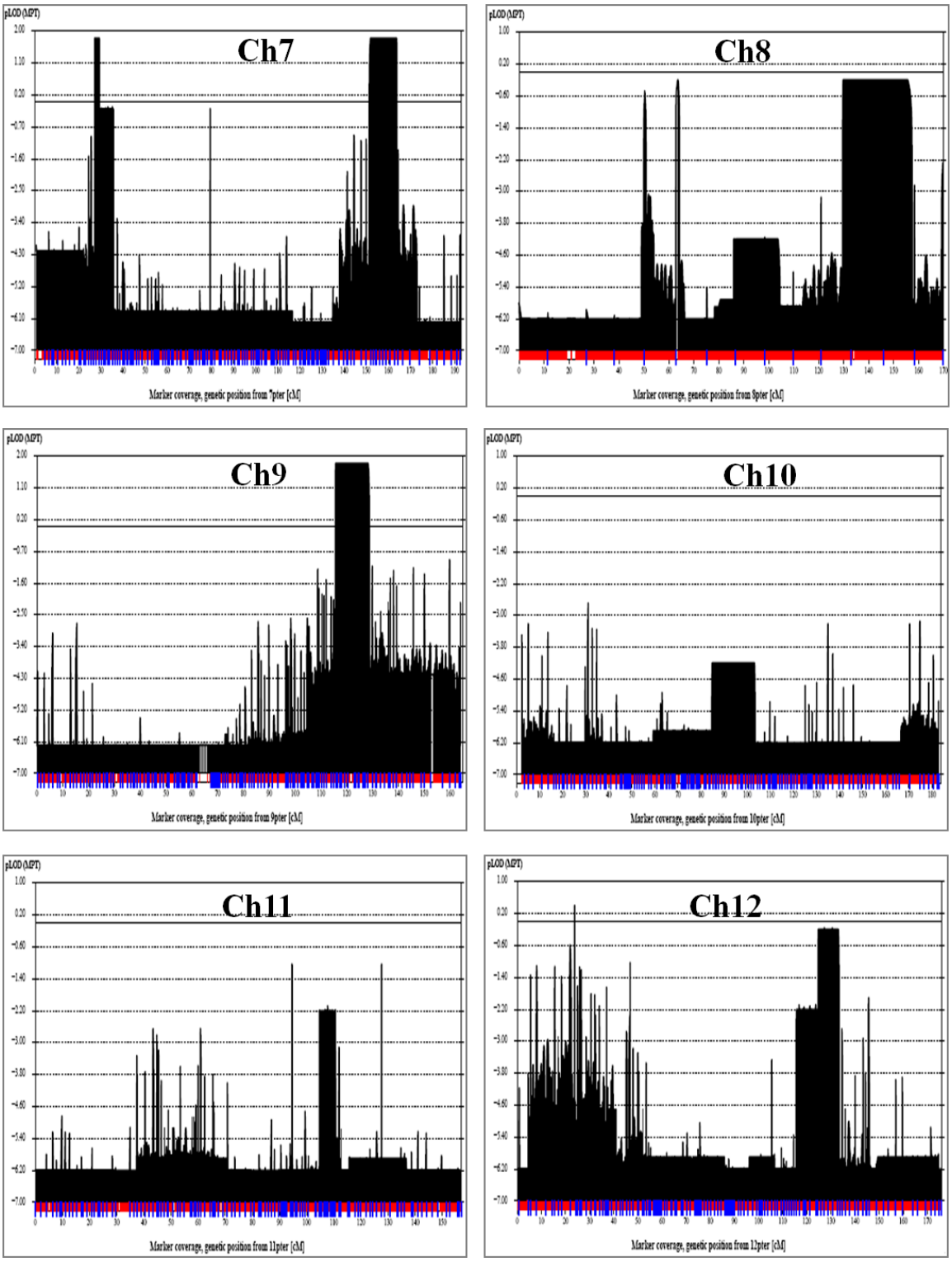

Figure A.3. Multipoint lod scores in a fully penetrant dominant model for MCL. Affected, subclinical and two unaffected sibs and subclinical mother are included. The results for all autosomal chromosomes and PAR regions are given (continued).

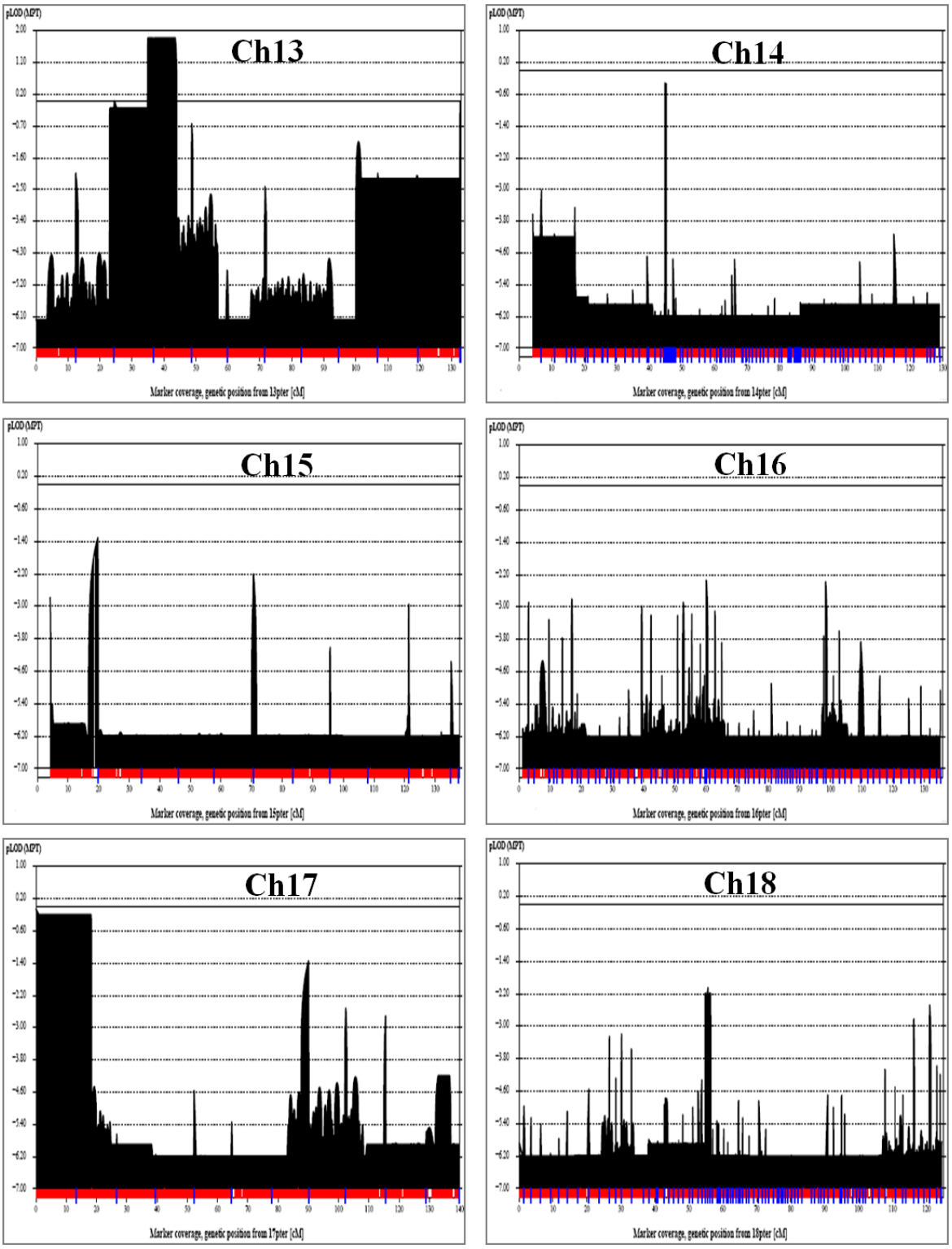

Figure A.3. Multipoint lod scores in a fully penetrant dominant model for MCL. Affected, subclinical and two unaffected sibs and subclinical mother are included. The results for all autosomal chromosomes and PAR regions are given (continued).

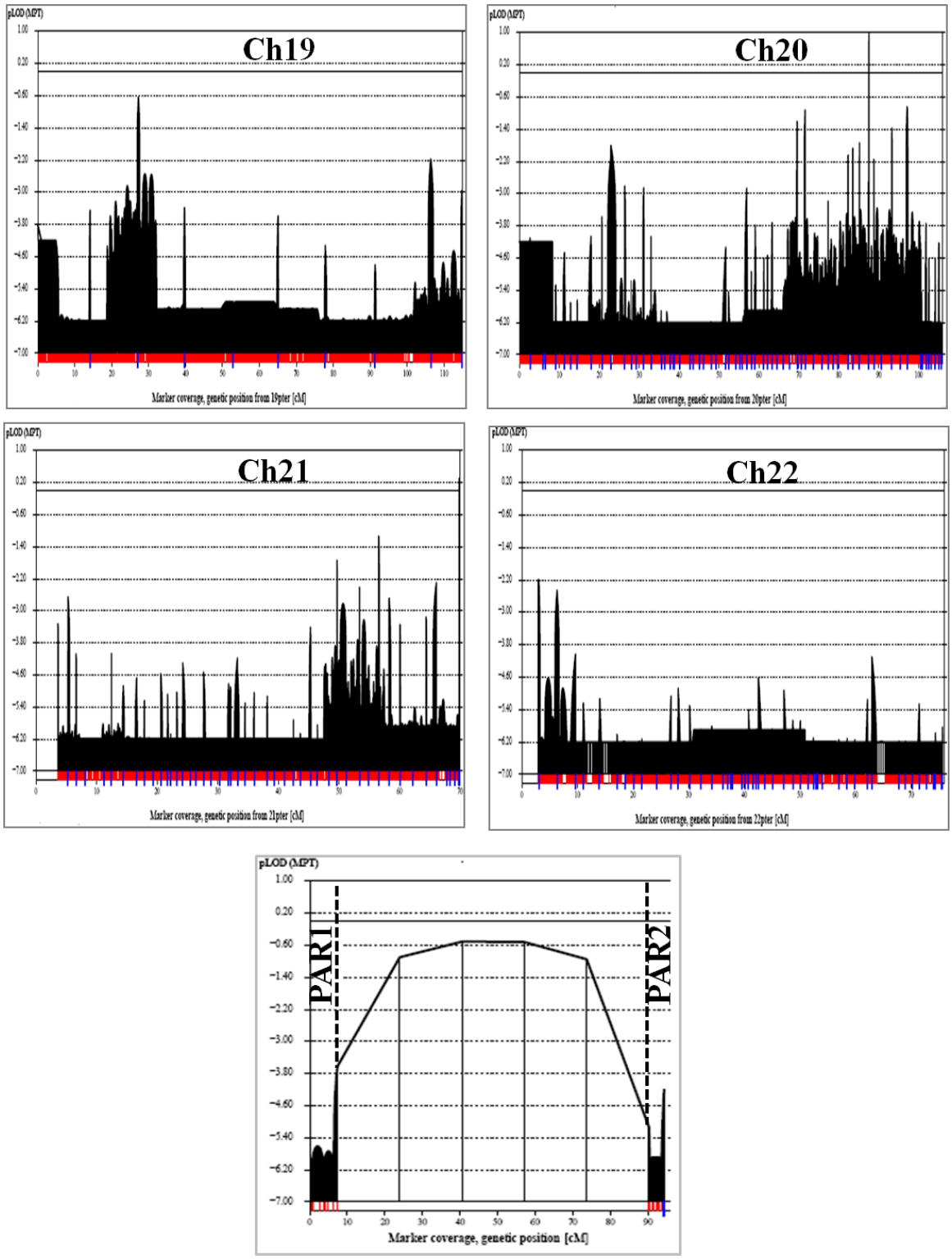

Figure A.3. Multipoint lod scores in a fully penetrant dominant model for MCL. Affected, subclinical and two unaffected sibs and subclinical mother are included. The results for all autosomal chromosomes and PAR regions are given (continued).

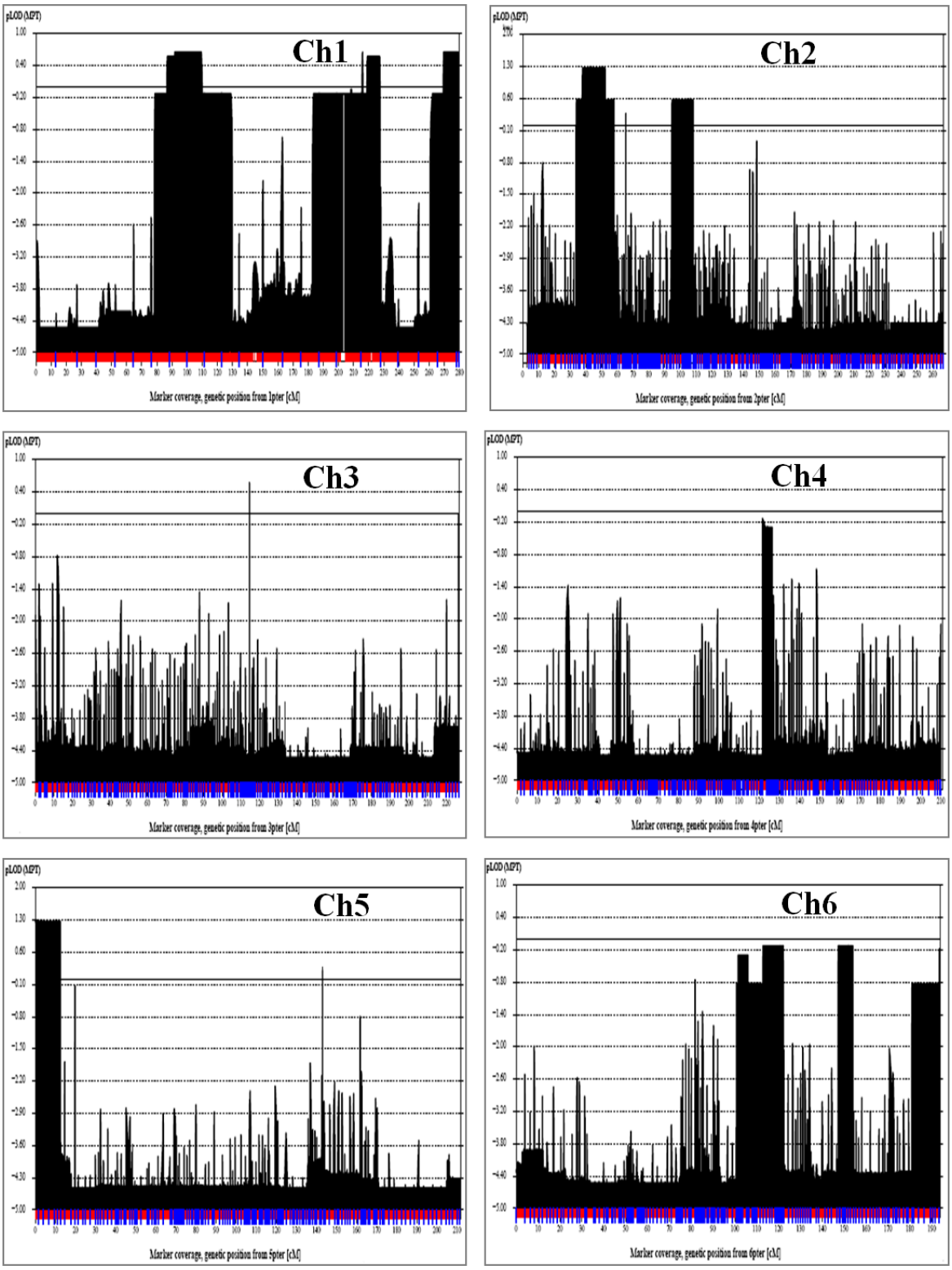

Figure A.4. Multipoint lod scores in an autosomal dominant model for MCL with 80 per cent penetrance. Three unaffected and all affected sibs are included. The results of all autosomal chromosomes and PAR regions are given.

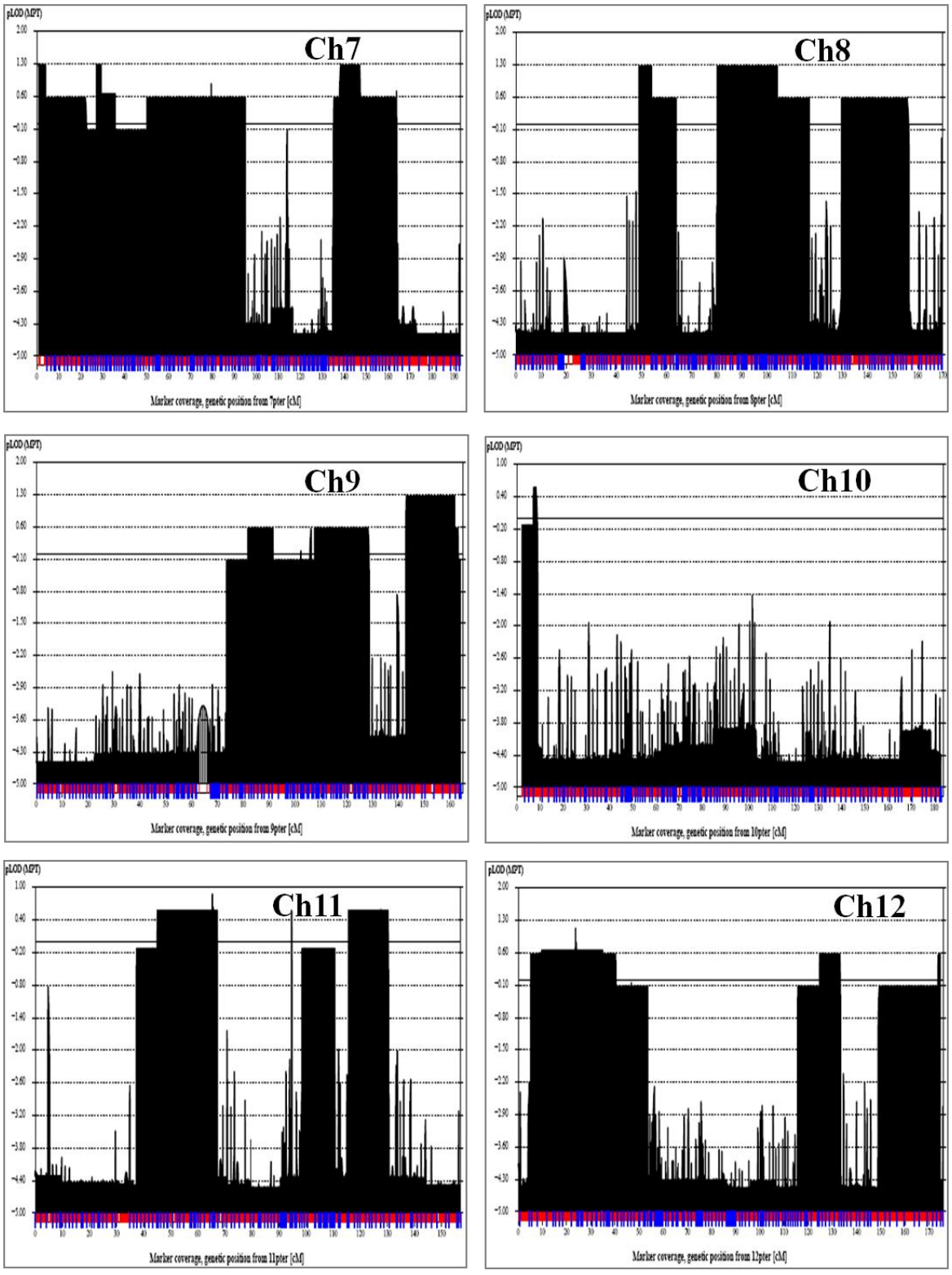

Figure A.4. Multipoint lod scores in an autosomal dominant model for MCL with 80 per cent penetrance. Three unaffected and all affected sibs are included. The results of all autosomal chromosomes and PAR regions are given (continued).

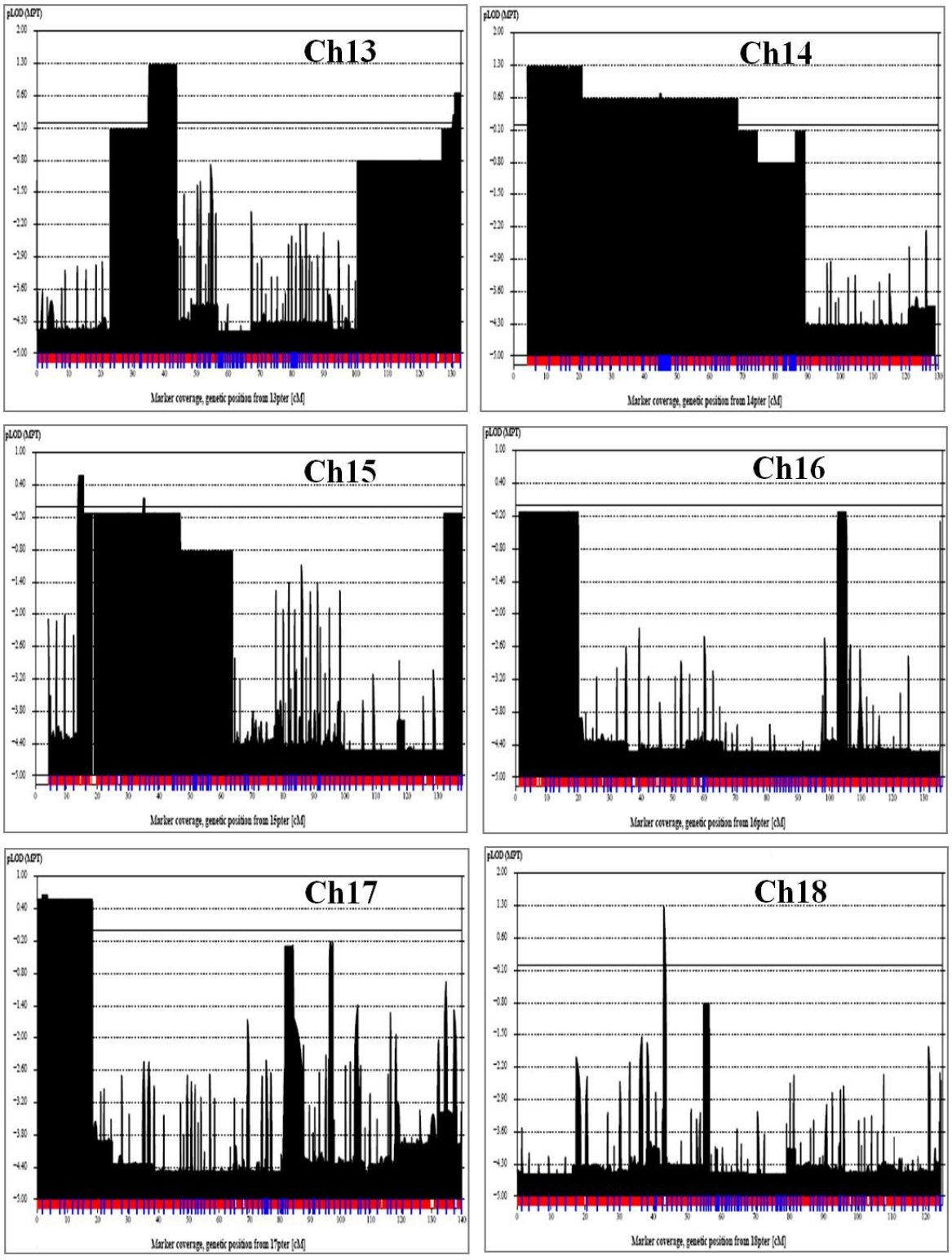

Figure A.4. Multipoint lod scores in an autosomal dominant model for MCL with 80 per cent penetrance. Three unaffected and all affected sibs are included. The results of all autosomal chromosomes and PAR regions are given (continued).

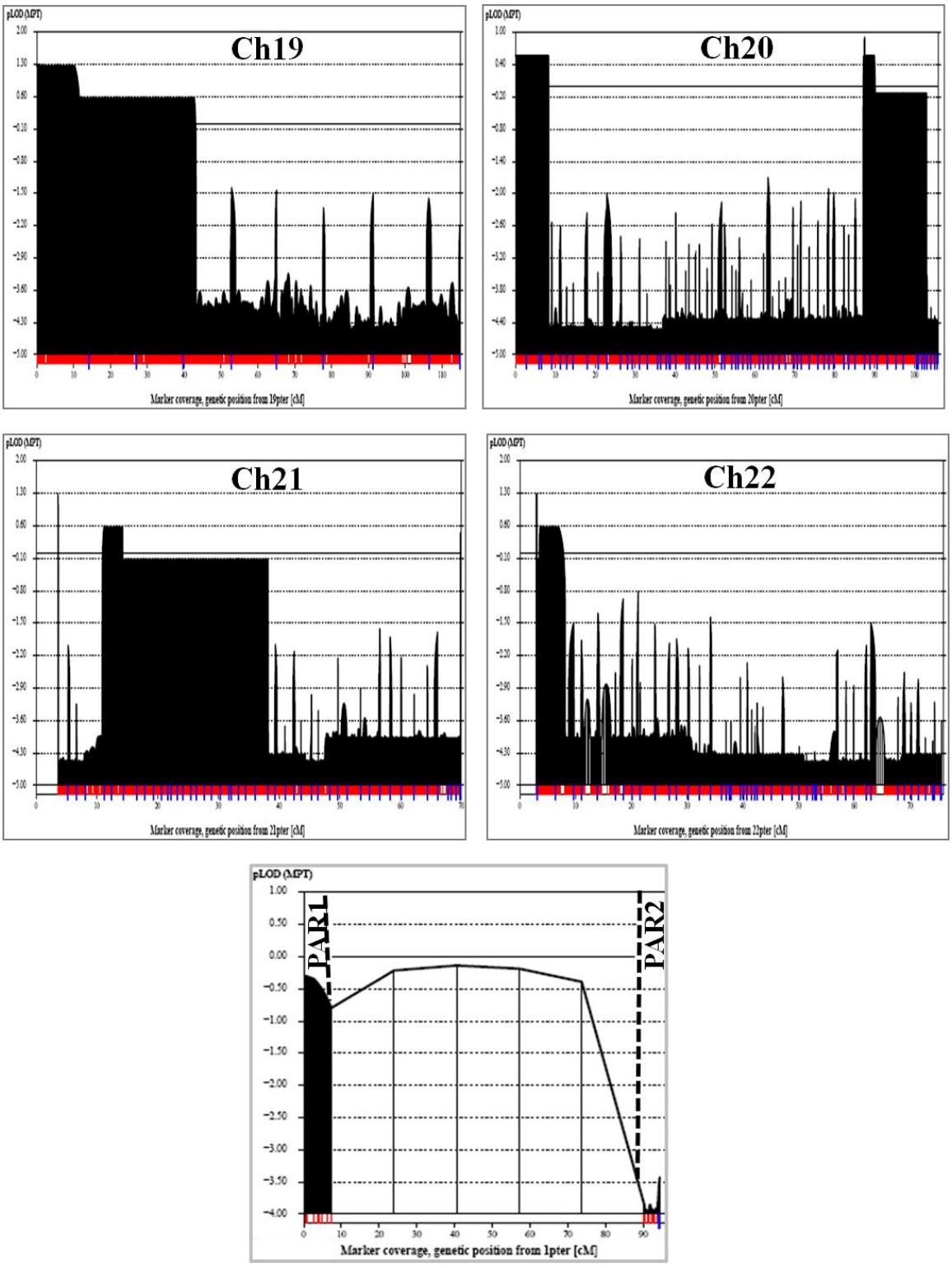

Figure A.4. Multipoint lod scores in an autosomal dominant model for MCL with 80 per cent penetrance. Three unaffected and all affected sibs are included. The results of all autosomal chromosomes and PAR regions are given (continued).

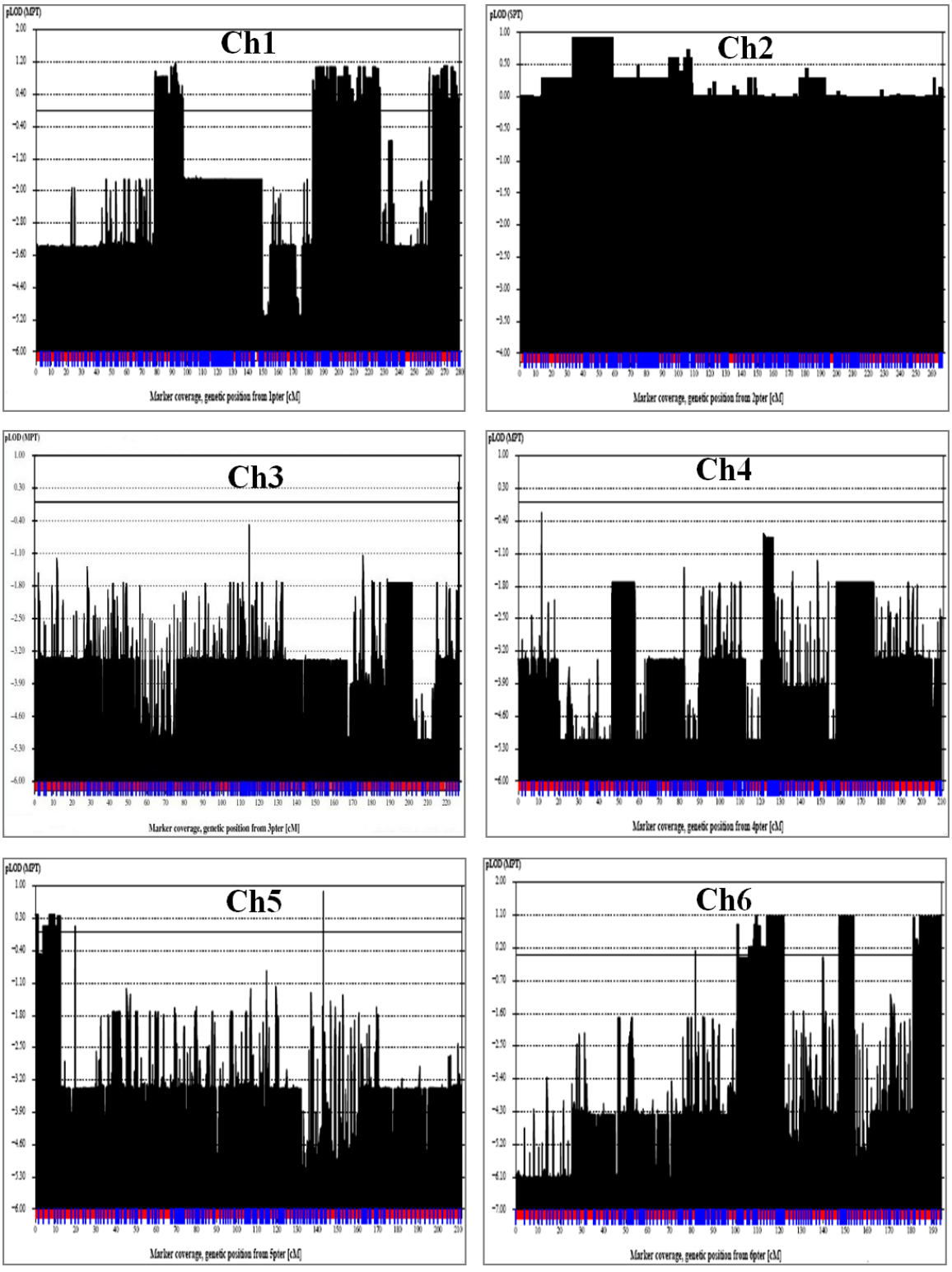

Figure A.5. Multipoint lod scores for MCL in an autosomal dominant model with 80 per cent penetrance using only the affected sibs. The results for all autosomal chromosomes and PAR regions are given.

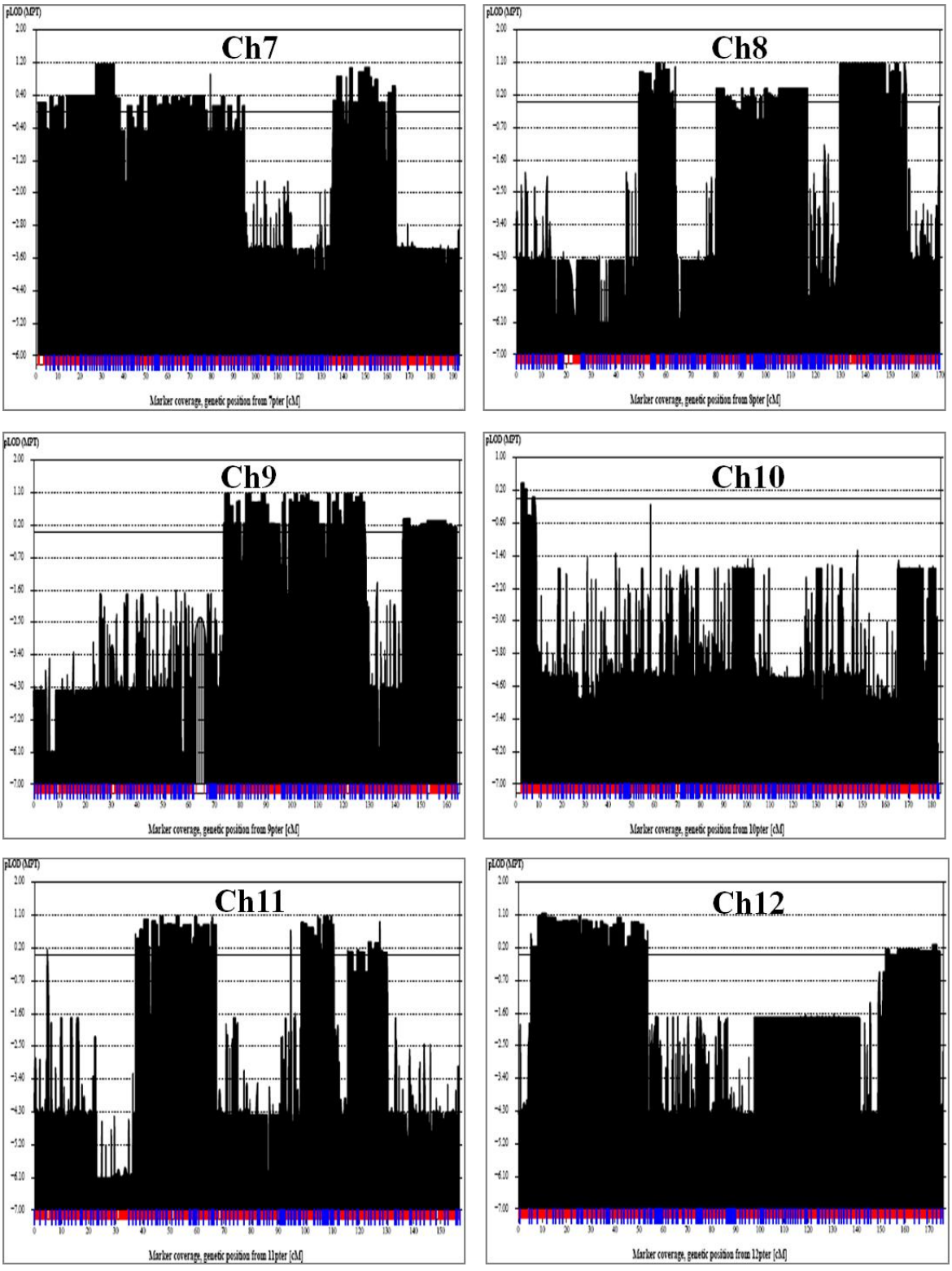

Figure A.5. Multipoint lod scores for MCL in an autosomal dominant model with 80 per cent penetrance using only the affected sibs. The results for all autosomal chromosomes and PAR regions are given (continued).

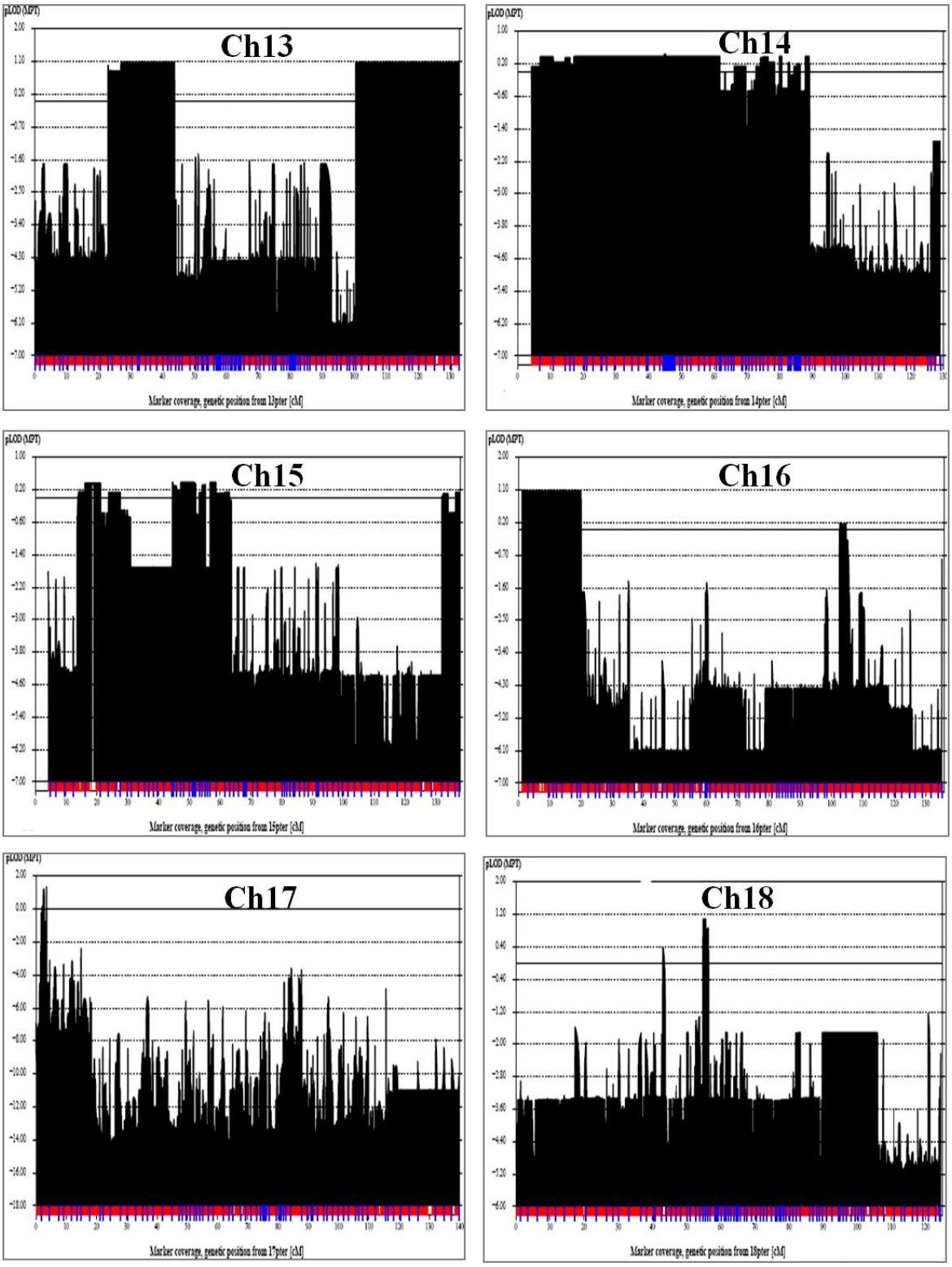

Figure A.5. Multipoint lod scores for MCL in an autosomal dominant model with 80 per cent penetrance using only the affected sibs. The results for all autosomal chromosomes and PAR regions are given (continued).

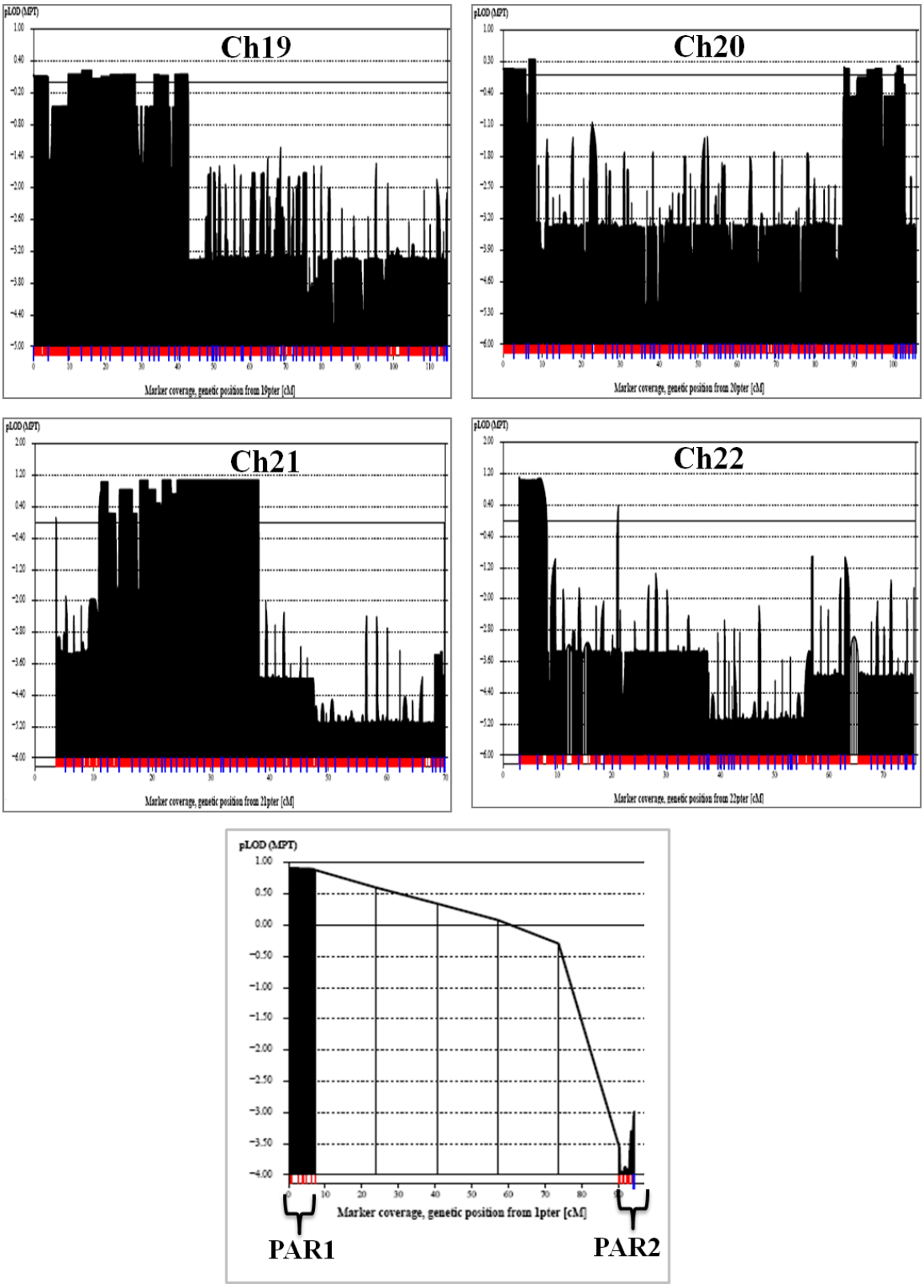

Figure A.5. Multipoint lod scores for MCL in an autosomal dominant model with 80 per cent penetrance using only the affected sibs. The results for all autosomal chromosomes and PAR regions are given (continued).

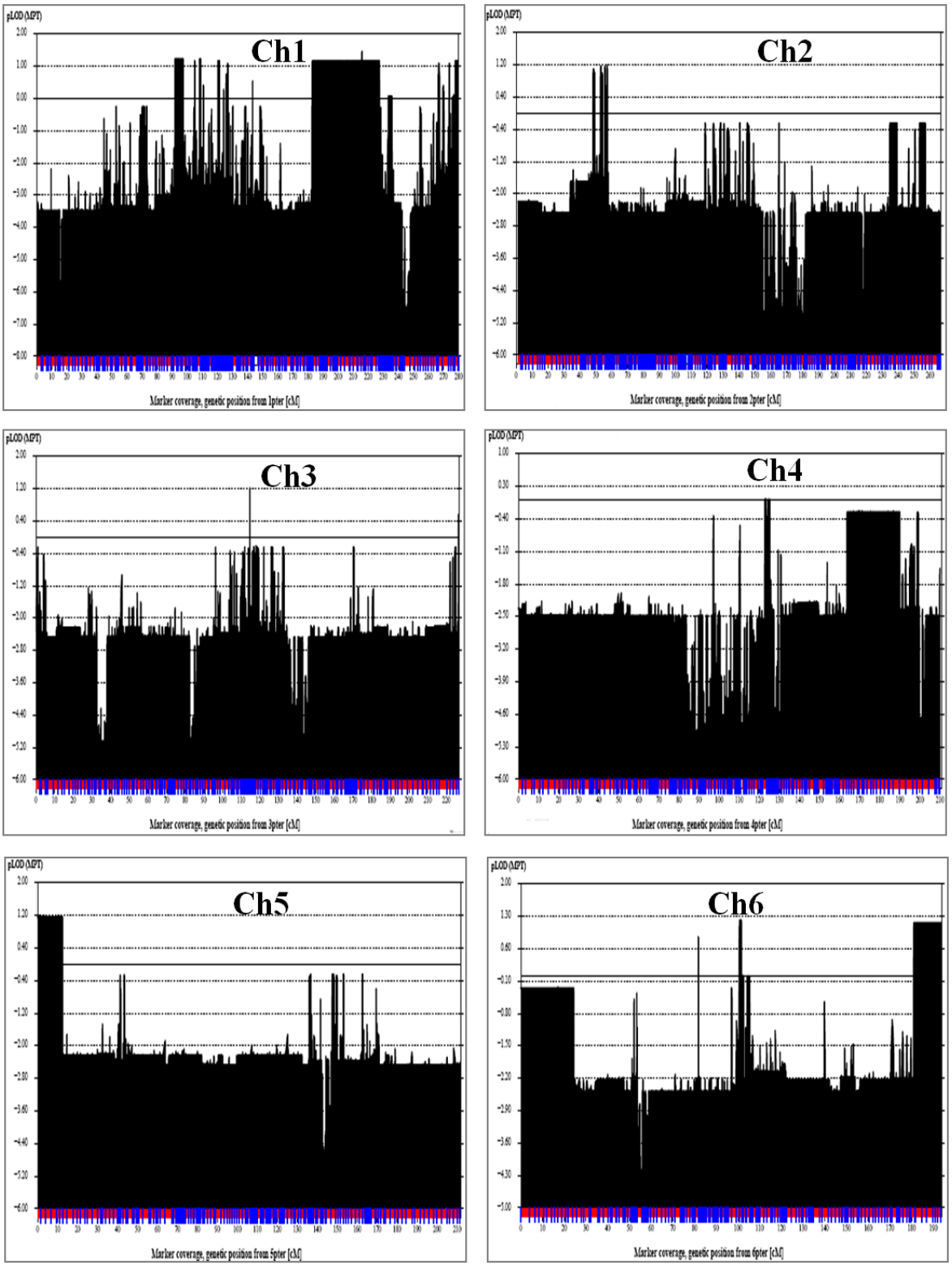

Figure A.6. Multi point lod score results for MCL in a dominant model with 80 per cent penetrance using the affected sibs and minimal cousins. The results for all autosomal chromosomes and PAR regions are given.

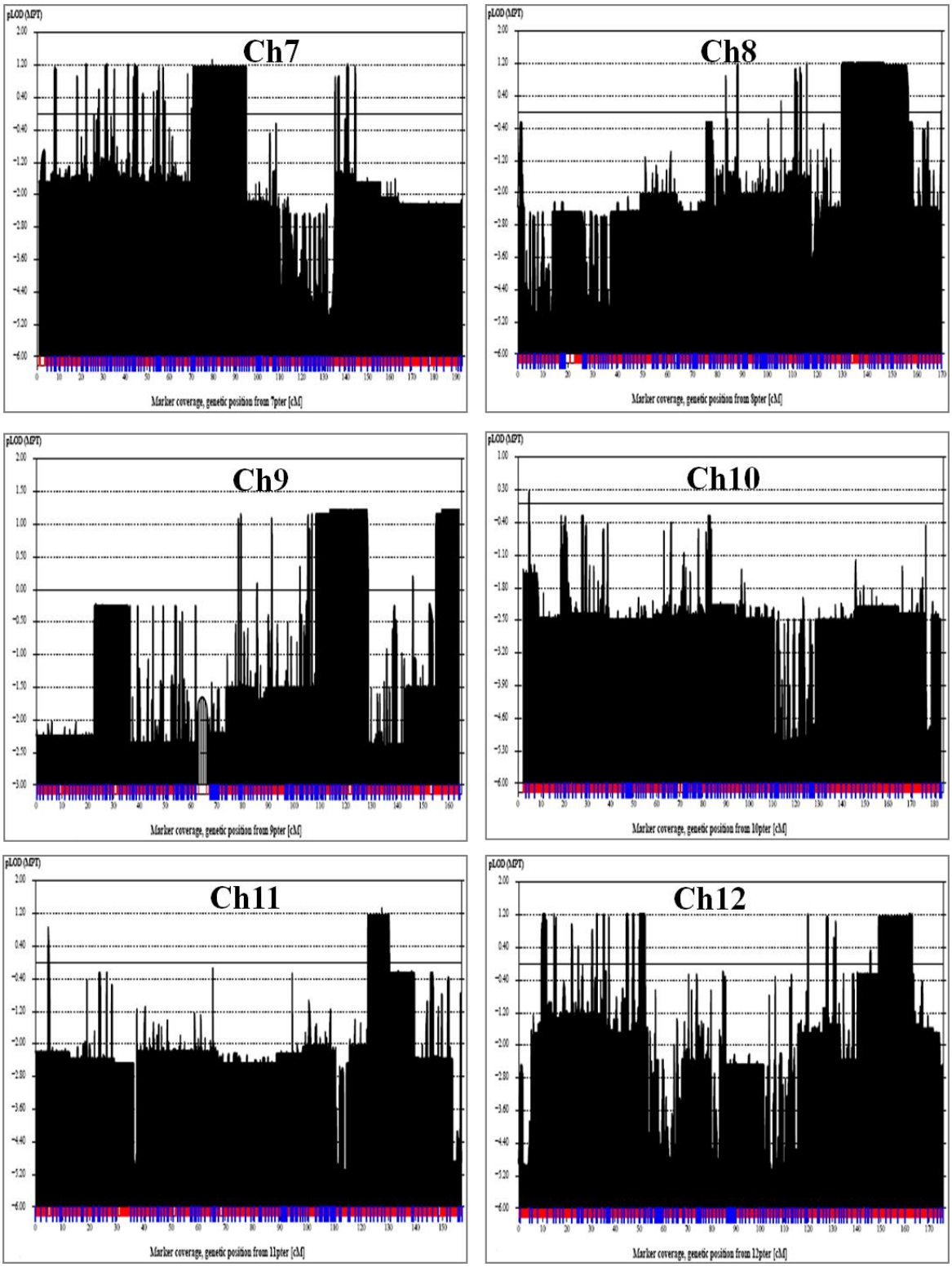

Figure A.6. Multi point lod score results for MCL in a dominant model with 80 per cent penetrance using the affected sibs and minimal cousins. The results for all autosomal chromosomes and PAR regions are given (continued).

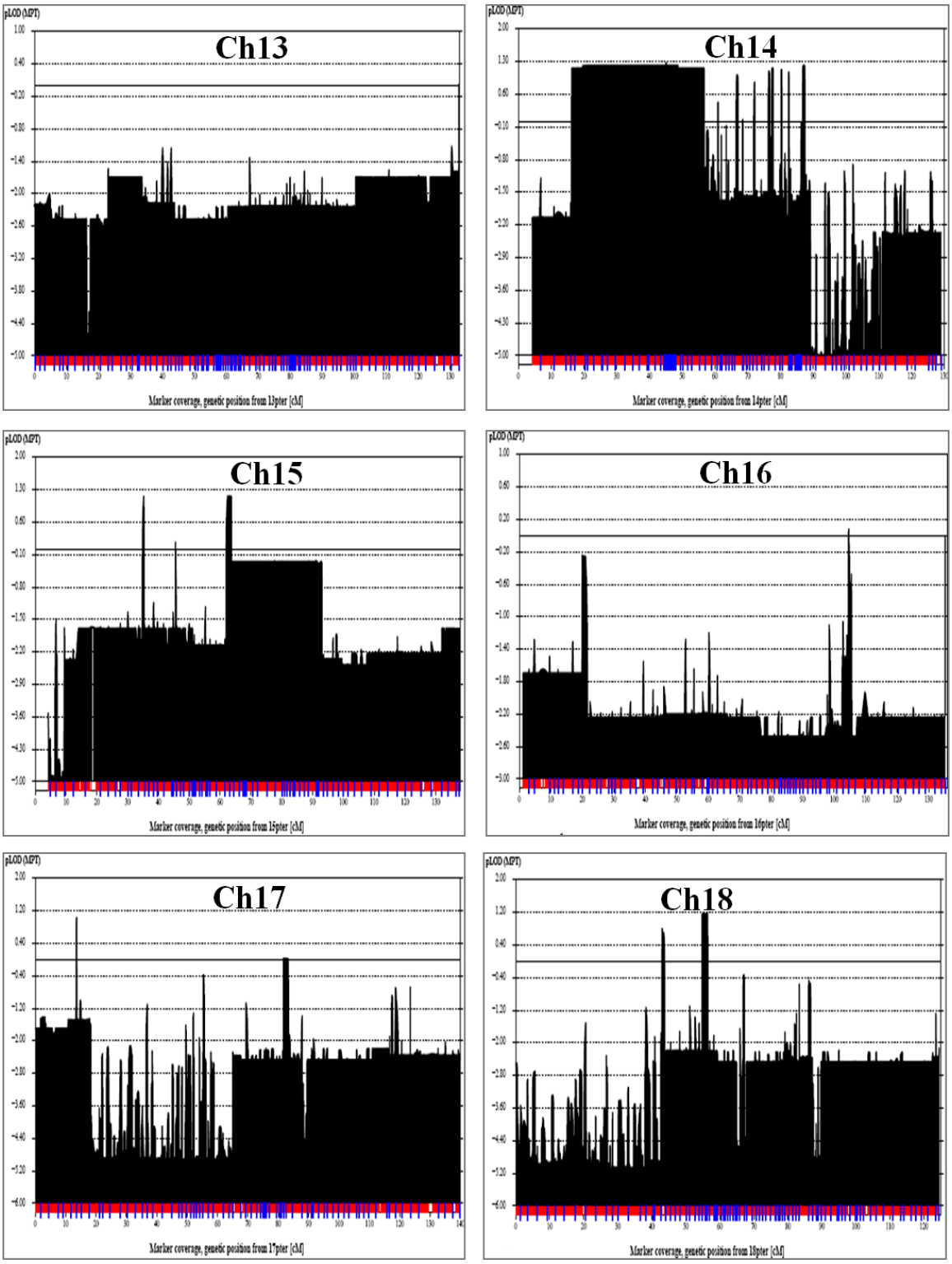

Figure A.6. Multi point lod score results for MCL in a dominant model with 80 per cent penetrance using the affected sibs and minimal cousins. The results for all autosomal chromosomes and PAR regions are given (continued).

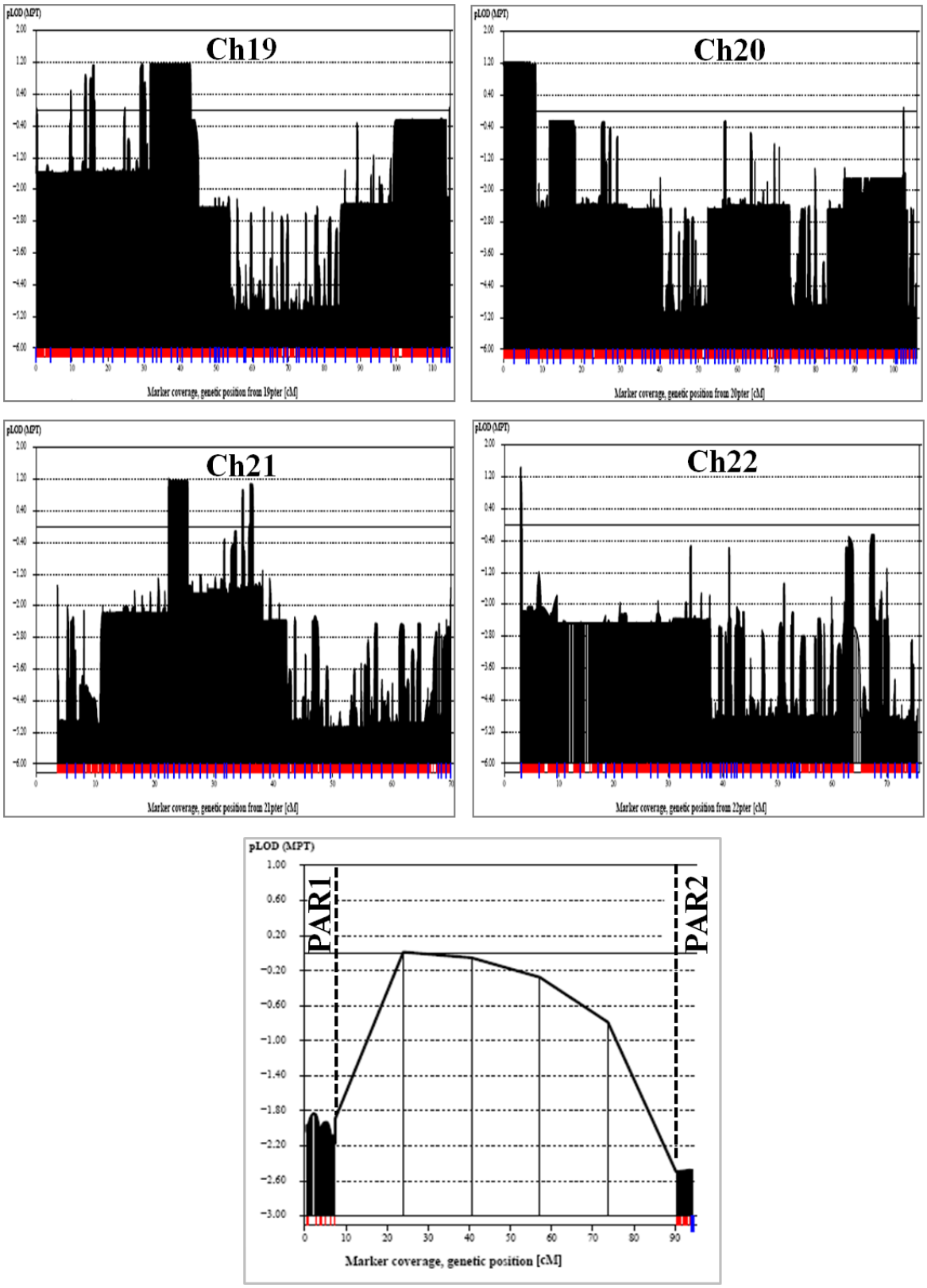

Figure A.6. Multi point lod score results for MCL in a dominant model with 80 per cent penetrance using the affected sibs and minimal cousins. The results for all autosomal chromosomes and PAR regions are given (continued).

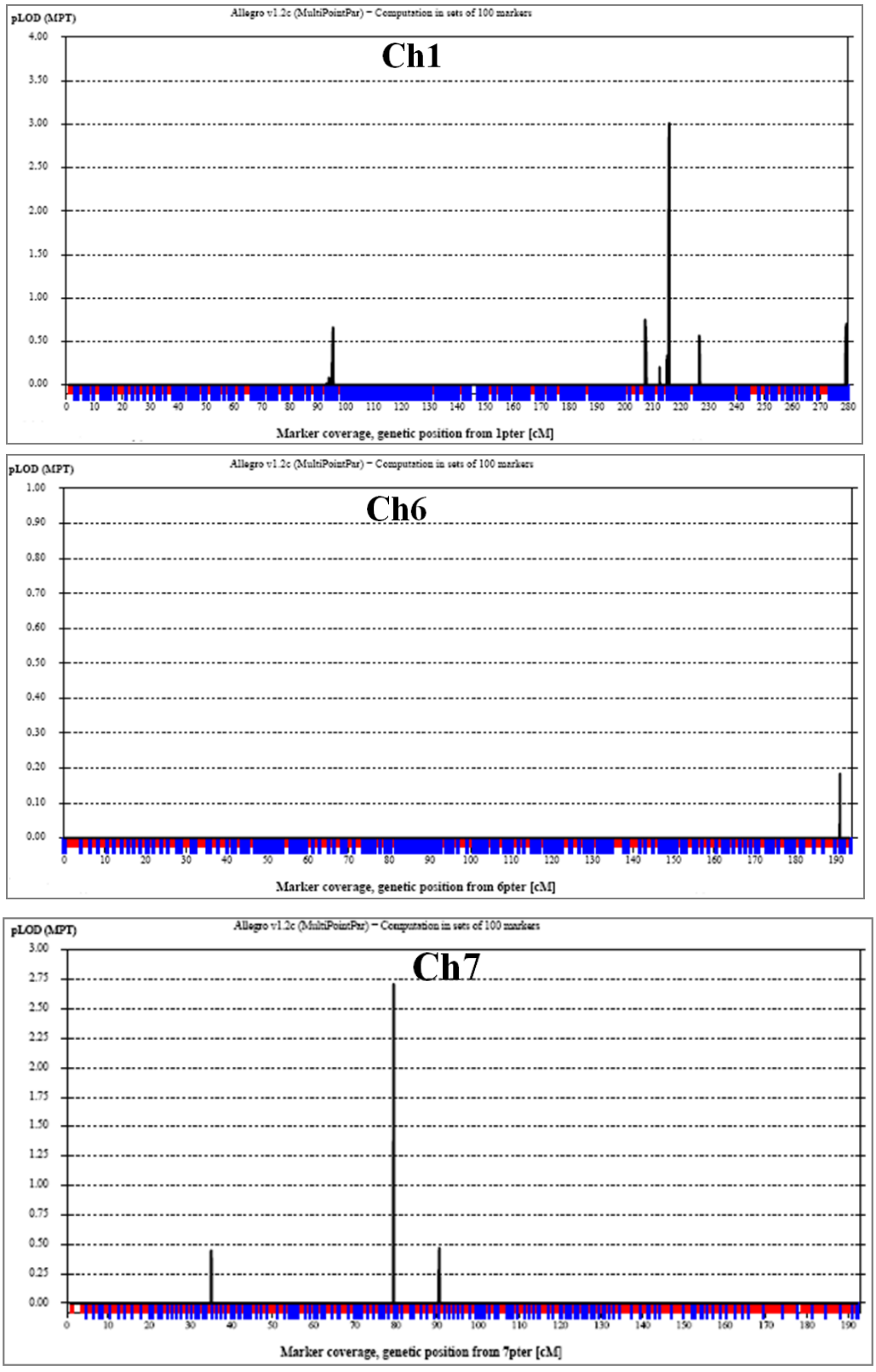

Figure A.7. Multipoint lod scores in a fully penetrant recessive model for MCL using the affected sibs and minimal cousins. The regions in all autosomal chromosomes and PAR regions that yielded positive scores are presented.

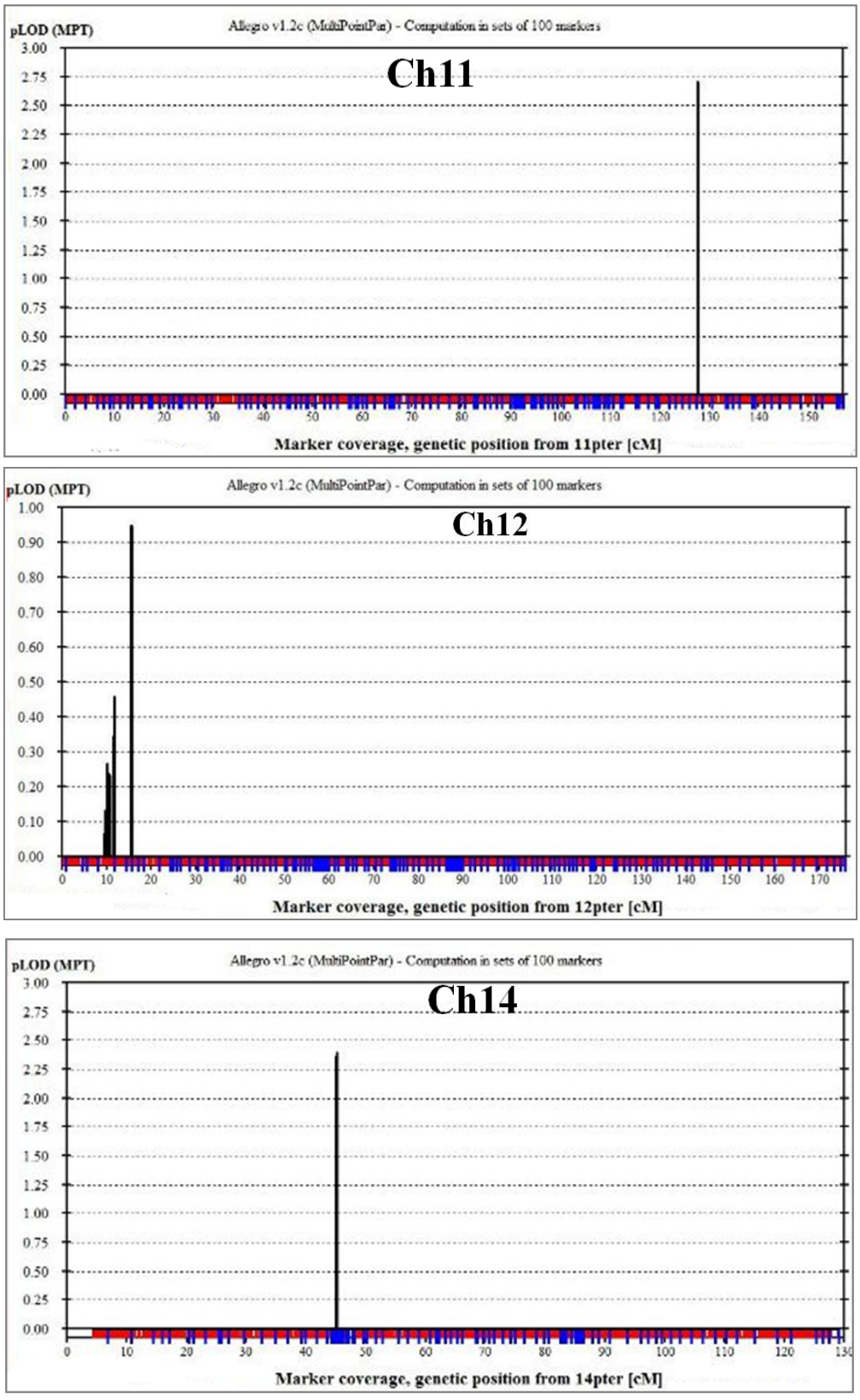

Figure A.7. Multipoint lod scores in a fully penetrant recessive model for MCL using the affected sibs and minimal cousins. The regions in all autosomal chromosomes and PAR regions that yielded positive scores are presented (continued).

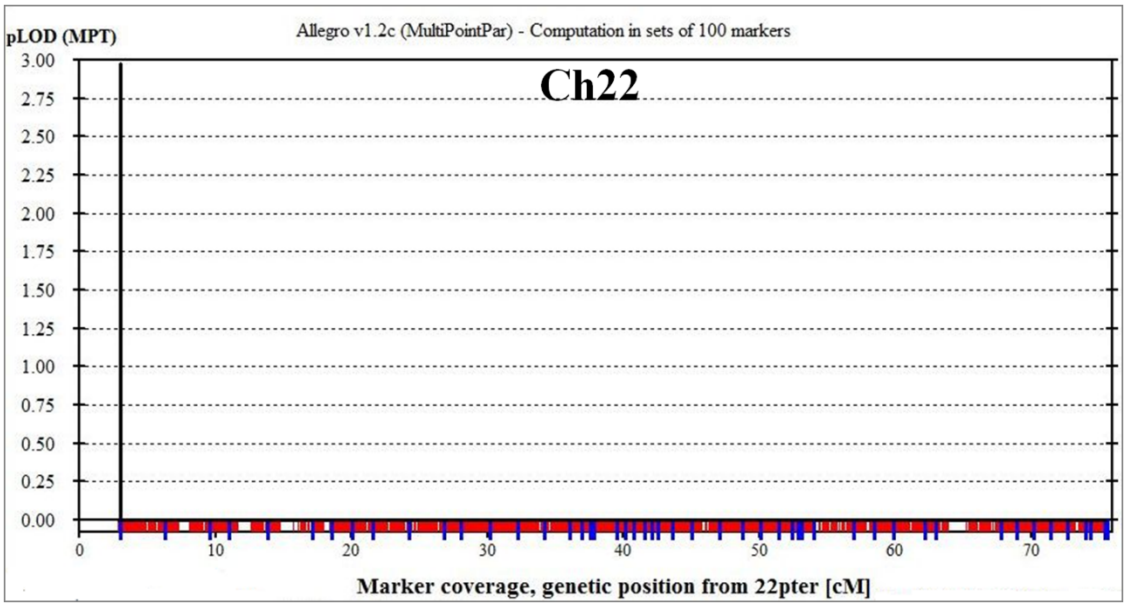

Figure A.7. Multipoint lod scores in a fully penetrant recessive model for MCL using the affected sibs and minimal cousins. The regions in all autosomal chromosomes and PAR regions that yielded positive scores are presented (continued).

8. REFERENCES

Al-Dosari, M. and F.F. Alkuraya, 2009, "A novel missense mutation in GORAB produces geroderma osteodysplastica phenotype indistinguishable from that caused by nullimorphic mutations", *American Journal of Medical Genetics Part A*, Vol. 149A, No. 10, pp. 2093-2098, May.

Al-Gazali, L.I., L. Sztriha, F. Skaff, and D. Haas, 2001, "Gerodermia osteodysplastica and wrinkly skin syndrome: are they the same?", *American Journal of Medical Genetics*, Vol. 101, No. 3, pp. 213-220, July.

Armstrong, A.P. and N. Waterhouse, 1996, "Tessier 30 median mandibular cleft: case report and literature review", *British Journal* of *Plastic Surgery*, Vol. 49, No. 8, pp. 536-538, December.

Barbara, D.A., A.R. Buckalew, and K.E. Leffler, 2005, "Effects of Epidermal Growth Factor (EGF), Transforming Growth Factor-(TGF), and 2,3,7,8- Tetrachlorodibenzo-p-dioxin on Fusion of Embryonic Palates in Serum-Free Organ Culture Using Wild-Type, EGF Knockout, and TGF Knockout Mouse Strains", *Birth Defects Research Part*, Vol. 73, No. 6, pp. 447-454, June.

Baumgartner, M.R., D. Rabier, M.C. Nassogne, J.L. Dufier, J.P. Padovani, P. Kamoun, D. Valle and J.M. Saudubray, 2005, "Delta1-pyrroline-5-carboxylate synthase deficiency: neurodegeneration, cataracts and connective tissue manifestationscombined with hyperammonaemia and reduced ornithine, citrulline, arginine and proline", *European Journal of Pediatrics*, Vol. 164, No. 1, pp. 31-36, January.

Beaty, T.H., J.C. Murray, M.L. Marazita, R.G. Munger, I. Ruczinski, J.B. Hetmanski, K.Y. Liang, T. Wu, T. Murray, M.D. Fallin, R.A. Redett, G. Raymond, H. Schwender, S.C. Jin, M.E. Cooper, M. Dunnwald, M.A. Mansilla, E. Leslie, S. Bullard, A.C. Lidral, L.M. Moreno, R. Menezes, A.R. Vieira, A. Petrin, A.J. Wilcox, R.T. Lie, E. W. Jabs, Y.H. Wu-Chou, P.K. Chen, H. Wang, X. Ye, S. Huang, V. Yeow, S.S.

Chong, S.H. Jee, B. Shi, K. Christensen, M. Melbye, K.F. Doheny, E.W. Pugh, H. Ling, E.E. Castilla, A.E. Czeizel, L. Ma, L.L. Field, L. Brody, F. Pangilinan, J.L. Mills, A.M. Molloy, P.N. Kirke, J.M. Scott, M. Arcos-Burgos and A.F. Scott, 2010, "A genome-wide association study of cleft lip with and without cleft palate identifies risk variants near MAFB and ABCA4", *Nature Genetics*, Vol. 42, No. 6, pp. 525-529, June.

Bicknell, L.S., J. Pitt, S. Aftimos, R. Ramadas, M.A. Maw and S.P. Robertson, 2008, "A missense mutation in ALDH18A1, encoding Delta1-pyrroline-5-carboxylate synthase (P5CS), causes an autosomal recessive neurocutaneous syndrome", *European Journal of Human Genetics,* Vol. 16, No. 10, pp. 1176-1186, October.

Bliek, B.J., R.H. van Schaik, I.P. van der Heiden, F.A. Sayed-Tabatabaei, C.M. van Duijn, E.A. Steegers and R.P. Steegers-Theunissen, 2009, "Eurocran Gene-Environment Interaction Group. Maternal medication use, carriership of the ABCB1 3435C > T polymorphism and the risk of a child with cleft lip with or without cleft palate", *American Journal of Medical Genetics Part A*, Vol. 149A, No. 10, pp. 2088-2092, October.

Broman, K.W., J.C. Murray, V.C. Sheffield, R. White and J. Weber, 1998, "Comprehensive human genetic maps: individual and sex-specific variation in recombination", *American Journal of Human Genetics*, Vol. 63, No. 3, pp. 861-869.

Carter T.C., A.M. Molloy, F. Pangilinan, J.F. Troendle, P.N. Kirke, M.R. Conley, D.J. Orr, M. Earley, E. McKiernan, E.C. Lynn, A. Doyle, J.M. Scott, L.C. Brody and J.L. Mills, 2010, "Testing reported associations of genetic risk factors for oral clefts in a large Irish study population", *Birth Defects Research Part A: Clinical and Molecular Teratology*, Vol. 88, No. 2, pp. 84-93, February.

Cetinkaya, M., Gene Hunt in Four Inherited Diseases, 2010, Bogazici University PhD Thesis.

Charoenchaikorn, K., T. Yokomizo, D.P. Rice, T. Honjo, K. Matsuzaki, Y. Shintaku, Y. Imai, A. Wakamatsu, S. Takahashi, Y. Ito, T. Takano-Yamamoto, I. Thesleff, M. Yamamoto and T. Yamashiro, 2009, "Runx1 is involved in the fusion of the primary and the secondary palatal shelves", *Developmental Biology*, Vol. 326, No. 2., pp. 392-402, February.

Chiquet, B.T., S.S. Hashmi, R. Henry, A. Burt, J.B. Mulliken, S. Stal, M. Bray, S.H. Blanton and J.T. Hecht, 2008, "Genomic screening identifies novel linkages and provides further evidence for a role of MYH9 in nonsyndromic cleft lip and palate", *European Journal of Human Genetics,* Vol. 17, No. 2, pp. 195-204, Februrary.

Dent, M., G. Raisman and F. Lai, 1996, "Expression of type 1 inositol 1,4,5-trisphosphate receptor during axogenesis and synaptic contact in the central and peripheral nervous system of developing rat", *Development*, Vol. 122, No. 3, pp. 1029-1039, March.

Ding, H., X. Wu, H. Boström, I. Kim, N. Wong, B. Tsoi, M. O'Rourke, G.Y. Koh, P. Soriano, C. Betsholtz, T.C. Hart, M.L. Marazita, L.L. Field, P.P. Tam and A. Nagy, 2004, "A specific requirement for PDGF-C in palate formation and PDGFR-alpha signaling", *Nature Genetics*, Vol. 36, No. 10, pp. 1111-1116, October.

Eppley, B.L., J.A. van Aalst, A. Robey, R.J. Havlik and A.M. Sadove, 2005, "The Spectrum of Orofacial Clefting", *Plastic Reconstruction Surgery*, Vol. 115, No. 7, pp. 101-114, June.

Fearon, J.A., 2008, "Rare craniofacial clefts: a surgical classification", *Journal of Craniofacial Surgery*, Vol. 19, No. 1, pp. 110-112, January.

Foskett, J.K., C. White, K. Cheung, and D. Mak, 2007, "Inositol trisphosphate receptor Ca^{2+} release channels", *Physiological Reviews*, Vol. 87, No. 2, pp. 593-658, April.

Grigoriou, M., A.S. Tucker, P.T. Sharpe and V. Pachnis, 1998, "Expression and regulation of Lhx6 and Lhx7, a novel subfamily of LIM homeodomain encoding genes,

suggests a role in mammalian head development", *Development*, Vol. 125, No. 11, pp. 2063-2074, June.

Guernsey, D.L., H. Jiang, S.C. Evans, M. Ferguson, M. Matsuoka, M. Nightingale, A.L. Rideout, S. Provost, K. Bedard, A. Orr, M.P. Dubé, M. Ludman and M.E. Samuels, 2009," Mutation in Pyrroline-5-Carboxylate Reductase 1 Gene in Families with Cutis Laxa Type 2", *American Journal of Human Genetics*, Vol. 85, No. 1, pp. 120-129, July.

Hennies, H.C., U. Kornak, H. Zhang, J. Egerer, X. Zhang, W. Seifert, J. Kuhnisch, B. Budde, M. Natebus, F. Brancati, R. William, W.R. Wilcox, D. Muller, P.B. Kaplan, A. Rajab, G. Zampino, V. Fodale, B. Dallapiccola, W. Newman, K. Metcalfe, J. Clayton-Smith, M. Tassabehji, B. Steinmann, F.A. Barr, P. Nurnberg, P. Wieacker and S. Mundlos, 2008, "Gerodermia osteodysplastica is caused by mutations in GORAB , a Rab-6 interacting golgin", *Nature Genetics*, Vol. 40, No. 12, pp. 1410-1412, December.

Hirsch, C., R. Gauss, S.C. Horn, O. Neuber and T. Sommer, 2009, "The ubiquitylation machinery of the endoplasmic reticulum", *Nature*, Vol. 458, No. 7237, pp. 453-60, March.

Hoegg, M., D. Browman, M. Resek, and S. Robbins, 2009, "Distinct regions within the erlins are required for oligomerization and association with high molecular weight complexes", *The Journal of Biological Chemistry*, Vol. 284, No. 12, pp. 7766-7776, March.

Hoffmann, K. and T.H. Lindner, 2005, "easyLINKAGE-Plus-Automated Linkage Analyses Using Large-Scale SNP Data", *Bioinformatics*, Vol. 21, No. 17, pp. 3565-3567, September.

Hunter, A.G., J.T. Martsolf, C.G. Baker, M.H. Reed, 1978, "Geroderma osteodysplastica. A report of two affected families", *Human Genetics*, Vol. 40, No. 3, pp. 311-324, February.

Iijima, T., T. Imai, Y. Kimura, A. Bernstein, H.J. Okano, M. Yuzaki and H. Okano, 2005, "Hzf protein regulates dendritic localization and BDNF-induced translation of type 1 inositol 1,4,5-trisphosphate receptor mRNA", *The Proceedings of the National Academy of Sciences Online (US)*, Vol. 102, No.47, pp. 17190-171905, November.

Ikegawa, S., M. Isomura, Y. Koshizuka and Y. Nakamura, 1999, "Cloning and characterization of a novel gene (C8orf2), a human representative of a novel gene family with homology to C. elegans C42.C1.9", *Cytogenetics and Cell Genetics*, Vol. 85, No. 3-4, pp. 227-231, March.

Inoue, M., M. Kawakami, K. Tatsumi, T. Manabe, M. Makinodan, H. Matsuyoshi, T. Kirita and A. Wanaka, 2006, "Expression and regulation of the LIM homeodomain gene L3/Lhx8 suggests a role in upper lip development of the chick embryo", *Anatomy and Embryology (Berlin)*, Vol. 211, No. 3, pp. 247-253, June.

Jordan, T., H. Jiang, H. Li and J.X. DiMario, 2005, "Regulation of skeletal muscle fiber type and slow myosin heavy chain 2 gene expression by inositol trisphosphate receptor 1", *Journal of Cell Science*, Vol. 118, No. 10, pp. 2295-2302, May.

Jugessur, A., P.G. Farlie and N. Kilpatrick, 2009, "The genetics of isolated orofacial clefts: from genotypes to subphenotypes", *Oral Diseases*, Vol. 15, No. 7, pp. 437-453, October.

Jugessur, A. and J.C. Murray, 2005, "Orofacial clefting: recent insights into a complex trait", *Current Opinion in Genetics and Development*, Vol. 15, No. 3, pp. 270-278, June.

Krishnan, N., M.B. Dickman and D.F. Becker, 2007, "Proline modulates the intracellular redox environment and protects mammalian cells against oxidative stress", *Free Radical Biology and Medicine*, Vol. 44, No. 4, pp. 671-681, February.

Kornak, U., E. Reynders, A. Dimopoulou, J. van Reeuwijk, B. Fischer, A. Rajab, B. Budde, P. Nürnberg, F. Foulquier, ARCL Debre´-type Study Group, D. Lefeber, Z.

Urban, S. Gruenewald, W. Annaert, H.G. Brunner, H. van Bokhoven, R. Wevers, E. Morava, G. Matthijs, L. Maldergem and S. Mundlos, 2008, "Impaired glycosylation and cutis laxa caused by mutations in the vesicular H(+)-ATPase subunit ATP6V0A2", *Nature Genetics*, Vol. 40, No. 1, pp. 32-34, January.

Liu, Y., G.L. Borchert, S.P. Donald, A. Surazynski, C.A. Hu, C.J. Weydert, L.W. Oberley and J.M. Phang, 2005, "MnSOD inhibits proline oxidase-induced apoptosis in colorectal cancer cells", *Carcinogenesis*, Vol. 26, No. 8, pp. 1335-1342, August.

Lynn, A., C. Kashuk, M.B. Petersen, J.A. Bailey, D.R. Cox, S.E. Antonarakis and A. Chakravarti, 2000, "Patterns of meiotic recombination on the long arm of human chromosome 21", *Genome Research*, Vol. 10, No. 9, pp. 1319-1332, September.

Marazita, M.L., A.C. Lidral, J.C. Murray, L.L. Field, B.S. Maher, T. Goldstein McHenry, M.E. Cooper, M. Govil, S. Daack-Hirsch, B. Riley, A. Jugessur, T. Felix, L. Morene, M.A. Mansilla, A.R. Vieira, K. Doheny K and E. Pugh, 2009, "Genome scan, fine-mapping, and candidate gene analysis of nonsyndromic cleft lip with or without cleft palate reveals phenotype specific differences in linkage and association results", *Human Heredity*, Vol. 68, No. 3, pp. 151-170, June.

Martínez-Glez, V., P. Lapunzina P, A. Delicado, A. Tendero, M.A. Mori, M.L. de Torres, L. Fernández, M. Palomares and I.L. Pajares, 2006 "Mietens-Weber syndrome: two new patients and a review", *Clinical Dysmorphology*, Vol.15, No.3, pp. 175-177, July.

Matsumoto, M., T. Nakagawa, T. Inoue, E. Nagata, K. Tanaka, H. Takano, O. Minowa, J. Kuno, S. Sakakibara, M. Yamada, H. Yoneshima, A. Miyawaki, Y. Fukuuchi, T. Furuichi, H. Okano, K. Mikoshiba and T. Noda, 1996, "Ataxia and epileptic seizures in mice lacking type 1 inositol 1,4,5-trisphosphate receptor", *Nature*, Vol. 379, No. 6561, pp. 168-171, January.

Miettinen, P.J., J.R. Chin, L. Shum, H.C. Slavkin, C.F. Shuler, R. Derynck and Z. Werb, 1999, "Epidermal growth factor receptor function is necessary for normal

craniofacial development and palate closure", *Nature Genetics*, Vol. 22, No. 1, pp. 69-73, May.

Mitchell, L.E., J.C. Murray, S. O'Brien and K. Christensen, 2003, "Retinoic acid receptor alpha gene variants, multivitamin use, and liver intake as risk factors for oral clefts: a population-based case-control study in Denmark, 1991-1994", *American Journal of Epidemiology*, Vol. 158, No. 1, pp. 69-76, July.

Morava, E., M. Guillard, D.J. Lefeber and R.A. Wevers, 2009, "Autosomal recessive cutis. laxa syndrome revisited", *Journal of Human Genetics*, Vol. 17, No. 9, pp. 1099-1110, September.

Mossey, P.A., J. Little, R.G. Munger, M.J. Dixon and W.C. Shaw, 2009, "Cleft lip and palate", *Lancet*, Vol. 374, pp. 1773-85.

Murray, J.C., 1995, "Face Facts: Genes, Environment, and Clefts", *American Journal of Human Genetics*, Vol. 57, No. 2, pp. 227-232, August.

Nagase, T., K.I. Ito, K. Kato, K. Kaneko, K. Kohda, M. Matsumoto, A. Hoshino, T. Inoue, S. Fujii, H. Kato and K. Mikoshiba, 2003, "Long-term potentiation and long-term depression in hippocampal CA1 neurons of mice lacking the IP(3) type 1 receptor", *Neuroscience*, Vol. 117, No. 4, pp. 821-830.

Nanda, A., Q.A. Alsaleh, H. Al-Sabah, E.E. Marzouk, A.M. Salam, M. Nanda and J.T. Anim, 2008, "Gerodermia osteodysplastica/wrinkly skin syndrome: Report of three patients and brief review of literature", *Pediatric Dermatology*, Vol. 25, No. 1, pp. 66-71, January-February.

Nyholt, D.R., 2000, "All LODs are not created equal", *American Journal of Human Genetics*, Vol. 67, No. 2, pp. 282-288, August.

Ogura, H., M., Matsumoto and K. Mikoshiba, 2001, "Motor discoordination in mutant mice heterozygous for the type 1 inositol 1,4,5-trisphosphate receptor", *Behavioural Brain Research*, Vol. 122, pp. 215–219, February.

Phang, J.M., J. Pandhare and Y. Liu, 2008, "The metabolism of proline as microenvironmental stress substrate", *Journal of Nutrition*, Vol. 138, No.10, pp. 2008-2015, October.

Picco, P., C. Marciano, D. Qaglino, G. Bisio, R. Biolcati, A. Buoncompagni, M.D Rocco, I. Ronchetti and C. Borrone, 1993, "Gerodermia Osteodysplastica: A clinical and biological report", *European Journal of Histochemistry*, Vol. 37, pp. 86-88.

Pietrement, C., G.H. Sun-Wada, N.D. Silva, M. McKee, V. Marshansky, D. Brown, M. Futai and S. Breton, 2005, "Distinct expression patterns of different subunit isoforms of the V-ATPase in the rat epididymis", *Biology of Reproduction*, Vol. 74, pp. 185-194.

Rahimov, F., M.L. Marazita, A. Visel, M.E. Cooper, M.J. Hitchler, M. Rubini, F.E. Domann, M. Govil, K. Christensen, C. Bille, R.P. Steegers-Theunissen, L.A. Pennacchio, B.C. Schutte and J.C. Murray, 2008, "Disruption of an AP-2alpha binding site in an IRF6 enhancer is associated with cleft lip", *Nature Genetics*, Vol. 40, No. 11, pp. 1341-1347, November.

Rajab, A., U. Kornak, B.S. Budde, K. Hoffmann, J. Jaeken, P. Nürnberg and S. Mundlos, 2008, "Geroderma osteodysplasticum hereditaria and wrinkly skin syndrome in 22 patients from Oman", *American Journal of Medical Genetics Part A*, Vol. 146A, No. 8, pp. 965-976, April.

Randolph, Y.H., 2002, "ER-associated degradation in protein quality control and cellular regulation", *Current Opinion in Cell Biology*, Vol. 14, No. 4, pp. 476-482.

Resnick, J.I. and H.K. Kawamoto Jr., 1990, "Rare craniofacial clefts: Tessier no. 4 clefts", *Plastic Reconstruction Surgery*, Vol. 85, No. 6, pp. 843-849, June.

Riley, B.M., M.A. Mansilla, J. Ma, S. Daack-Hirsch, B.S. Maher, L.M. Raffensperger, E.T. Russo, A.R. Vieira, C. Dodé, M. Mohammadi, M.L. Marazita and J.C. Murray, 2007, "Impaired FGF signaling contributes to cleft lip and palate", *The Proceedings of the National Academy of Sciences Online (US)*, Vol. 104, No. 11, pp. 4512-4517, March.

Schubert, U., L.C. Antón, J. Gibbs, C.C. Norbury, J.W. Yewdell and J.R. Bennink, 2000, "Rapid degradation of a large fraction of newly synthesized proteins by proteasomes", *Nature*, No. 404, No. 6779, pp. 770-774, April.

Seyhan, T. and H. Kýlýnç, 2002, "Median cleft of the lower lip: report of two new cases and review of the literature", *Annals of Otology, Rhinology and Laryngology*, Vol. 111, No. 3.1, pp. 217-221, March.

Sheth, N., X. Roca, M.L. Hastings, T. Roeder, A.R. Krainer and R. Sachidanandam, 2006, "Comprehensive splice-site analysis using comparative genomics", *Nucleic Acids Research*, Vol. 34, No. 14, pp. 3955-67, August.

Shi, M., A. Mostowska, A. Jugessur, M.K. Johnson, M.A. Mansilla, K. Christensen, R.T. Lie, A.J. Wilcox and J.C. Murray, 2009, "Identification of microdeletions in candidate genes for cleft lip and/or palate", *Birth Defects Research Part A: Clinical and Molecular Teratology*, Vol. 85, No. 1, pp. 42-51, January.

Sivertsen, A., A.J. Wilcox, R. Skjaerven, H.A. Vindenes, F. Abyholm, E. Harville and R.T. Lie, 2008, "Familial risk of oral clefts by morphological type and severity: population based cohort study of first degree relatives", *British Medical Journal*, Vol. 336, No. 7641, pp. 432-534, February.

Sull, J.W., K.Y. Liang, J.B. Hetmanski, M.D. Fallin, R.G. Ingersoll, J.W. Park, Y.H. Wu-Chou, P.K. Chen, S.S. Chong, F. Cheah, V. Yeow, B.Y. Park, S.H. Jee, E.W. Jabs, R. Redett, A.F. Scott and T.H. Beaty, 2008, "Excess maternal transmission of markers in TCOF1 among cleft palate case-parent trios from three populations",

American Journal of Medical Genetics Part A, Vol. 146A, No. 18, pp. 2327-2331, September.

Takei, K., R. Shin, T. Inoue, K. Kato, and K. Mikoshiba, 1998, "Regulation of nerve growth mediated by inositol 1,4,5-trisphosphate receptors in growth cones", *Science*, Vol. 282, pp. 1705-1708.

Taylor, C.W., A.A. Genazzani and S.A. Morris, 1999, "Expression of inositol trisphosphate receptors", *Cell Calciu*m, Vol. 26, No.6, pp. 237–251.

Thomas, P.S., J. Kim, S. Nunez, M. Glogauer and V. Kaartinen, 2010, "Neural crest cell-specific deletion of Rac1 results in defective cell-matrix interactions and severe craniofacial and cardiovascular malformations", *Developmental Biology*, Vol. 340, No. 2, pp. 613-25, April.

Türkmen, S., G. Guo, M. Garshasbi, K. Hoffmann, A. Alshalah, C. Mischung, A. Kuss, N. Humphrey, S. Mundlos and P. Robinson, 2009, "CA8 mutations cause a novel syndrome characterized by ataxia and mild mental retardation with predisposition to quadrupedal gait", *PLoS Genetics*, Vol. 5, No. 5, pp 1000487, May.

Vembar, S.S. and J.L. Brodsky, 2008, "One step at a time: endoplasmic reticulum-associated degradation", *Nature Reviews Molecular Cell Biology,* Vol. 9, No. 12, pp. 944-957, December.

Vieira, A.R., 2008, "Unraveling Human Cleft Lip and Palate Research", *Journal of Dental Research*, Vol. 87, No. 2, pp. 119-125.

Vieira, A.R., R. Meira, A. Modesto and J.C. Murray, 2004, "MSX1, PAX9, and TGFA contribute to tooth agenesis in humans", *Journal of Dental Research*. Vol. 83, No. 9, pp. 723-727, September.

Vieira, A.R., T.G. McHenry, S. Daack-Hirsch, J.C. Murray and M.L. Marazita, 2008, "Candidate gene/loci studies in cleft lip/palate and dental anomalies finds novel

susceptibility genes for clefts", *Genetics in Medicine*, Vol. 10, No. 9, pp. 668-74, September.

Warner, D.R., M.M. Pisano, E.A. Roberts and R.M. Greene, 2003, "Identification of three novel Smad binding proteins involved in cell polarity", *FEBS Letters*, Vol. 539, No. 1-3, pp. 167-73, March.

Wortmann, S.B., R. Rodenburg, B. Schwahn, J.A. Smeitink and E. Morava, 2007, "Distal joint contractures, mental retardation, characteristic face and growth retardation: Chitayat syndrome revisited", *Genetic Counseling*, Vol. 18, No. 1, pp. 119-23.

Yang, L.T. and V. Kaartinen, 2007, "Tgfb1 expressed in the Tgfb3 locus partially rescues the cleft palate phenotype of Tgfb3 null mutants", *Developmental Biology*, Vol. 312, No. 1, pp. 384-395, December.

Yildirim, Y., A. Tolun and B. Tüysüz, 2010, "The Phenotype Caused by PYCR1 Mutations Corresponds to Geroderma Osteodysplasticum Rather than Autosomal Recessive Cutis Laxa Type 2", *American Journal of Medical Genetics*, Under Revision.

Young, D.L., R.A. Schneider, D. Hu and J.A. Helms, 2000, "Genetic and teratogenic approaches to craniofacial development", *Critical Reviews in Oral Biology and Medicine*, Vol. 11, No. 3, pp. 304-317.

Zhao, Y., O. Marín, E. Hermesz, A. Powell, N. Flames, M. Palkovit, J.L. Rubenstein and H. Westphal, 2003, "The LIM-homeobox gene Lhx8 is required for the development of many cholinergic neurons in the mouse forebrain", *The Proceedings of the National Academy of Sciences Online (US)*, Vol. 100, No. 15, pp. 9005-9010, July.

Zhao, Y., Y.J. Guo, A.C. Tomac, N.R. Taylor, A. Grinberg, E.J. Lee, S. Huang and H. Westphal, 1999, "Isolated cleft palate in mice with a targeted mutation of the LIM homeobox gene lhx8", *The Proceedings of the National Academy of Sciences Online (US)*, Vol. 96, No. 26, pp. 15002-15006, December.